# Endocytosis, Phagocytosis, and Innate Immune Responses: A Dissertation

# ENDOCYTOSIS, PHAGOCYTOSIS, AND INNATE IMMUNE RESPONSES

A Dissertation Presented By

Christine A. St. Pierre

submitted to the Faculty of the

University of Massachusetts Graduate School of Biomedical Sciences, Worcester

in partial fulfillment of the requirements for the degree of

DOCTOR OF PHILOSOPHY

July 13, 2010

Biomedical Sciences

ENDOCYTOSIS, PHAGOCYTOSIS, AND INNATE IMMUNE RESPONSES

A dissertation presented by

Christine A. St. Pierre

The signatures of the Dissertation Defense Committee signifies completion and approval as to style and content of the Dissertation

Robert W. Finberg, M.D., Thesis Advisor

Evelyn A. Kurt-Jones, Ph.D., Member of Committee

Silvia Corvera, M.D., Member of Committee

Katherine Fitzgerald, Ph.D., Member of Committee

Amy Hise, M.D., M.P.H., Member of Committee

The signature of the Chair of the Committee signifies that the written dissertation meets the requirements of the Dissertation Committee

Alan Rothman, M.D., Chair of Committee

The signature of the Dean of the Graduate School of Biomedical Sciences signifies that the student has met all graduation requirements of the school.

Anthony Carruthers, Ph.D.,
Dean of the Graduate School of Biomedical Sciences

Immunology and Virology Program

July 13, 2010

## ACKNOWLEDGEMENTS

I would first like to thank my mentor Dr. Robert Finberg for allowing me to perform my graduate research in his laboratory. I have grown immensely as a scientist under his direction and will be forever grateful for his guidance, support, and humor throughout my graduate career. I would like to thank Dr. Evelyn Kurt-Jones, whom I consider my co-mentor, for helping me to grow not only as a scientist but also as a scientific writer. She has provided me with countless hours of scientific discussion and allowed me to be a part of several grant-writing processes. I would also like to thank all the members of the Finberg/Kurt-Jones lab for all their support throughout the years. I would especially like to thank Dr. Jennifer Wang, Dr. Shenghua Zhou, and Melvin Chan for their assistance in experimental design and many scientific discussions. I would like to thank my fellow graduate student, Ryan Nistler, for all his help in optimizing experiments and for being a great friend.

I would like to thank my collaborators, Dr. Ryan Hayward in the Department of Polymer Science and Engineering at UMass Amherst, and Dr. David Ayers in the Department of Orthopedics here at UMass Medical School, for allowing me to take part in really exciting projects and I look forward to future collaborations with them.

I would like to thank Dr. Donna Ambrosino and her team and MassBiologics for all her help and support during my first years as a graduate student. She introduced me to several projects, and trusted me to work with her team when I had very little experience.

I would like to thank my current and former committee members, Dr. Eicke Latz, Dr. Katherine Fitzgerald, Dr. Silvia Corvera, Dr. Evelyn Kurt-Jones, Dr. Alan Rothman, and my outside member Dr. Amy Hise, for all their comments, suggestions, and support of my work. They have assisted me in moving my projects into a direction that I am proud of.

Finally, I would not be where I am today if it weren't for the love and support of my family and friends. They have always, and continue to believe in me in all that I do, and I am forever grateful. I will always cherish the friendships I have made in graduate school, and wish them all the best in their scientific careers. Last, but not least, I would like to thank Dr. Michael Vaine for making my last three years of graduate school the best years of my life. It has been great to be able to share all of my experiences with someone, especially a fellow scientist. He has pushed me to become a better person, both at home and professionally, and I love him dearly for that.

## ABSTRACT

In this dissertation, the roles of endocytosis and phagocytosis pathways in a variety of clinically relevant scenarios were examined. These scenarios include antibody-mediated internalization of cell surface proteins, titanium wear-particle uptake in failed joint replacements, and polymeric microparticle uptake and immune responses for drug delivery or adjuvant use.

The use of antibodies specific for cell surface proteins has become a popular method to deliver therapeutics to target cells. As such, it is imperative to fully understand the ability of antibodies to mediate internalization and endosomal trafficking of the surface protein that it recognizes, so that drug delivery can be optimized. By comparing the internalization and endosomal localization of two different antibody-bound proteins, the transferrin receptor (TfR) and rabies G, we have found that there is a specific antibody-mediated internalization pathway that occurs when an antibody binds to a cell surface protein. Interestingly, the internalization pathway induced by antibody binding is different than that seen with recycling receptor internalization after ligand binding. This may have broad implications for the future development of antibody-based therapeutics.

Joint replacement failure is a major clinical problem. Studies have indicated that a large amount of metal and polyethylene wear debris is found in the synovial membrane and tissue surrounding failed replacements. Through examination of the immune response following uptake of titanium particles, our results suggest that titanium wear-particle induced inflammation and subsequent joint replacement failure

may be due to activation of the NLRP3 inflammasome, leading to increased IL-1β secretion and IL-1 associated signaling. These findings introduce IL-1 as a target for potential therapeutics for patients exhibiting significant inflammation.

Polymeric microparticles have been widely used in a variety of therapeutic applications, including drug delivery and vaccine adjuvants. It is essential to understand the ability of such particles to either activate or inhibit an immune response following uptake. Through comparison of particles with varying surface morphology, we have determined that particles with regions of high surface curvature (budding) are more immunogenic than particles with low surface curvature (spherical). Budding particles were more rapidly phagocytosed and induced higher levels of the inflammasome-associated cytokine, IL-1β, when exposed to mouse macrophages. Additionally, budding particles induced a more rapid neutrophil response in vivo, when compared to spherical particles. These findings have broad implications for the development of future targeting vehicles for delivery of vaccines, drugs, proteins, and siRNA therapeutics.

# TABLE OF CONTENTS

## LIST OF FIGURES

Page

### CHAPTER 1



### CHAPTER 2

**CHAPTER 3**

**CHAPTER 4**

## ABBREVIATIONS USED

**ASC**: Apoptosis-associated speck-like protein

**ATP**: Adenosine triphosphate

**BIR**: Baculovirus inhibitor of apoptosis

**CARD**: Caspase recruitment domain

**CCV**: Clathrin-coated vesicle

**DMEM**: Dulbecco's modified eagle's medium

**DN**: Dominant-negative

**EE**: Early endosome

**EGFR**: Epidermal growth factor receptor

**ELISA**: Enzyme-linked immunosorbent assay

**ER**: Endoplasmic reticulum

**FcR**: Fc receptor

**FCS**: Fetal calf serum

**Rabies G**: Rabies glycoprotein

**GDP**: Guanosine diphosphate

**GFP**: Green fluorescent protein

**GM-CSF**: Granulocyte-macrophage colony stimulating factor

**GTP**: Guanosine triphosphate

**H&E**: Hematoxylin and eosin

**HEK**: Human embryonic kidney

**HIV**: Human immunodeficiency virus

**IL-1α**: Interleukin-1 alpha

**IL-1α/β**: Interleukin-1 alpha and beta

**IL-1β**: Interleukin-1 beta

**IL-1R**: Interleukin-1 receptor

**IL-1Ra**: Interleukin-1 receptor antagonist

**IL-6**: Interleukin-6

**i.p.**: Intra-peritoneal

**ITAM**: Immune receptor tyrosine activation motif

**IRF**: Interferon responsive factor

**KO**: Knockout

**LA**: Latrunculin A

**lamps**: Lysosomal-associated membrane proteins

**LDL**: Low density lipoprotein

**LDLR**: Low density lipoprotein receptor

**LE**: Late endosome

**lgp**: Lysosome membrane glycoprotein

**LPS**: Lipopolysaccharide

**LRR**: Leucine rich repeat

**MARCO**: Macrophage receptor with collagenous structure

**MCP-1**: Monocyte chemotactic protein 1

**MDP**: Muramyl dipeptide

**MHC**: Major histocompatibility complex

**MIP-1α**: Macrophage inflammatory protein 1 alpha

**MIP-1β**: Macrophage inflammatory protein 1 beta

**MNA**: Mouse neuroblastoma

**MNAG**: Mouse neuroblastoma expressing rabies glycoprotein

**MPR**: Mannose-6-phosphate receptor

**MSU**: Monosodium urate

**NACHT**: domain present in NAIP, CIITA, HET-E, and TP-1

**NAIP**: Neuronal apoptosis inhibitory protein

**NF-κB**: Nuclear factor kappa B

**NLR**: Nucleotide-binding domain, leucine-rich repeat containing (formally termed NOD-like receptor)

**NOD**: Nucleotide-binding oligomerization domain

**PAMP**: Pattern-associated molecular pattern

**PBS**: Phosphate buffered saline

**PEC**: Peritoneal exudate cell

**$PGE_2$**: Prostaglandin E2

**PMA**: Phorbol 12-myristate 13-acetate

**PRRs**: Pattern recognition receptors

**PS-PEO**: Polystyrene-block-poly (ethylene oxide)

**PYD**: Pyrin domain

**RE**: Recycling endosome

**ROS**: Reactive oxygen species

**s.c.**: Sub-cutaneous

**SEM**: Scanning electron microscopy; standard error of the mean

**siRNA**: small interfering RNA

**SR-A**: Scavenger receptor A

**TEM**: Transmission scanning electron microscopy

**Tf**: Transferrin

**TfR**: Transferrin receptor

**TGN**: Trans-golgi network

**Ti**: Titanium

**TIR**: Toll/interleukin-1 receptor

**TIRF**: Total internal reflection fluorescence

**TLR**: Toll-like receptor

**TNF**: Tumor necrosis factor

**YFP**: Yellow fluorescence protein

**WT**: Wild type

## COPYRIGHT NOTICE

Some of the work presented in this thesis can be found in the following publication:

**St. Pierre, C.A.**, Chan, M., Iwakura, Y., Ayers, D.C., Kurt-Jones, E.A., Finberg, R.W. 2010. Periprosthetic Osteolysis: Characterizing the innate immune response to titanium wear-particles. *J Orthop Res*. In press. DOI: 10.1002/jor.21149

# CHAPTER I

## Introduction

Internalization of exogenous and cell-associated products is a highly regulated process that is involved in a number of functions that are essential for the cell, including receptor recycling and signaling, cell homeostasis, antigen presentation, and protection from extracellular pathogens. The ability of cells to internalize ligand- or antibody-bound cell surface receptors and to phagocytose foreign pathogens or particles has broad therapeutic implications for the treatment of a variety of diseases and disorders. In order to generate effective treatments, it is essential to fully understand the mechanisms involved in the various internalization pathways and, in the case of phagocytosis, the subsequent immune response.

### A. INTERNALIZATION PATHWAYS

There are several internalization pathways that cells utilize to perform the important functions listed above. A brief description of what is known for each of these pathways is outlined below.

Cellular internalization pathways include pinocytosis, phagocytosis, clathrin-independent internalization, and clathrin-dependent receptor-mediated internalization. Pinocytosis, or cell drinking, refers to the internalization of small particles (i.e., those less than 200 nm in size) and is a way for cells to ingest fluids. Phagocytosis, or cell eating, refers to internalization of large particles (i.e., those greater than 200 nm in size)

and is a way for immune cells to ingest foreign pathogens, dead or dying cells, and other particulate debris (1). Clathrin-independent internalization refers to a variety of endocytosis mechanisms including caveolae-mediated, RhoA-mediated, CDC42-medited, and ARF6-mediated pathways (2) for proteins like cholera toxin subunit B (3, 4) and GPI-anchored proteins (4, 5). Most receptor-mediated endocytosis processes in the cell, however, involve associations with clathrin and clathrin-mediated internalization. Receptor-mediated internalization, also referred to as clathrin-mediated internalization, involves the binding of a protein to a particular receptor on the surface of the cell, like transferrin (Tf) and the transferrin receptor (TfR), resulting in cellular signaling, recruitment of clathrin and adaptor proteins and internalization of the cargo into the cell. Both phagocytosis and receptor-mediated internalization pathways involve the cooperation of a variety of cellular processes in order to function properly.

**Phagocytosis Pathways**

Phagocytosis is generally a receptor-mediated, actin-dependent, and clathrin-independent mechanism of entry into cells for large cargo (>200 nm) (6, 7). In mammals, phagocytosis is carried out by a specialized subset of cells termed ‘professional phagocytes’, including neutrophils, monocytes, macrophages, and dendritic cells (8). Phagocytosis serves as a defense against microorganisms, via pathogen-specific receptors or by opsonin-mediated (complement or antibody) binding. Phagocytosis also serves as a means to remove cellular and non-cellular particulate material from the extracellular space.

Phagocytosis begins with recognition of the foreign, or dangerous, particle by a phagocyte. Association of particles with the surface of phagocytic cells induces actin polymerization at the site of binding to assist in internalization (6-8). Internalized vesicles containing phagocytosed material, termed phagosomes, through association with adaptor proteins involved in the endocytosis pathway, eventually fuse with lysosomes to form phagolysosomes, which contain acidic lysosomal components, including cathepsins (8-10). Phagocytosis can occur through association with one of several different cell surface proteins, including complement receptors, Fc-receptors (FcR), scavenger receptors, and pathogen-specific receptors, like Toll-like receptors (TLRs), mannose receptors, and lectins (7, 11).

Complement-mediated phagocytosis can occur via one of the three major complement pathways in cells: the alternative pathway, the classical pathway, and the mannose binding lectin pathway. The details of each pathway have been well characterized and have been reviewed extensively (12). The major opsonins, or proteins involved in pathogen binding and recognition by macrophages, generated from these pathways include C3b, C3bi, and C4b. Several complement receptors (CR) participate in the phagocytosis of complement-opsonized particles, including CR1, CR3, and CR4. CR1 binds C3b, C4b, and C3bi, and is associated with particle binding (7). CR3 and CR4 are integrin family members that bind C3bi and are associated with particle internalization (7). Complement-mediated phagocytosis requires a secondary stimulus, such as cytokines or chemokines, in order to occur. Additionally, uptake via

complement does not lead to the release of certain inflammatory mediators, including reactive oxygen species (ROS) (7).

FcRs that are involved in phagocytosis include FcγRI, FcγRIIA (in humans), and FcγRIII (13). Binding of the Fc region of antibodies to the FcR results in receptor cross-linking and subsequent tyrosine phosphorylation of immune receptor tyrosine activation motifs (ITAMs) on the receptor itself (FcγRIIA) or on common γ subunits (FcγRI and FcγRIII (7) via src-family kinases (14). This activation leads to the recruitment and activation of Syk kinases, which are responsible for cytoskeletal rearrangement, actin assembly, and downstream transcriptional activation of inflammatory cytokines (15, 16), via participation of PI-3 kinases, rho-GTPases, protein kinase C, and motor proteins (reviewed in (7)).

There are two major scavenger receptors involved in phagocytosis, Scavenger receptor A (SR-A) and macrophage receptor with collagenous structure (MARCO). SR-A, which is expressed in most macrophage populations (17-19), binds to whole microbes, recognizing LPS and lipoteichoic acids (20) while MARCO, expressed on certain subsets of macrophages (17, 18), recognizes a variety of Gram-positive and Gram-negative bacteria (21) as well as artificial latex and $TiO_2$ (18), silica (22), and polystyrene particles (23).

Binding to TLRs and other pathogen/pattern recognition receptors like mannose receptors or lectins on the surface of immune cells represents another mechanism for phagocytosis. Each receptor recognizes a particular moiety on the surface of pathogens,

and once bound, induces intracellular signaling pathways, including internalization and the release of pro-inflammatory cytokines including IL-6, TNF, and IL-1β.

**Clathrin-dependent receptor-mediated internalization**

Receptor-mediated internalization, also commonly referred to as clathrin-mediated internalization, involves the binding of a ligand to a receptor expressed on the surface of cells. Clathrin-mediated internalization is most commonly associated with endocytosis of cell surface receptors and cell surface proteins. The functional subunit of clathrin is the triskelion, formed from the interactions of three clathrin heavy chains and three light chains that create a three-legged polymer structure (24). These triskelions then associate with each other through interactions between antiparallel proximal domains to create a hexagonal lattice coating on budding vesicles (25).

The internalization process starts with the formation of a structure known as a coated pit. Formation of the coated pit is thought to begin with the recruitment of adaptor proteins, including AP-2, to a docking site on the plasma membrane. Adaptor proteins then recruit clathrin, which self assembles into higher order triskelion structures to form a clathrin-coated pit (1, 26, 27). With the help of several other adaptor and accessory proteins, including dynamin, the clathrin-coated pit moves away from the plasma membrane, until it eventually pinches off to form a clathrin-coated vesicle (CCV) (28). Clathrin and most adaptor proteins are quickly shed from these vesicles and recycled back to the surface where they can participate in other pit formations (29, 30).

**Role of actin in clathrin-mediated endocytosis**

It has long been believed that actin plays a role in endocytosis, however it has been difficult to determine the specific requirement or function of actin in these pathways. The role of actin in clathrin-mediated endocytosis is even more controversial since different groups have demonstrated that actin is both essential (31-34) and not essential (34-36).

Several groups have provided evidence arguing for a role of actin in receptor-mediated internalization. Lamaze et al. demonstrated that treatment of perforated or intact A431 cells with actin monomer sequestering drugs, like LA, inhibited receptor-mediated endocytosis, including internalization of the TfR (31). Yarar and colleagues have shown that actin dynamics are essential for a number of stages in clathrin-mediated endocytosis, including coated-vesicle formation, invagination, and subsequent internalization (32). Several recent reports have come out linking budding yeast proteins essential for endocytosis and actin nucleation to mammalian homologues that associate with clathrin adaptors (reviewed in (33)).

Other groups have provided evidence that actin is not essential for receptor-mediated internalization. Sandvig et al. have shown that drugs that inhibit actin polymerization, like cytochalasin D, have no effect on TfR internalization in mammalian cells, but do inhibit some fluid-phase endocytosis events (35). Treatment of polarized epithelial cells with cytochalasin D inhibited endocytosis from the apical

surface with no effect of endocytosis from the basolateral surface (36), including recycling of the TfR.

Although the role of actin in clathrin-mediated internalization remains unclear, its role in other internalization pathways including phagocytosis has been verified (6-8). The question of whether actin plays a dispensable or indispensable role in clathrin-mediated internalization may depend on several variables, including the localization of membrane proteins on the plasma membrane, the type of cell, the ligand being studied, as well as the cellular growth conditions (34).

## B. ENDOSOMAL COMPARTMENTS

As described above, once internalized within a cell, the CCV quickly uncoats and the subunits, namely clathrin and adaptor proteins, are recycled to participate in new rounds of internalization (29, 30). Newly uncoated vesicles move along microtubules to fuse with other vesicles (37), and eventually move to early endosomes, where they are sorted into various compartments of the endosomal pathway based on cargo (Figure 1.1). These compartments and their associated proteins exhibit specific functions for cargo sorting, delivery, and movement within the cell. The major endocytic compartments and their functions are described in detail below.

There are four major classes of endosomal compartments in cells termed early endosomes (EE), late endosomes (LE), recycling endosomes (RE), and lysosomes. The endosomal compartments are differentially characterized by their expression of proteins of the Rab family of small GTPases (Figure 1.1). Lysosomes, on the other hand, are

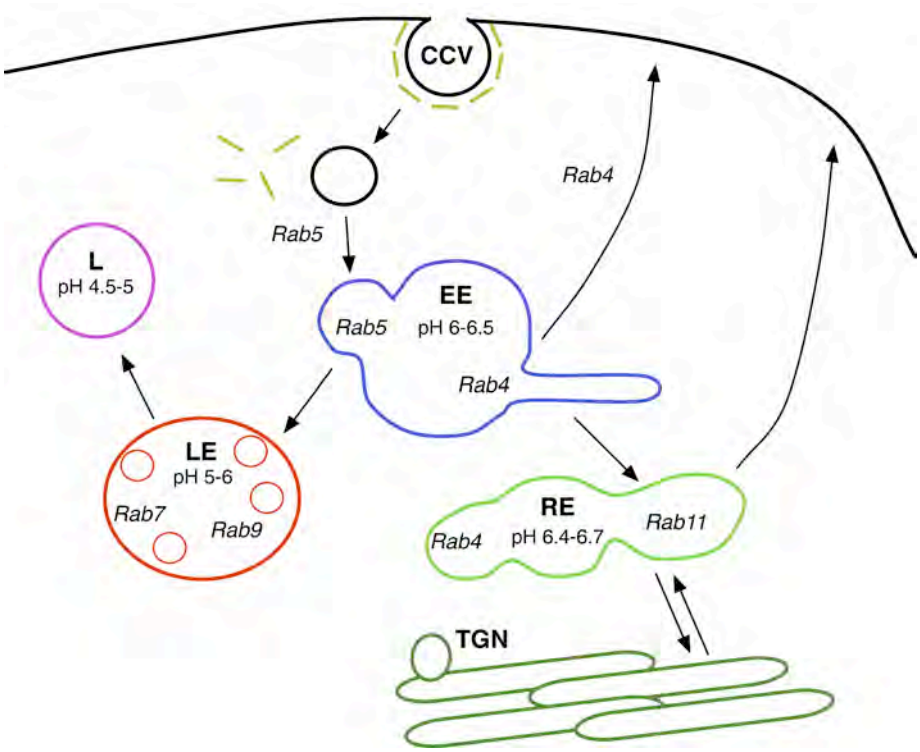


**Figure 1.1: Endocytic compartments and associated proteins.** Cargo is internalized via clathrin into clathrin-coated vesicles (CCV). CCV are delivered to early endosomes (EE) expressing Rab5 and Rab4. Rapid recycling from EE to the plasma membrane is mediated by Rab4. Slow recycling involves movement of cargo through tubular regions of EE to recycling endosomes (RE) expressing Rab11. Cargo in RE is recycled to the plasma membrane or transported to the trans-golgi network (TGN). Vesicular regions of the EE are delivered to late endosomes (LE) expressing Rab7 and Rab9. Final degradation of cargo in LE occurs following delivery to lysosomes (L).

characterized by their low pH, level of expression of specific glycoproteins including lysosome membrane glycoproteins (lgps) and lysosome-associated membrane proteins (lamps), as well as a high density on Percoll (38). In order to function properly, Rab GTPases must cycle between the active GTP-bound and inactive GDP-bound states. In the GTP-bound, active form, Rab proteins recruit specific effector proteins to the membrane to perform a variety of functions including membrane budding, fusing, docking, or movement along the cytoskeletal network (reviewed in (39, 40)).

**Early Endosomes**

The first stop for newly uncoated vesicles is the EE. Early or sorting endosomes are the crossing guards of the endosomal pathway, sorting cargo from all budding vesicles (37, 41). EE are dispersed throughout the cytoplasm and contain two morphologically different domains, tubular regions and vesicular regions (42). The tubular regions are generally 50-60 nm in diameter and up to 4 μm in length (43), while the vesicular regions range from 400-700 nm in diameter (44). Cargo can exit EE along several different pathways, including movement to RE, LE and lysosomes, or to the trans-Golgi-network (TGN). Association of cargo with the endosomal membrane is thought to mediate these initial sorting events. Receptors and other membrane proteins occupy a large surface area within the endosomes, and are therefore transported to RE through tubular regions. Soluble cargo, on the other hand, require more fluid volume, but little association with the membrane, and are therefore transported to LE through vesicular regions (1, 45).

The pH of EE, ranging from 6-6.5 (46-48), is low enough to dissociate certain ligands from receptors, such as the low density lipoprotein (LDL) and Tf, but high enough to leave receptors intact to allow for recycling back to the surface, like the low density lipoprotein receptor (LDLR) and TfR (49). EE express several Rab proteins, based on the destination of the cargo. These include Rab5, Rab4, and, to a lesser extent, Rab11.

The small GTPase Rab5 is a key regulator of early endocytosis, including movement from clathrin-coated vesicles to EE as well as fusion between early endosomal compartments (39, 50-52). Uncoated vesicles move first into Rab5-positive endosomes, which then fuse to each other and move to the early endosomal compartment. Rab5 also plays a direct role in the association and movement of EE along microtubules (53).

Rab4 is expressed in both EE and RE, and is involved in early sorting events as well as rapid recycling of membrane proteins from EE to the plasma membrane (39, 54). Rab4 localizes to both vesicular and tubular regions of the EE and requires cycling between membrane-bound and unbound forms into order to function properly (55). Rab4 is also thought to work with Rab5 to help maintain a balance in trafficking between the plasma membrane and endosomes (56). This cooperation has been proven further with the discovery that the Rab5 effector protein Rabaptin-5 also binds to Rab4 (57).

**Recycling endosomes**

REs, located in the perinuclear cytoplasm, are thought to arise from the tubular extensions of EE, as mentioned above. There are two different types of recycling pathways, rapid recycling and slow recycling. Rapid recycling directly from the EE to the plasma membrane is thought to involve initial localization with Rab4-enriched regions of the EE, followed by movement to the plasma membrane. Slow recycling involves movement to perinuclear RE (pH 6.4-6.7) located near the microtubule-organizing center (48, 58).

Rab11 is expressed in slow-recycling endosomes and perinuclear RE and regulates traffic at the TGN/RE boundary (59-61). Activation of Rab11 by GTP is necessary for the delivery of membrane proteins, including the TfR, to the plasma membrane from perinuclear RE (59, 61). Rab11 also plays a role in early endosomal compartmentalization, so that proteins can be delivered to the appropriate compartments, including REs and the TGN (62).

**Late endosomes and lysosomes**

Movement from EE to LE involves the budding and dissociation of vacuolar regions of EE into carrier vesicles (63), which travel along microtubules to the perinuclear cytoplasm (44). These carrier vesicles may contain several internal vesicles and are therefore also termed multivesicular bodies (64). LEs, defined by the accumulation of multiple carrier vesicles, are enriched for the mannose-6-phosphate receptor (MPR), Rab7, and Rab9 (65, 66).

Rab9 is expressed in and regulates trafficking within late endosomes (39, 60). Depletion of Rab9 leads to a decreased number of LE and lysosomes. Additionally, in the absence of Rab9, LE and lysosomes localize closer to the nucleus. Thus, Rab9 plays an important role in regulating LE size, number, and endosomal location (67). Rab9 is also involved in the transport of MPR from LE to the TGN and, as such, involved in lysosome biogenesis (68-70). MPR plays an important role in delivering lysosomal enzymes to and from LE and the TGN. Without Rab9, MPR does not recycle between the two compartments and lysosomal enzymes are inefficiently sorted (69).

Following trafficking to LE, cargo is delivered to lysosomes. Lysosomes function as the final degradative compartment for many cellular processes, including material internalized via endocytosis, phagocytosis (phagolysosomes), and autophagy (38). Lysosomes are characteristically very similar to LE, as both express lgps and lamps and both contain acid hydrolases. However, when compared to LE, lysosomes have a higher density on Percoll due to increasing digested material, contain more active acid hydrolases, have a lower pH (pH 4.5-5 versus pH 5-6) (6, 46, 48), no longer express MPR, and express higher levels of lgps and lamps (38, 65).

## C. RECYCLING OF THE TRANSFERRIN RECEPTOR

One of the most well-characterized internalization pathways is the recycling pathway of the TfR and its ligand Tf. Most of what we know about recycling endosomes, endosomal sorting, and receptor-mediated internalization has been derived

from studies of the TfR/Tf pathway. Brief descriptions of the receptor, ligand, and internalization pathway are given below.

The TfR is a transmembrane glycoprotein that exists as a homodimer on the surface of most cells (71). The TfR binds to the serum glycoprotein Tf to deliver iron into cells. Each receptor can bind two molecules of Tf (71), with a similar relative affinity of 7-13 x $10^{-9}$ $M^{-1}$ for either iron-bound (diferric) Tf at pH 7.0 or iron-depleted (apo) Tf at pH ~5.4 (72). Expression of the TfR is dependent on the amount of extracellular iron available, as receptor numbers are decreased when cells are grown in iron-rich media, and vice-versa (73, 74).

Tf is a serum glycoprotein that delivers iron to most body tissues (73, 75). Tf contains two iron-binding sites, which bind to iron with very high affinity at pH 7.0 and low affinity at low pH (75). When bound to two molecules of iron, diferric-Tf binds to the TfR with high affinity (72), and the complex is internalized via clathrin-mediated endocytosis. Although this process occurs constitutively, regardless of whether the receptor is bound to ligand (76), recycling rates are significantly increased when the receptor is bound to Tf or to a TfR-specific antibody, due to an increase in $Ca^{2+}$ influx (76).

Endocytosis of the TfR does not involve recruitment of adaptor proteins, but rather involves movement of the complexed receptor to already formed clathrin-coated pits, as the TfR is permanently associated with the clathrin adaptor protein, AP-2, via a cytoplasmic tyrosine-containing motif (77). This allows for rapid internalization from the cell surface. Once internalized, the complex localizes to Rab5- and Rab4-positive

EE within 2-4 min. Iron is released from the Tf/TfR complex in EE, leaving the TfR bound to iron-depleted (apo) Tf, due to its high affinity for the receptor at low pH (72). From here, the complex can directly recycle to the plasma membrane via Rab4 and the fast-recycling pathway or move to Rab11-positive RE (5-7 min) through the slow-recycling pathway (58). These REs translocate to the perinuclear cytoplasm, near the microtubule-organizing center. From there, traffic continues to the plasma membrane (10-12 min) where apo-Tf is released to bind more iron (6, 45).

## D. ANTIBODIES AS THERAPEUTICS

The use of antibodies to target specific cells or cell types has become an increasingly popular method of treatment for a variety of diseases. Targets for antibody-mediated internalization include both endogenous cell surface proteins as well as virus-associated surface proteins. In order for an antibody or antibody-conjugate to be functional, it must internalize and localize with EE, LE, and lysosomes, so that the antibody/protein complex will be degraded or, in the case of a drug-conjugate, the drug, will be released into the cytoplasm (78-80). Many studies examining the potential of an antibody to be used as a therapeutic either focus on determining whether or not an antibody will localize with LE (78, 81) or involve the use of antibodies that recognize proteins known to internalize through a degradation pathway, e.g. the epidermal growth factor receptor (EGFR).

**Antibody-mediated internalization of cellular proteins**

Studies have shown that the use of antibodies to target cellular proteins can be beneficial for the treatment of various diseases and cancers. The presence of antibodies specific for the β-amyloid peptide on the surface of neuronal cells, which can mediate internalization and degradation of the protein (80), have been shown to slow cognitive deterioration and reduce plaque burden in mice and Alzheimer's patients (82-84). Several groups have shown that antibodies against altered growth factor receptors or adhesion molecules can be utilized in targeting specific cell types or cells within a particular activation state to suppress gene expression (78, 85, 86). For example, monoclonal antibodies conjugated to cytotoxic drugs can slow development of choroidal neovascularization (CNV), the major complication associated with macular degeneration, through targeting the integrin molecule α4β3, which is highly expressed in CNV membranes (87). Additionally, antibodies conjugated to chemokines/cytokines have been shown to decrease tumor formation in a cancer model and decrease inflammation in a rheumatoid arthritis model, by targeting the EMD domain of fibronectin, which is highly expressed in tumor cells and at sites of arthritis (81, 88).

**Antibody-mediated internalization of viral proteins**

Studies have also indicated the benefit of using antibodies to treat viral infections. Virus-specific antibodies are known to modulate or neutralize viral infection and decrease virus-induced cell death (89). One potential mechanism for inhibiting viral release is to mediate the internalization of the viral glycoproteins expressed on the

surface of infected cells. It is possible that this internalization renders virus within a cell unable to appropriately bud from an infected cell, leading to a decrease in viral titers and an ineffective viral infection (90, 91). Additionally, it has been shown that antibody-mediated internalization of viral proteins could be used to target antiviral therapeutics to infected cells only. For example, Song et al. reported that an antibody against the HIV glycoprotein can specifically deliver functional siRNA only to infected cells, leading to a decrease in viral protein expression (79). Others have shown that antibodies directed against the hepatitis B surface antigen can effectively deliver antiviral siRNAs to infected cells both *in vitro* and *in vivo* leading to decreased viral gene expression (92).

## E. IMMUNE RESPONSE TO INTERNALIZED MATERIAL

Internalization of cargo via the pathways listed above usually represents a single event with no further cellular consequences other than those directly associated with the event, such as iron delivery via TfR/Tf complexes. However, certain internalization events, especially those involving the phagocytosis pathway, can also activate the host immune system, depending on the cargo and the associated cell. As mentioned above, neutrophils, monocytes, and macrophages are the major cell types involved in phagocytosis. Their ability to recognize and respond appropriately to phagocytosed material is necessary for proper maintenance and activation of the innate immune response. Aberrations in this response can cause debilitating disease and autoimmune disorders.

**The role of macrophages in immune recognition**

Neutrophils and monocytes, generated in the bone marrow, enter the circulation in response to hematopoietic and chemotactic factors. After up-regulation of adhesion molecules on endothelial venules (93), these cells can rapidly migrate to sites of tissue damage (94). Neutrophils are generally short-lived, around 1 to 2 days, and are considered 'first-responders', as they arrive to sites of inflammation hours before monocytes (93). Because of this rapid response, neutrophils represent the hallmark of an acute inflammatory response. Monocytes, which in the presence of various chemokines and cytokines differentiate into macrophages, can remain in the circulation for days, weeks, even years (8), representing a more robust, sustained, inflammatory response (94).

Innate immune cells, especially monocytes and macrophages, express several different types of receptors in order to appropriately respond to foreign material. These include Fc- and complement-receptors as well as receptors specific for particle- or pathogen-associated molecular patterns (PAMPs). These receptors, referred to as pattern recognition receptors (PRRs), include TLRs, which are expressed on both the cell surface and endosomal membranes, and NLRs (nucleotide-binding domain, leucine-rich repeat containing receptors – formally termed NOD-like receptors), which are expressed in the cytosol. TLRs are transmembrane proteins that contain an extracellular leucine-rich repeat (LRR) domain, and an intracellular Toll/interleukin-1 receptor (TIR) domain (95). TLRs recognize a wide variety of PAMPs including LPS,

peptidoglycans, flagellin, and microbial/viral RNA or DNA (96). Recognition of PAMPs by TLRs occurs through the C-terminal LRR domains (95), which induces recruitment of adaptor molecules to intracellular TIR domains, leading to downstream signaling events including activation of MAP kinases, interferon-responsive factors (IRFs), and the NF-κB response (97).

**NLR proteins and inflammasomes**

Structurally, NLRs usually contain an N-terminal effector domain [pyrin domain (PYD), caspase recruitment domain (CARD), or baculovirus inhibitor of apoptosis (BIR) domain], a central nucleotide-binding domain [domain present in neuronal apoptosis inhibitory protein (NAIP), CIITA, HET-E, and TP1 (NACHT)], and a C-terminal receptor domain composed of LRRs (98). NLRs, like TLRs, recognize molecular patterns through their LRR domains (99). NLRs normally exist in the cytosol in an inactive conformation. The LRRs fold back onto the NACHT domain, inhibiting oligomerization of the NACHT domains. Once NLRs are exposed to ligands through interaction with LRRs, a conformational change occurs, exposing the NACHT domain and triggering oligomerization, which is required for activation (98). Following oligomerization, NLRs recruit caspases, adaptor proteins, or kinases through homotypic interactions with the effector domain and proteins expressing a CARD, PYD, or BIR domain, depending on the NLR (98). Through oligomerization and adaptor molecule recruitment, these proteins have been observed to form large molecular complexes in the cytosol, termed inflammasomes (100). The NLR family can be divided into two

major sub-families, the CARD-containing NODs and PYD-containing NLRPs (formally termed NALPs). To date, there are currently 14 known human NLRPs (101) which have been shown to recognize a variety of molecular ligands such as MDP, anthrax lethal toxin, flagellin, ATP, and Nigericin, as well as various live pathogens including *Candida albicans*, *Staphylococcus aureus*, *Salmonella typhimurium*, *Legionella pneumophila*, and *Listeria monocytogenes* (102, 103).

**NLRP3 recognition of particulate material**

The NLRP3 inflammasome has been shown to be involved in the inflammatory response to particulates including silica, asbestos, monosodium urate (MSU) crystals, and cobalt/chromium metal alloys (104-107). The process leading to NLRP3 activation begins with internalization of the particles by phagocytosis. Phagosomes containing internalized particles generally fuse with lysosomes, creating phagolysosomes.

Following uptake, the actual trigger for NLRP3 activation and oligomerization is unknown, however it is unlikely to be a direct ligand interaction, due to the broad range of known stimuli. There are two major models for NLRP3 activation; the first involves interaction with ROS. ROS are highly reactive free radicals that are produced from a variety of cellular processes including oxygen synthesis, NADPH oxidase activity and innate immune activation (108). In order to regulate the amount of ROS in cells, which can induce cell damage at high levels, enzymes with anti-oxidant activities, such as thioredoxin, will neutralize ROS (108). Studies have indicated that a

thioredoxin interacting protein, TXNIP, can directly bind to NLRP3 in the presence of ROS, leading to activation and formation of the inflammasome complex (109).

The alternative model is that NLRP3 senses changes in membrane integrity and membrane disruption (102). It is thought that uptake of a large amount of particles induces phagolysosomal destabilization and eventually rupture of the lysosomal compartment, leading to release of lysosomal contents, including cathepsins, into the cytosol (104, 110). In this model, NLRP3 is activated following an interaction with cathepsins, leading to formation of the inflammasome complex (111).

As mentioned previously, activation of the NLRP3 inflammasome (Figure 1.2) involves a conformational change in NLRP3 into its active form, which then associates with the adaptor protein ASC (112) through PYD interactions. This complex leads to the recruitment of pro-caspase-1 through CARD interactions (98, 99, 113). Pro-caspase-1 is cleaved into its active form, caspase-1. Active caspase-1 cleaves pro-IL-1β into its active, secreted form, IL-1β. Secreted IL-1β can bind to and activate the IL-1 receptor (IL-1R), leading to additional pro-inflammatory signaling, including NF-κB activation, pro-inflammatory cytokine production, and neutrophil recruitment. Polymorphisms in NLRP3 are linked to a spectrum of auto-inflammatory diseases with unchecked IL-1 production, termed cryopyrinopathies (114). These diseases, which include Muckle-Wells syndrome, familial cold autoinflammatory syndrome, and chronic infantile neurologic cutaneous articular syndrome, usually present with periodic episodes of fever and neutrophil-mediated inflammation, sometimes causing arthritis and joint destruction (115).

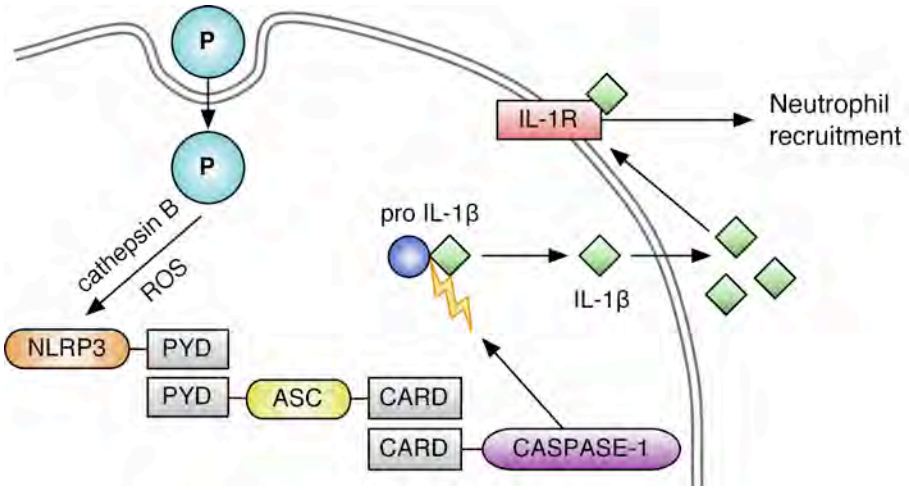


**Figure 1.2: NLRP3 activation and inflammasome complex formation.** Internalization of a particle (P) induces the production of reactive oxygen species (ROS) and cathepsin B release, which activate NLRP3. Active NLRP3 forms a complex with ASC through pyrin domain (PYD) interactions. ASC then activates and recruits caspase-1 through caspase recruitment domain (CARD) interactions. Active caspase-1 cleaves pro-IL-1β into active, secreted IL-1β, which can bind to and activate its receptor, IL-1R, causing an acute inflammatory response and neutrophil recruitment.

**Role of IL-1 in immune cell activation**

IL-1 is a multifunctional cytokine. It affects most cell types and also influences the expression and production of other cytokines. There are two major forms of IL-1, IL-1α and IL-1β. Both forms are produced as a precursor (pro) form, without a signal peptide (116). Pro-IL-1α is fully active, and is usually found dispersed throughout the cytoplasm of cells. The reverse is true for pro-IL-1β, which is inactive until cleaved by caspase-1 (116). Although IL-1α can be found outside of cells in regions of high inflammation, functions for IL-1α are mainly intracellular. For example, following stimulation with cytokines and TLR ligands, intracellular pro-IL-1α translocates to the nucleus, where it participates in activation of NF-κB and AP-1 and induces the synthesis of pro-inflammatory cytokines, including IL-6 and more IL-1α (116-118).

Gene expression and generation of mature, secreted IL-1β is much more tightly regulated than IL-1α, as its functions are much more broad and, likely, systemic. Gene expression regulation includes specific promoter binding sites, transcriptional repressors, and mRNA stabilizers (116). Once synthesized, further regulatory steps are taken to ensure appropriate control of cleavage to the active, secreted form. *In vitro*, two signals are required for optimal production and cleavage of pro-IL-1β into secreted IL-1β (102, 119, 120). The first signal, which up-regulates pro-IL-1β, can be achieved through NF-κB activation by PRR interactions. The most common first signal used *in vitro* is bacterial LPS, which is recognized by TLR4. The second signal requires caspase-1 cleavage and activation through NLRP-inflammasome induction. In order for

caspase-1 to cleave pro-IL-1β, it must first be activated through self-cleavage of pro-caspase-1 (121), introducing another regulatory step.

Both IL-1α and IL-1β can be secreted by a number of cells including macrophages, monocytes, neutrophils, lymphocytes, and epithelial cells (122). IL-1α and IL-1β both signal through the type 1 IL-1R. The IL-1R is a high affinity, transmembrane receptor expressed on a variety of cells, including lymphocytes and thymocytes (116, 122). The IL-1R consists of an extracellular ligand-binding domain, organized similarly to members of the Ig-superfamily, and a cytoplasmic region containing a TIR domain (122). Signaling through the IL-1R requires many of the same adaptor proteins associated with TLR signaling, including MyD88, IRAK, and TRAF6, which leads to NF-κB activation and inflammatory cytokine production (122).

As mentioned above, IL-1 signaling and activation plays a major role in a variety of pathways. Two major functions of IL-1β include osteoclast activation (123-125) and neutrophil recruitment (104, 126-128). Studies have found that both bone resorption, mediated by osteoclasts, and neutrophil recruitment can be inhibited through the use of the IL-1R antagonist, IL-1Ra. IL-1Ra is produced as two major forms, soluble (sIL-1Ra) and intracellular (icIL-1Ra), following cellular stimulation (116). sIL-1Ra competes with both IL-1α and IL-1β for binding to the IL-1R.

It is thought that since IL-1Ra has only one functional binding site for the receptor, while IL-1α and IL-1β have two, IL-1Ra can bind to the IL-1R without causing downstream signaling and activation (129). Commercially available sIL-1Ra, known as Anakinra™, has proven to be highly effective at improving joint function in

rheumatoid arthritis patients (130-132). Additionally, treatment of animals with sIL-1Ra has been highly effective at reducing the severity of inflammation in a variety of inflammation models (105, 133).

## F. THESIS OBJECTIVES

As described above, endocytosis and phagocytosis pathways are important for many cellular functions. Both pathways involve internalization of cargo, followed by movement through portions of the endocytic compartments. These pathways differ, however, in the downstream implications of internalization. Endocytosis pathways (or receptor-mediated internalization in non-phagocytic cells) are utilized for cell survival, receptor recycling, and other maintenance functions, whereas phagocytosis pathways (or internalization of cargo by professional phagocytes) are utilized for the protection and defense against non-self, including pathogens and particulate material. Understanding the mechanisms surrounding these two essential functions of cells will aid in the development of targeted therapeutics for a variety of applications, including viral inactivation and clearance, pathogen removal, anti-cancer therapies, and many more.

In this thesis, the roles of endocytosis and phagocytosis pathways in a variety of clinically relevant scenarios will be examined: antibody-mediated internalization of cell-surface proteins, titanium wear-particle uptake in failed joint replacements, and immune responses to polymeric microparticle uptake for drug delivery or adjuvant use. The specific aims of each are explained below:

**Project 1. Divergence of surface proteins into a degradation pathway by antibody binding.**

Through understanding receptor-mediated endocytosis pathways and characterizing the endosomal compartments within cells, the ability to use antibodies to mediate the internalization of surface proteins has become an increasingly popular therapeutic avenue. However, it is still unclear as to how antibodies direct the internalization of proteins into a particular endosomal pathway. One major question remains: Does the surface protein or the ligand specify the internalization pathway? In order to answer this, work described herein will aim to determine whether an antibody can alter the internalization pathway of the TfR, which internalizes through recycling endosomes when bound to its ligand, Tf. Work will also examine whether antibody-mediated internalization can be utilized to target rabies virus infected cells through the use of a viral glycoprotein-specific antibody and cells expressing the rabies glycoprotein on the surface.

**Project 2. Characterizing the innate immune response to titanium wear-particles.**

Osteolysis of bone surrounding joint replacements is a major clinical problem affecting approximately 10% of all joint replacement patients (134, 135). Studies have shown that small wear particles, generated through normal use, become dislodged and released into the tissues surrounding the joint, where they can be taken up by monocytes and macrophages (135, 136). These cells become activated, releasing various pro-

inflammatory cytokines including IL-1β, suggesting a role for the NLRP3 inflammasome in inflammation and subsequent bone loss. Titanium remains an important alloy used in many hip and knee replacements and high levels of titanium wear-particles are often found in tissues (137, 138). The NLRP3 response to titanium wear particles has not previously been characterized. The work described here will aim to identify if the NLRP3 inflammasome plays a role in the inflammatory response to phagocytosed titanium wear particles.

**Project 3. Examining the role of surface curvature in innate immune activation by synthetic microparticles.**

Polymeric microparticles have been widely investigated as platforms for drug delivery, adjuvants, and as imaging contrast agents. Certain types of particles are phagocytosed by macrophages more efficiently than others (139). Additionally, different particles can induce significant inflammation or may be relatively well tolerated. However, the physical and chemical characteristics that determine the uptake and subsequent immune response to different particles remain undefined. In order to utilize microparticle technology to its full potential, it is essential to understand the ability of such particles to either activate or inhibit an immune response following uptake. Work described in this section will aim to define the role of microparticle shape in activating the immune response, which has important implications for engineering of delivery vehicles and implant materials.

# CHAPTER II

## Divergence of surface proteins into a degradation pathway by antibody binding

### INTRODUCTION

The use of antibodies to target specific cells or cell types has become an increasingly desirable method of treatment for a variety of diseases. The presence of antibodies specific for the β-amyloid peptide on the surface of neuronal cells, which can mediate internalization and degradation of the protein (80), have been shown to slow cognitive deterioration and reduce plaque burden in mice and Alzheimer's patients (82-84). Antibodies against altered growth factor receptors or adhesion molecules have also been utilized in targeting specific cell types or cells within a particular activation state to suppress gene expression in cancerous tissues (78, 85, 86). In order for an antibody to efficiently promote the internalization and subsequent degradation of target surface proteins, it must be delivered to a low pH, late endosomal or lysosomal compartment associated with the degradation pathway (78-80). Due to the broad-range of cell surface proteins that have been successfully utilized for antibody-based internalization or delivery, we hypothesized that the internalization pathway observed when an antibody is bound to a cell surface protein may remain the same, regardless of the natural internalization pathway of the membrane protein to which the antibody is specific. In order to examine this, we analyzed the internalization of an endogenous cell surface protein, the transferrin receptor, when bound to an antibody (αCD71) and compared this

to the well-known, recycling pathway observed when the receptor is bound to its ligand, transferrin.

Antibody-mediated delivery has also been exploited to target virus-infected cells and deliver antiviral agents, while sparing uninfected cells, using cell surface-expressed viral proteins (79, 92). It is known that glycoprotein-specific antibodies can mediate internalization of viral glycoproteins (89, 140-142), and studies have suggested that the ability of antibodies to inhibit viral release from infected cells is partially due to the fact that it efficiently binds to and internalizes the envelope protein to which it is specific (89, 90). This mechanism of inhibition has been shown to be effective with influenza virus-infected cells and antibodies specific for the virus envelope protein, neuraminidase (91). To examine whether antibodies can be utilized to mediate the internalization of the rabies virus glycoprotein (G), we characterized the internalization of a rabies G-specific antibody, termed ARG1, in cells expressing rabies G on the surface. To define whether the antibody-bound glycoprotein would be delivered to a degradative pathway, we analyzed its co-localization with known markers of the degradative pathway, including the Rab GTPase Rab9 and low pH lysosomes.

We find that transferrin bound to the transferrin receptor and ARG1 bound to rabies G follow distinctly different endocytic pathways. However, when an antibody is used to target the transferrin receptor, it is diverted to the pathway followed by the antibody-bound rabies G. Thus, we theorize that antibody binding can overcome the endosomal sorting signals inherent to cell surface proteins and mediate their delivery to a generalized antibody-mediated degradative pathway.

## B. MATERIALS AND METHODS

### Cells and cell culture:

MNA cells (generous gift of Massachusetts Biologic Laboratories) and HEK293T cells (ATCC) were grown in complete medium (Dulbecco's Modified Eagle's Medium (DMEM) supplemented with 10% fetal bovine serum and 1% penicillin-streptomycin, 1% L-glutamine, and 1% sodium pyruvate) at 37˚C with 10% $CO_2$. For antibody binding and localization experiments, 60-80% confluent cells were transfected with 1 μg of Rabies G-, clathrin-GFP-, or Rab-XFP-expressing plasmids using GeneJuice reagent (Novagen) according to the manufacturer's protocol. Cells were imaged 24 h after transfection.

### Plasmids:

The Rabies G glycoprotein expression plasmid, a generous gift from Massachusetts Biologic Laboratories, has been previously characterized (143). Fluorescently tagged Rab4, Rab9, and Rab11 expression plasmids were provided by Eicke Latz (University of Massachusetts, Worcester, MA). To generate dominant negative Rab5a (S34N), site-directed mutagenesis was performed on a GFP-tagged Rab5a expression plasmid using a Phusion site-directed mutagenesis kit (Finnzymes).

### Antibodies and reagents:

ARG1 antibody (gift from Massachusetts Biologic Laboratories) was purified from hybridomas generated from rabies vaccine-immunized HuMAb (Medarex) mice, as described previously (143). Mouse anti human CD71 (αCD71) antibody was obtained from BD Biosciences. Antibodies were directly labeled with Alexa Fluor 647 (for confocal studies) or Alexa Fluor 568 (for TIRF studies) using Alexa Fluor protein-labeling kits (Molecular Probes, Invitrogen). Fluorescent human Tf and LysoTracker Green DND-26 were obtained from Molecular Probes (Invitrogen). LA, used at a concentration of 1.25 μM for inhibition studies, was purchased from Sigma.

**Flow Cytometric Analysis:**

Cells were grown to subconfluency on 6-well dishes (Falcon) in complete medium. Cells were resuspended in FACS buffer (PBS containing 1% BSA and 0.01% sodium azide) and surface stained with indicated antibodies for 1 hour at 4˚C. When necessary, secondary anti-human IgG-APC (Invitrogen) was added to cells for 1 hour at 4˚C in FACS buffer. Following staining, cells were washed with PBS and analyzed on a LSRII (BD Biosciences). Data were acquired by DIVA (BD Biosciences) and were analyzed with FlowJo 8.8.6 software (Tree Star Inc.).

**Confocal Microscopy:**

Cells were cultured on glass-bottom 35-mm tissue-culture dishes (MatTek) in complete medium. Images were taken on a Leica SP2 AOBS confocal laser-scanning microscope with a 63x objective, using Leica Confocal Software. Multicolor images were acquired

by sequential scanning with only one laser active per scan to avoid cross-excitation. Overall brightness and contrast of images were optimized using Adobe Photoshop CS3.

**TIRF Microscopy:**

Cells were cultured on 25-mm coverslips (Thomas Scientific, No. 1.5) in complete medium. Cells were transferred from complete medium to KRH (125 mM NaCl, 5 mM KCl, 1.3 mM $CaCl_2$, 1.2 mM $MgSO_4$, 25 mM HEPES pH 7.4, 2 mM sodium pyruvate, and 0.5% BSA (bovine serum albumin)) just prior to imaging, at 35°C. Two Coherent Innova 70C lasers were used. Argon ion and argon-krypton ion lasers were used to produce the 488 and 568 nm light, respectively. The combined beams were coupled into a single mode fiber using a KineFLEX fiber coupler manufactured by Point Source (Hamble, UK). A modified Olympus IX81 inverted microscope, a modified Olympus TIRF fiber illuminator and an Olympus Plan APO 60x objective with a numerical aperture (NA) of 1.45 were used. TIRF illumination was introduced through the edge of the objective at an angle set between 65° and 68° giving a penetration depth of 90-121 nm at 488 nm and 105-141 nm at 568 nm. Light was collimated through the objective and a layer of immersion oil onto the coverslip. The quality of the collimation was set halfway between the best for 488 nm and 568 nm. Light from the fluorophores was collected and relayed onto a 640x448 pixel CCD camera developed with Lincoln Labs (MIT). A Physik Instruments pifoc was used for fine focus control. The entire microscope was contained in a heated chamber held at 35°C. Imaging hardware and software were previously described (144).

**Co-localization analysis:**

The total number and percent of co-localized pixels per image was calculated as described previously (144, 145). Briefly, single fluorophore raw images were corrected by subtracting the background fluorescence outside the cell. Next, regions of potential co-localization were cropped and saved as new files for analysis. From this, the intensity of all positive-valued pixels was set to one and all other pixels to zero to generate a binary masking image. Co-localized pixels were identified from the overlap of the masked images of each fluorophore. Non-specific (background) co-localization was defined as that seen when pixel-rich regions were rotated 180 degrees relative to each other (flipped images).

**Statistical Analysis:**

A two-way ANOVA followed by Bonferroni's correction for post-test comparisons was used to determine statistical significance. Values of $p < 0.05$ were considered significant. Statistics were performed using GraphPad (Prism v5.0a) software.

## C. RESULTS

### Internalization and endosomal localization of the transferrin receptor/transferrin complex

It has been suggested that in order for a therapeutic antibody to mediate degradation of its target protein or to specifically deliver compounds into cells, the

internalization pathway must occur through receptor-mediated endocytosis, including localization with clathrin, early endosomes, late endosomes and/or lysosomes, associated with the degradation pathway (78-80).

We examined the internalization pathway of an endogenous cell surface protein, the transferrin receptor (TfR), bound to an antibody or to its ligand, transferrin (Tf). We first verified the natural internalization pathway of the TfR in HEK cells. TfR bound to Tf is known to internalize via clathrin-coated vesicles almost exclusively through a recycling pathway (58, 146, 147). To examine localization with clathrin, fluorescent Tf was added to HEK cells transfected with clathrin-GFP. Tf localization to clathrin was examined using total internal reflection fluorescence (TIRF) microscopy, an imaging technique in which fluorophores residing within approximately 100-300 nm from the plasma membrane can be selectively excited (145, 148, 149). In order to determine localization, we examined the total number and the percent of Tf and clathrin co-localized pixels over a 20 min time course. As expected, Tf localized with clathrin very rapidly after addition to cells, consistent with published findings (144) (Figure 2.1a). TIRF analysis revealed a mean (± S.D.) of 220.5 (± 94.7) total and 31.21 (± 11.89) percent Tf co-localized pixels, respectively. This was higher than background co-localization (flipped images), which exhibited a mean (± S.D.) of 20.88 (± 23.64) total and 2.692 (± 2.4) percent co-localized pixels. Background co-localization was calculated when the images (Tf and clathrin) were flipped 180 degrees relative to each other.

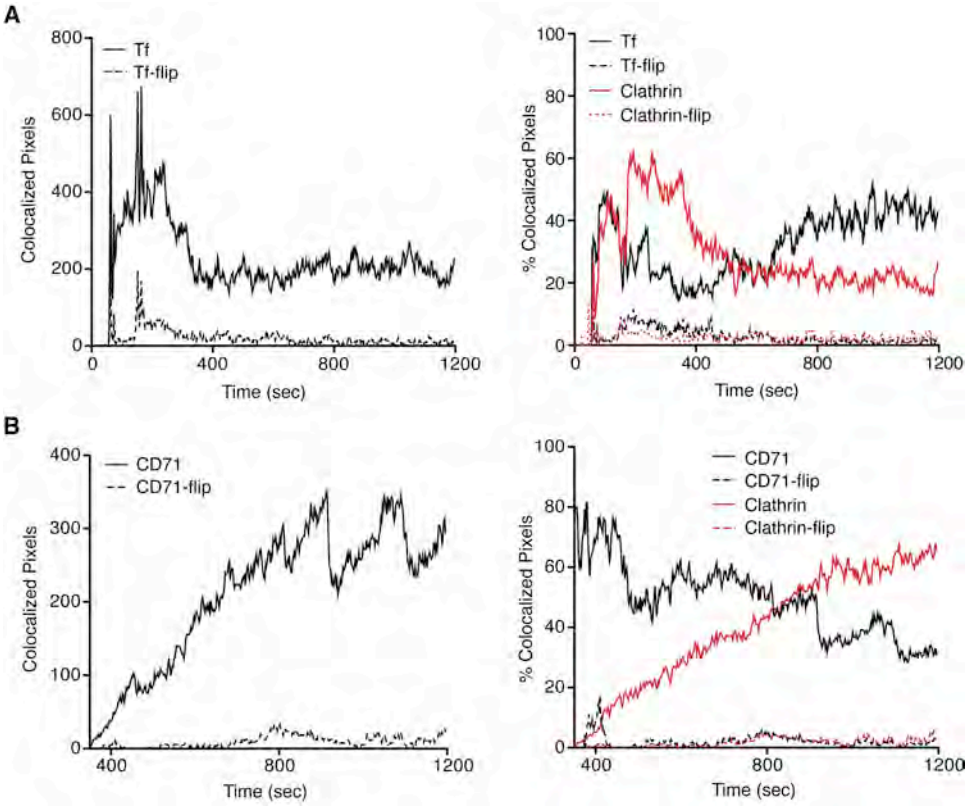


**Figure 2.1: Ligand and antibody-mediated internalization of the TfR localizes with clathrin.** (A, B) HEK cells were transfected with clathrin-GFP followed by incubation with either transferrin (Tf, A) or antibody (αCD71, B). Graphs show the total number (left) or percent (right) of co-localized pixels from addition to cells (T = 0 or 400) to 20 min following addition (T = 1200). Images on the left show the total number of Tf (A) or αCD71 (B) pixels that are co-localized with clathrin. Images on the right show the percent of Tf (A) or αCD71 (B) pixels co-localized with clathrin as well as the percent of clathrin pixels co-localized with either Tf (A) or αCD71 (B). Background co-localization, flipped images, were generated by rotating red and green pictures 180 degrees relative to each other. Images were taken using TIRF microscopy. Data are representative of three separate experiments.

The endosomal internalization pathway consists of various endosomal compartments that are differentially characterized by their expression of proteins of the Rab family of small GTPases, including Rab4, Rab5a, Rab9, and Rab11. Rab4 is expressed in early endosomes and recycling endosomes, and is thought to play a role in early sorting events (39, 60). Rab5a is a key regulator of early endocytosis, including movement from clathrin-coated vesicles to early endosomes as well as fusion between early endosomal compartments (39, 50-52). Rab9 is expressed in and regulates trafficking within late endosomes (39, 60). Rab11 is expressed in recycling endosomes and regulates traffic at the trans-golgi network/recycling endosome boundary (59, 60). To examine endosomal localization of Tf-bound TfR, HEK cells were transfected with Rab4-GFP, Rab5a-GFP, Rab9-YFP, or Rab11-GFP expressing plasmids and imaged using confocal microscopy. As expected, when bound to fluorescent Tf, internalized TfR localized with the early endosomal markers Rab4-GFP (Figure 2.2a) and Rab5a-GFP (Figure 2.2b) and the recycling endosomal marker Rab11-GFP (Figure 2.3a) at all time points tested, but not with the late endosomal marker, Rab9-YFP (Figure 2.3b). This data verifies that, in our system, the TfR/Tf complex internalizes through a recycling endosomal pathway.

**Endosomal localization of the transferrin receptor/antibody complex**

We next examined whether or not the internalization of the TfR to recycling endosomes would be affected if the receptor were bound to an antibody instead of Tf. To mimic an antibody-based therapeutic scenario, we used an antibody specific for the

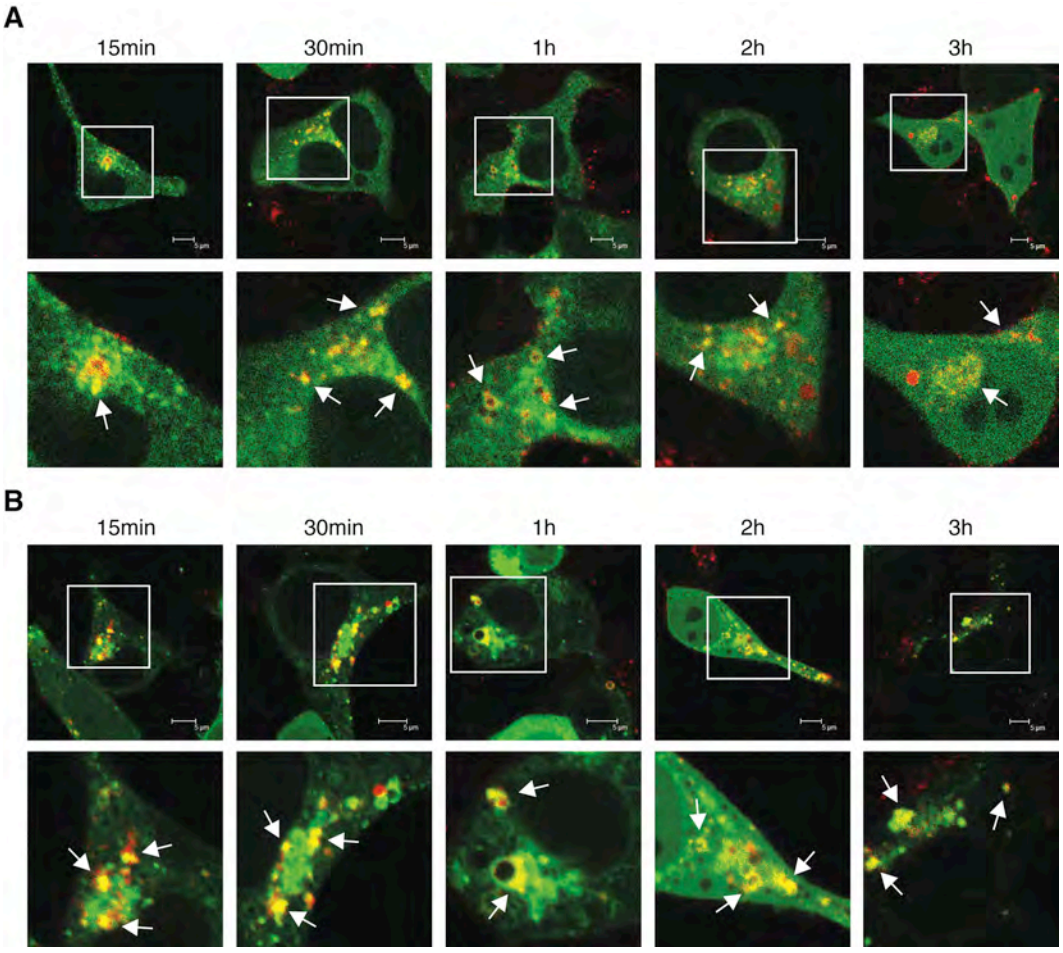


**Figure 2.2: Ligand-mediated transferrin receptor internalization involves early endosomes.** HEK cells were transfected with Rab4-GFP (A) or Rab5-GFP (B) and incubated with Tf (red) for given time points in complete medium. Top panels display the original image. Bottom panels display a magnified region of interest (boxed areas in top panels). Data are representative of three separate experiments. Arrows indicate regions of co-localization. Scale bar: 5 μm.

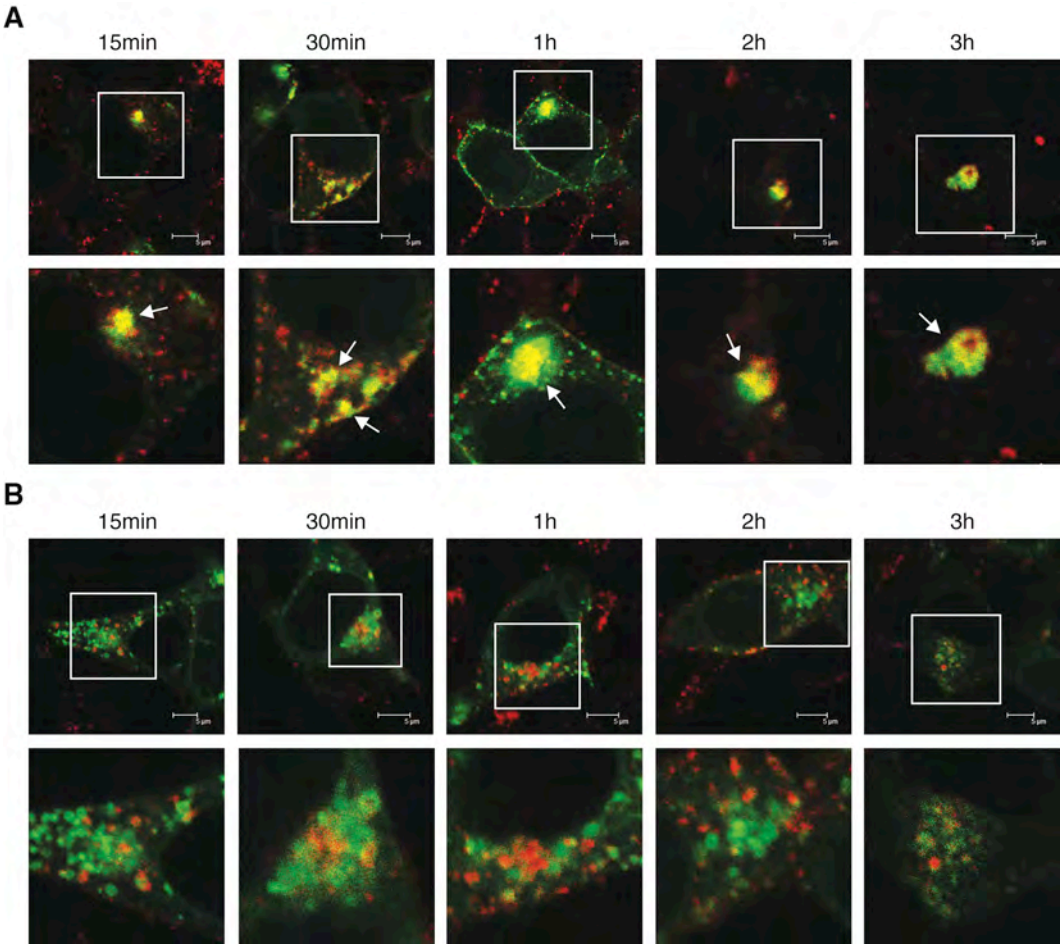


**Figure 2.3: Ligand-mediated transferrin receptor internalization does not involve late endosomes.** HEK cells were transfected with Rab11-GFP (A) or Rab9-YFP (B) and incubated with Tf (red) for given time points in complete medium. Top panels display the original image. Bottom panels display a magnified region of interest (boxed areas in top panels). Data are representative of three separate experiments. Arrows indicate regions of co-localization. Scale bar: 5 μm.

exofacial domain of the transferrin receptor protein, αCD71. As described above, HEK cells were transfected with Rab4-GFP, Rab5a-GFP, Rab9-YFP, or Rab11-GFP. Surprisingly, when bound to fluorescent αCD71, the TfR/αCD71 complex localized with all endosomal markers, including the late endosomal marker, Rab9-YFP (Figures 2.4 and 2.5), which was not seen in the natural TfR/Tf internalization pathway. Internalized antibody also localized with clathrin, similar to that seen with the TfR/Tf complex (Figure 2.1b).

To quantify the apparent shift in trafficking to include late endosomes, the total number of co-localized pixels between the TfR/Tf complex or the TfR/αCD71 complex and Rab9-YFP were compared. The number of co-localized pixels between the TfR/Tf complex and Rab9 were at levels similar to background (flipped images) at all time points tested, ranging from a mean (± S.D.) of 49.33 (± 17.93) to 116 (± 21.22) total and 9.84 (± 1.48) to 13.93 (± 1.83) percent co-localized pixels. Comparatively, the number of co-localized pixels between the TfR/αCD71 complex and Rab9 were significantly higher ($p \leq 0.01$) than background at all time points, ranging from a mean (± S.D.) of 200.5 (± 34.79) to 422.67 (± 99.86) total and 19.22 (± 3.22) to 24.98 (± 2.35) percent co-localized pixels (Figure 2.5b). These results indicate that, when bound to an antibody, the internalization pathway of the TfR can shift from an exclusively recycling endosomal pathway to include localization with late endosomes.

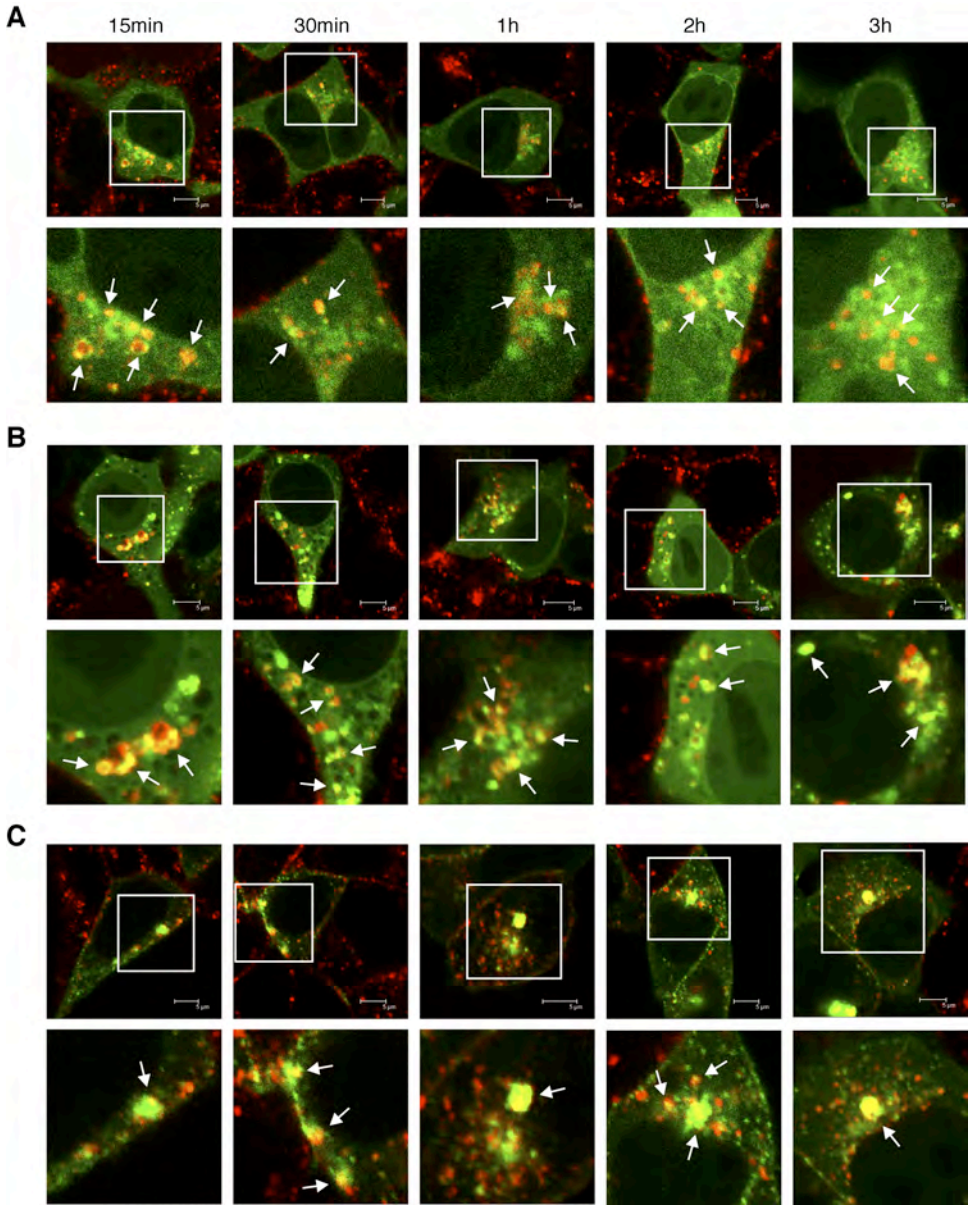


**Figure 2.4: Antibody-mediated transferrin receptor early and recycling endosomal localization is similar to that of the natural pathway.** HEK cells were transfected with Rab4-GFP (A), Rab5a-GFP (B), or Rab11-GFP (C) and incubated with αCD71 (red) for given time points in complete medium. Top panels display the original image. Bottom panels display a magnified region of interest (boxed areas in top panels). Arrows indicate regions of co-localization. Data are representative of three separate experiments. Scale bar: 5 μm.

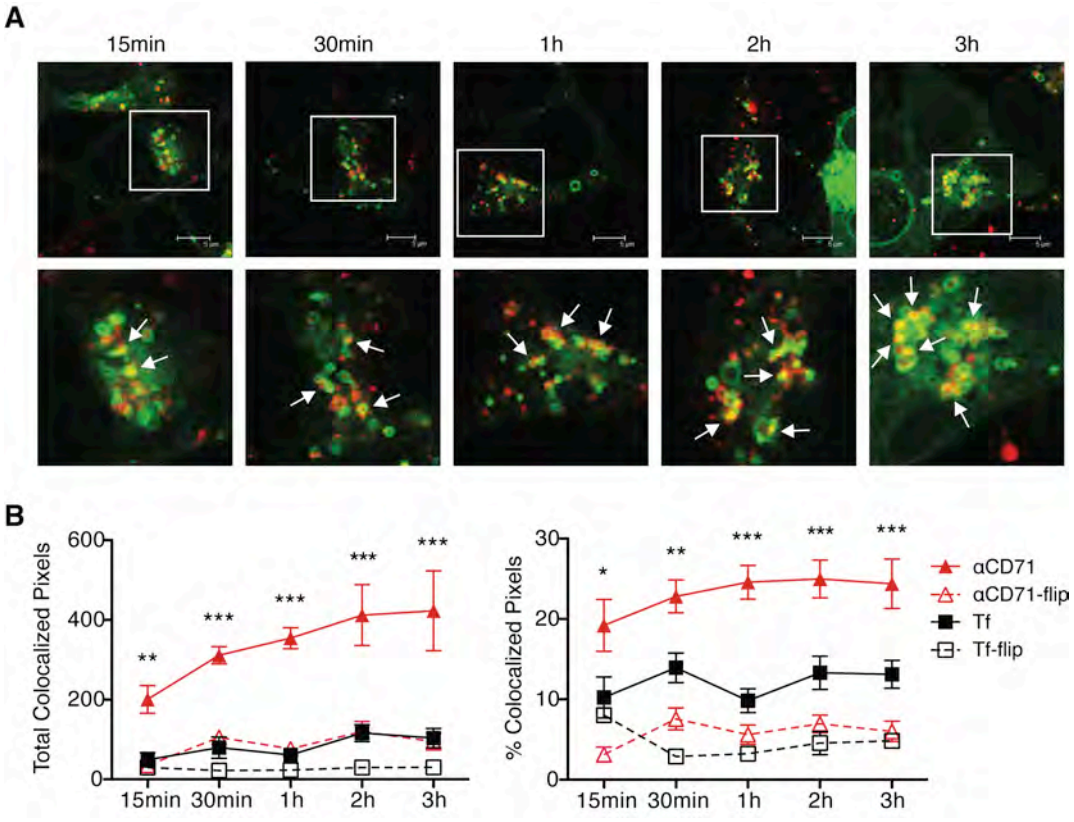


**Figure 2.5: Antibody-mediated transferrin receptor internalization includes movement though late endosomes.** A) HEK cells were transfected with Rab9-YFP (green) and incubated with αCD71 (red) for given time points in complete medium. Top panels display the original image. Bottom panels display a magnified region of interest (boxed areas in top panels). Arrows indicate regions of co-localization. Scale bar: 5 μm. B) Analysis of total and percent of Rab9/Tf versus Rab9/αCD71 co-localized pixels (n ≥ 5 per time point). Background co-localization (flipped images) was generated by rotating red and green pictures 180 degrees relative to each other. Data are representative of three separate experiments. Graphs show mean ± s.e.m. Significance values are shown relative to Rab9/Tf levels. P-values are shown as *** ≤ 0.0001; ** < 0.01; * <0.05.

**Internalization of the ARG1/rabies G complex**

Since antibody-mediated delivery has also been utilized in the treatment of viral infections, we examined the internalization and fate of a viral cell surface glycoprotein, rabies G, by using a fluorescent rabies-specific antibody, ARG1, which specifically binds to and internalizes in mouse neuroblastoma cells expressing rabies G (MNAG) on the surface (Figure 2.6). In order to generate a potential antibody-based therapeutic, it is essential to fully understand the internalization pathway of the target protein. Although the natural endocytic pathway of the TfR has been well characterized, the internalization of the rabies G glycoprotein has not been studied. We therefore performed a more in-depth analysis of the endocytic pathway of ARG1-bound rabies G, beginning with its association with clathrin.

To examine the role of clathrin in fluorescent ARG1 internalization, MNAG cells were transfected with GFP-clathrin and ARG1 localization was assessed by TIRF microscopy. We found that internalized ARG1 quickly localizes with clathrin-GFP after addition to cells and remains co-localized through 20 min (Figure 2.7a). Total co-localized ARG1 pixels ranged from 220-480 pixels and the percent of ARG1 pixels co-localized with clathrin ranged from 33-56 percent. This was significantly higher than background localization levels (flipped images), which ranged from 90-270 total and 18-34 percent co-localized pixels. We also examined ARG1 localization to clathrin at later time points using confocal microscopy. Similar to TIRF results, internalized antibody localized with clathrin up to 30 min after addition to cells (Figure 2.7b, arrows) with no localization by 1 hour. Taken together, these data suggest that the

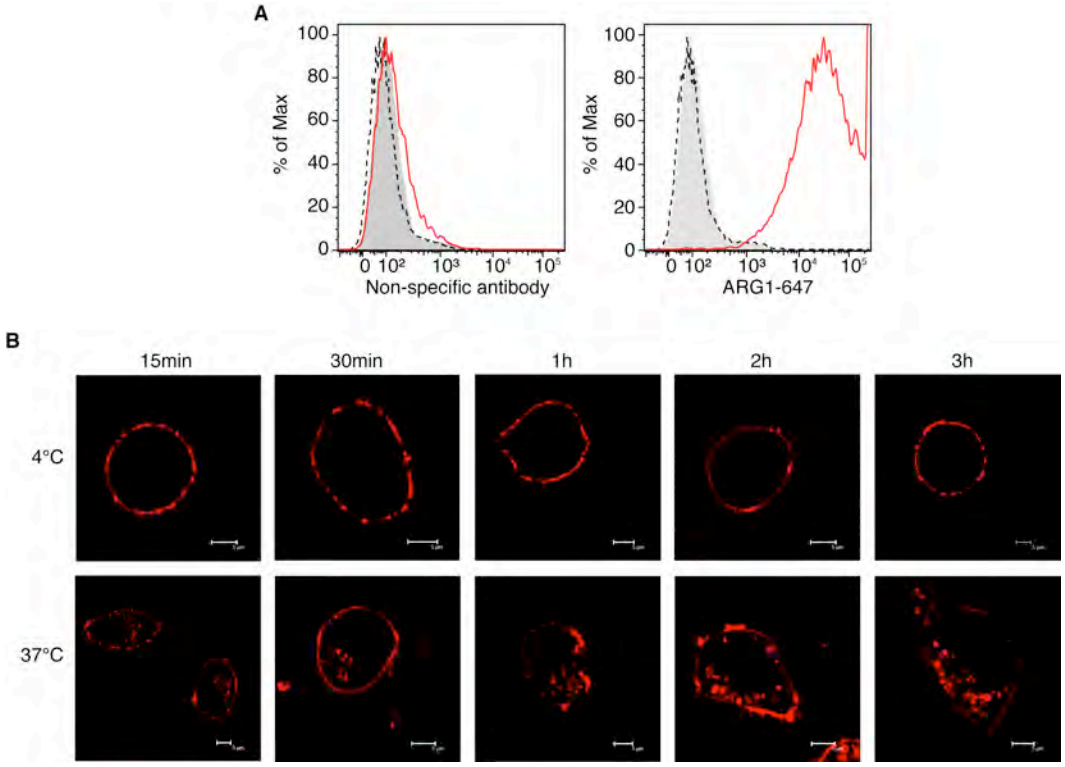


**Figure 2.6: ARG1 specifically binds to and internalizes in Rabies G-expressing cells.** A) MNA cells were transfected with Rabies G (red lines), or empty vector (dashed lines) and surface stained with indicated humanized antibodies (non-specific or ARG1). Gray plots indicate isotype staining. B) MNAG cells were incubated with ARG1 at 4˚C (top panels) and 37˚C (bottom panels) for given time points in complete medium. Data are representative of two separate experiments. Scale bar: 5 μm.

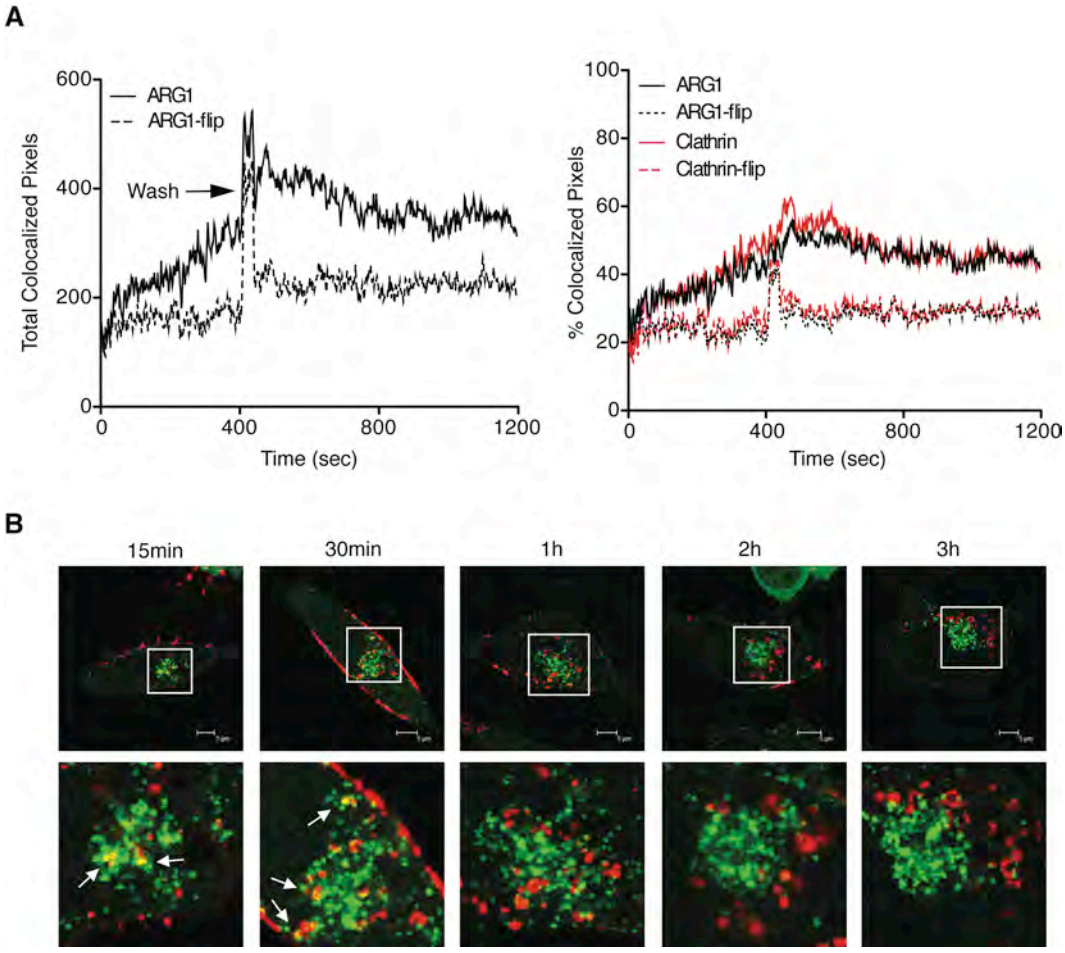


**Figure 2.7: ARG1 localizes with clathrin-expressing vesicles at early time points following addition to cells.** A, B) MNA cells were co-transfected with Rabies G and clathrin-GFP. A) Amount of total and percent ARG1/clathrin co-localized pixels from addition to cells (T = 0) to 20 min following addition (T = 1200). Images were taken using TIRF microscopy. Background co-localization, flipped images, were generated by rotating red and green pictures 180 degrees relative to each other. Arrow indicates a wash step. B) ARG1 (red) was incubated with cells for given time points in complete medium and imaged using confocal microscopy. Top panels display the original image. Bottom panels display a magnified region of interest (boxed areas in top panels). Arrows indicate regions of co-localization. Data are representative of three separate experiments. Scale bar: 5 μm.

ARG1/rabies G complex internalizes in MNAG cells via a clathrin-mediated endocytosis pathway, similar to that seen with other antibody-bound viral glycoproteins (89, 141).

Studies have indicated that actin polymerization is necessary for receptor-mediated endocytosis and antibody-directed endocytosis of viral glycoproteins in mammalian cells (31, 141). To examine the role of actin in ARG1 endocytosis, internalization was analyzed in the presence of the actin-specific inhibitor, Latrunculin-A (LA) using confocal microscopy. When actin polymerization was blocked by LA, there was no internal staining at any time point when compared to untreated cells (Figure 2.8). Overall, these results indicate that the ARG1/rabies G complex internalizes through a clathrin-associated and actin-dependent mechanism of entry.

**Early endosomal localization of the ARG1/rabies G complex**

To examine early endosomal localization, the role of Rab5a in ARG1 internalization was assessed in cells expressing wild type Rab5a-GFP through confocal microscopy. Internalized ARG1 localized with Rab5a-positive endosomes at early time points after addition to cells (Figure 2.9a, solid arrows), with maximal localization at 15 min and a complete loss of localization by 1 hour. To quantify the apparent co-localization, we also analyzed the total number and percent of co-localized pixels at the given time-points. We saw a significant amount of co-localized pixels at 15 and 30 minutes, with a mean (± S.D.) of 132.25 (± 18.23) and 81.25 (± 23.52) total pixels, respectively. The amount of ARG1/Rab5a co-localized pixels decreased over time,

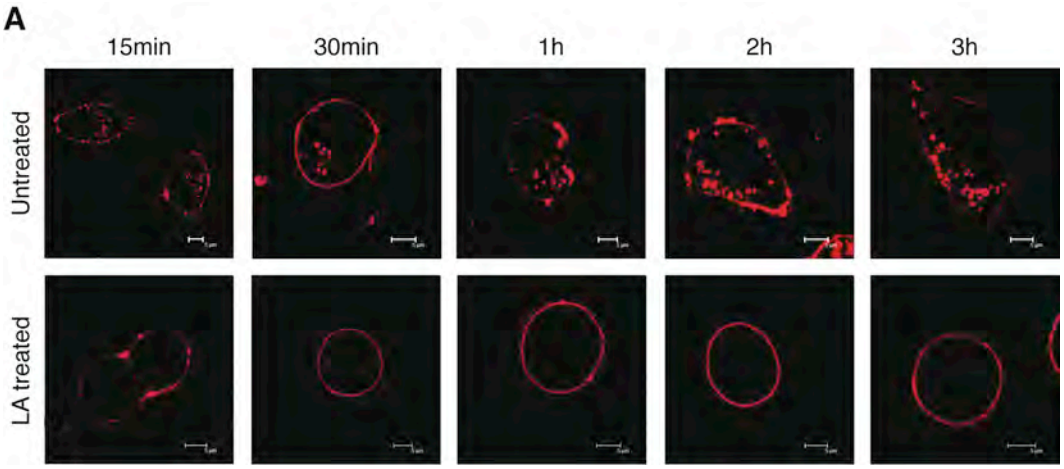


**Figure 2.8: ARG1 internalization requires actin polymerization.** MNAG cells were treated with 1.25 μM of Latrunculin-A (LA treated) or DMSO carrier alone (untreated) for 30 min prior to addition of ARG1 antibody (red) in complete medium for given time points. Data are representative of two separate experiments. Scale bar: 5 μm.

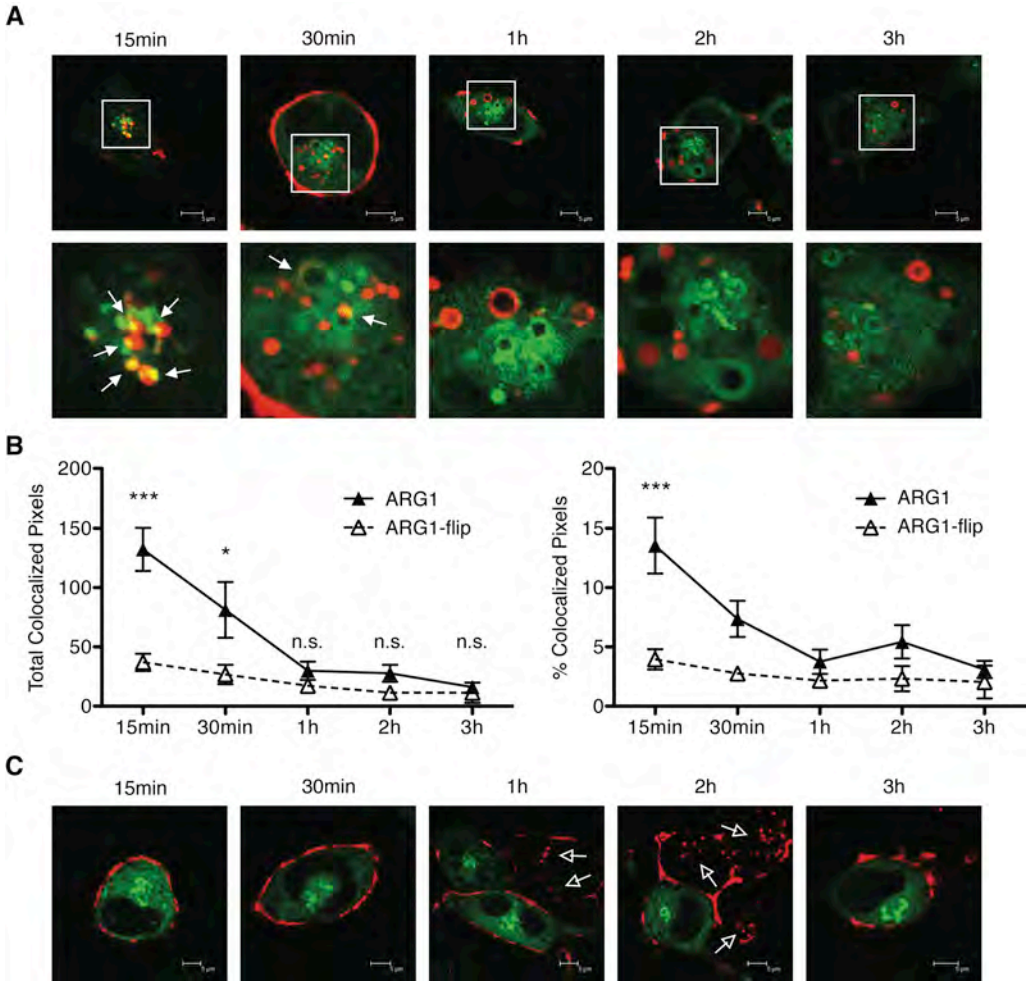


**Figure 2.9: Internalized ARG1 localizes to and requires Rab5a-positive endosomes.** MNA cells were co-transfected with Rabies G and either WT-Rab5a-GFP (A, B) or DN-Rab5a-GFP (C) and incubated with ARG1 (red) for given time points in complete medium. (A) Top panels display the original image. Bottom panels display a magnified region of interest (boxed areas in top panels). Solid arrows indicate regions of co-localization. (B) Analysis of total and percent ARG1/WT-Rab5a co-localized pixels ($n \geq 5$ per time point). (C) Open arrows show internalized antibody. Background co-localization, flipped images, were generated by rotating red and green pictures 180 degrees relative to each other. Data are representative of three separate experiments. Graphs show mean ± s.e.m. Significance values are shown relative to background levels. P-values are shown as *** $\leq 0.0001$; * $< 0.05$; n.s. = not significant. Scale bars: 5 μm.

with numbers similar to background (flipped images) by 1 to 3 hours ranging from a mean (± S.D.) of 29.88 (± 7.66) to 16 (± 4.23) co-localized pixels, respectively (Figure 2.9b). The percent of ARG1 pixels co-localized to Rab5a followed a similar pattern, with the highest percentage at 15 min (Figure 2.9b).

To determine the requirement for functional Rab5a, fluorescent ARG1 internalization was also assessed in cells expressing a GFP-tagged dominant-negative (DN) Rab5a. In order to function properly, Rab5a must cycle between the active GTP-bound and inactive GDP-bound states. The DN form of Rab5a contains a S34N amino acid change that is unable to be phosphorylated to the active GTP-bound state and, thus, remains GDP-bound (150). No internalization of ARG1 occurred in the presence of mutant (DN) Rab5a, (Figure 2.9c, green cells). As a control, ARG1 internalization was unaffected in cells that did not express GFP and were, therefore, not transfected with the DN-form, (Figure 2.9c, open arrows). These results indicate that ARG1 internalization following binding to rabies G localizes with and is dependent on the presence of functional Rab5a, a key regulator of endosomal trafficking.

**ARG1 localization with Rab4, Rab11, and Rab9**

To further characterize the intracellular localization of the ARG1/rabies G complex, internalization was compared to several different endosomal proteins, Rab4, Rab11, and Rab9. The association of these proteins with fluorescent ARG1 was assessed in cells expressing GFP-tagged Rab4 and Rab11 or YFP-tagged Rab9 plasmids through confocal microscopy. ARG1 did not localize with recycling endosomal

proteins, Rab4 or Rab11 at any time point tested (Figure 2.10). However, internalized ARG1 began to significantly localize with the late endosomal protein, Rab9 by 1 hour after addition to cells, with maximal co-localized pixels at 2 and 3 hours (Figure 2.11) exhibiting a mean (± S.D.) of 402.58 (± 45.92) and 432.09 (± 59.79) total and 28.11 (± 2.39) and 31.46 (± 2.8) percent co-localized pixels, respectively. Background co-localized pixels at all time points exhibited a range (± S.D.) of 11.25 (± 7.57) to 86.09 (± 20.66) total and 1.4 (± 0.99) to 6.65 (± 0.61) percent co-localized pixels (Figure 2.11b). To define a possible role for Fc-receptors in antibody internalization or trafficking, the internalization of ARG1 $F(ab')_2$ fragments was assessed. Fluorescently labeled $F(ab')_2$ fragments of ARG1 exhibited a staining and localization pattern similar to that of full length ARG1 (Figure 2.12), indicating that the Fc region of ARG1 does not play a role in internalization and endosomal localization.

**ARG1 localization with lysosomes**

Lysosomal localization of the ARG1/rabies G in MNAG cells was also assessed through confocal microscopy. Internalized ARG1 began to localize with the cell-permeant, acidotrophic dye, LysoTracker Green DND-26, at 1 hour after addition to cells (Figure 2.13). The total number of co-localized pixels increased over time, maximal co-localized pixels at 3 hours exhibiting a mean (± S.D.) of 345 (± 55.78) total and 33.54 (± 5.39) percent co-localized pixels (Figure 2.13b). These results indicate that the ARG1/rabies G complex traffics from Rab5a-positive early endosomes to

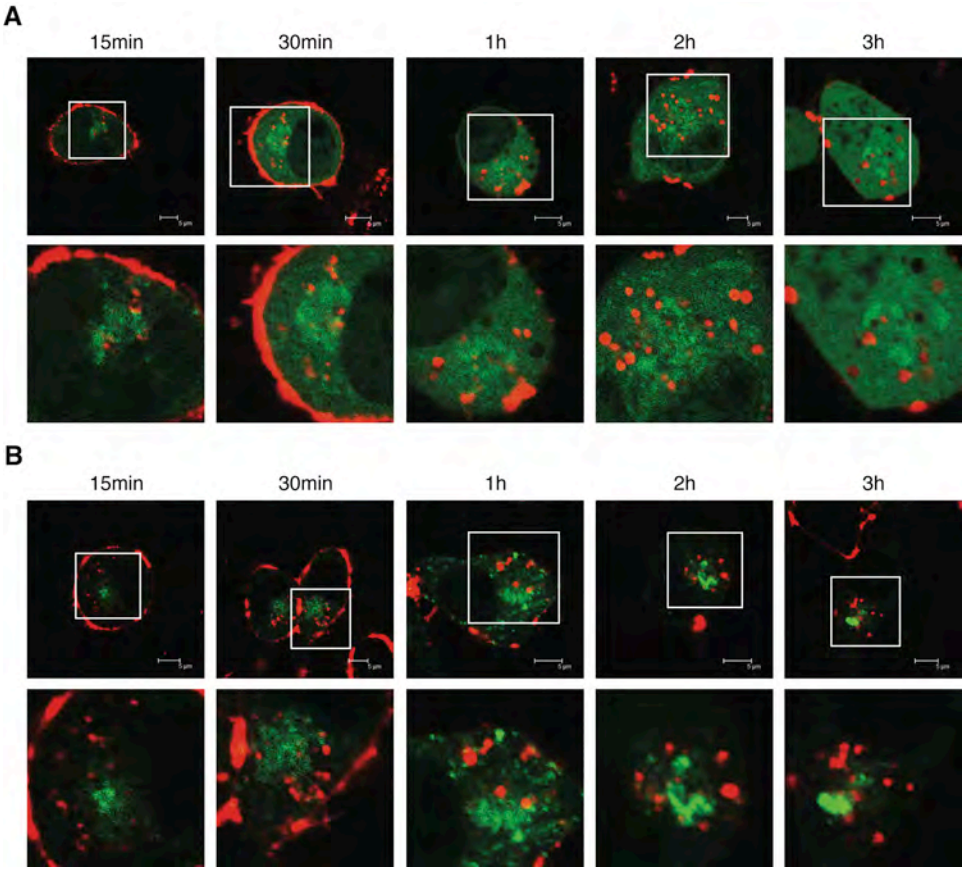


**Figure 2.10: ARG1 does not localize with recycling endosomal proteins.** MNA cells were co-transfected with Rabies G and either Rab4-GFP (A) or Rab11-GFP (B) and incubated with ARG1 (red) for given time points in complete medium. Top panels display the original image. Bottom panels display a magnified region of interest (boxed areas in top panels). Data are representative of three separate experiments. Scale bar: 5 μm.

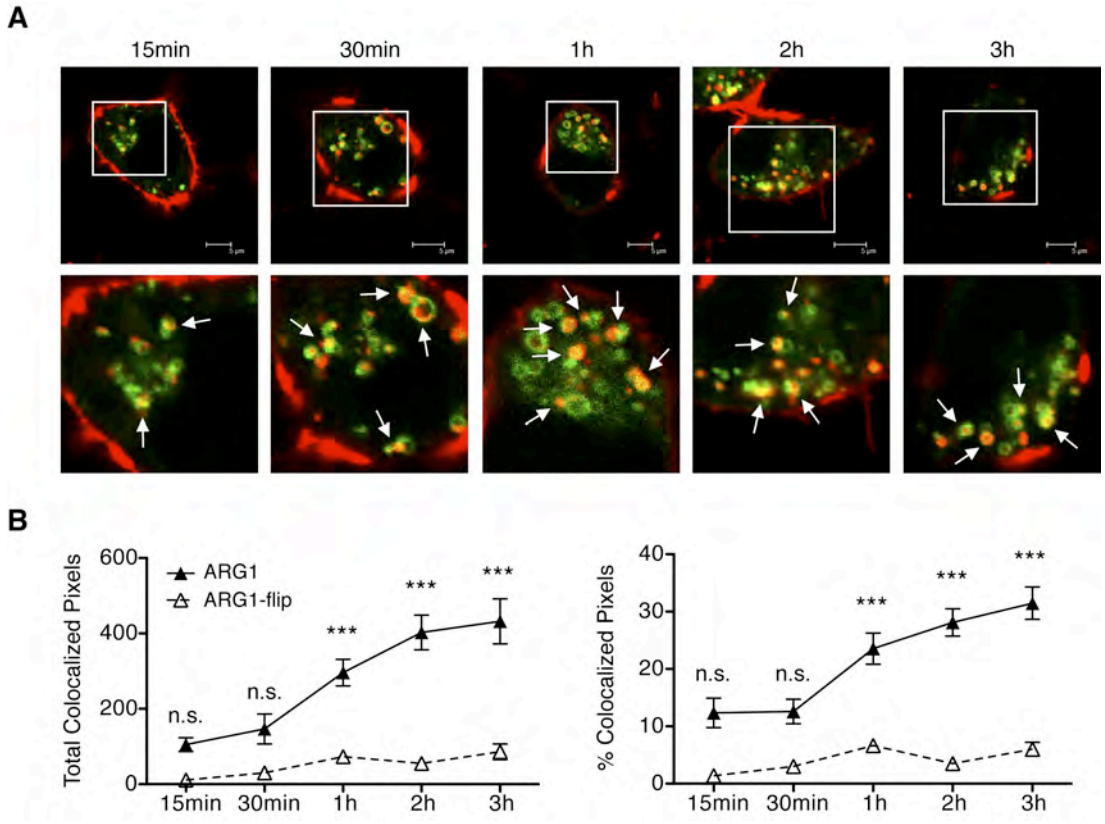


**Figure 2.11: Internalized ARG1 traffics to late endosomes.** (A, B) MNA cells were co-transfected with Rabies G and Rab9-YFP and incubated with ARG1 (red) for given time points in complete medium. Top panels display the original image. Bottom panels display a magnified region of interest (boxed areas in top panels). Arrows indicate regions of co-localization. (B) Analysis of total and percent ARG1/Rab9 co-localized pixels (n ≥ 4 per time point). Background co-localization, flipped images, was generated by rotating red and green pictures 180 degrees relative to each other. Data are representative of three separate experiments. Graphs show mean ± s.e.m. Significance values are shown relative to background levels. P-values are shown as *** ≤ 0.0001; n.s. = not significant. Scale bar: 5 μm.

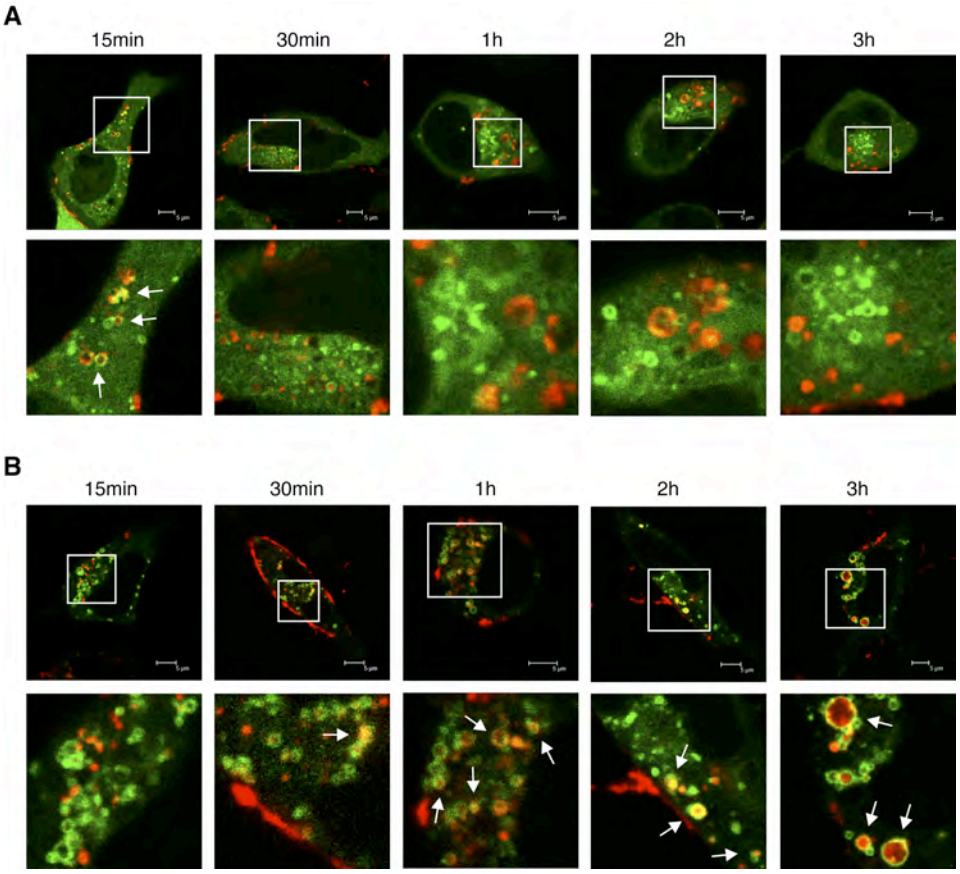


**Figure 2.12: F(ab')$_2$ internalization and endosomal localization is similar to full length ARG1.** MNA cells were co-transfected with Rabies G and WT-Rab5a-GFP (A) or Rab9-YFP (B) and incubated with F(ab')$_2$-ARG1 (red) for given time points in complete medium. Top panels display the original image. Bottom panels display a magnified region of interest (boxed areas in top panels). Data are representative of two separate experiments. Arrows indicate regions of co-localization. Scale bar: 5 μm.

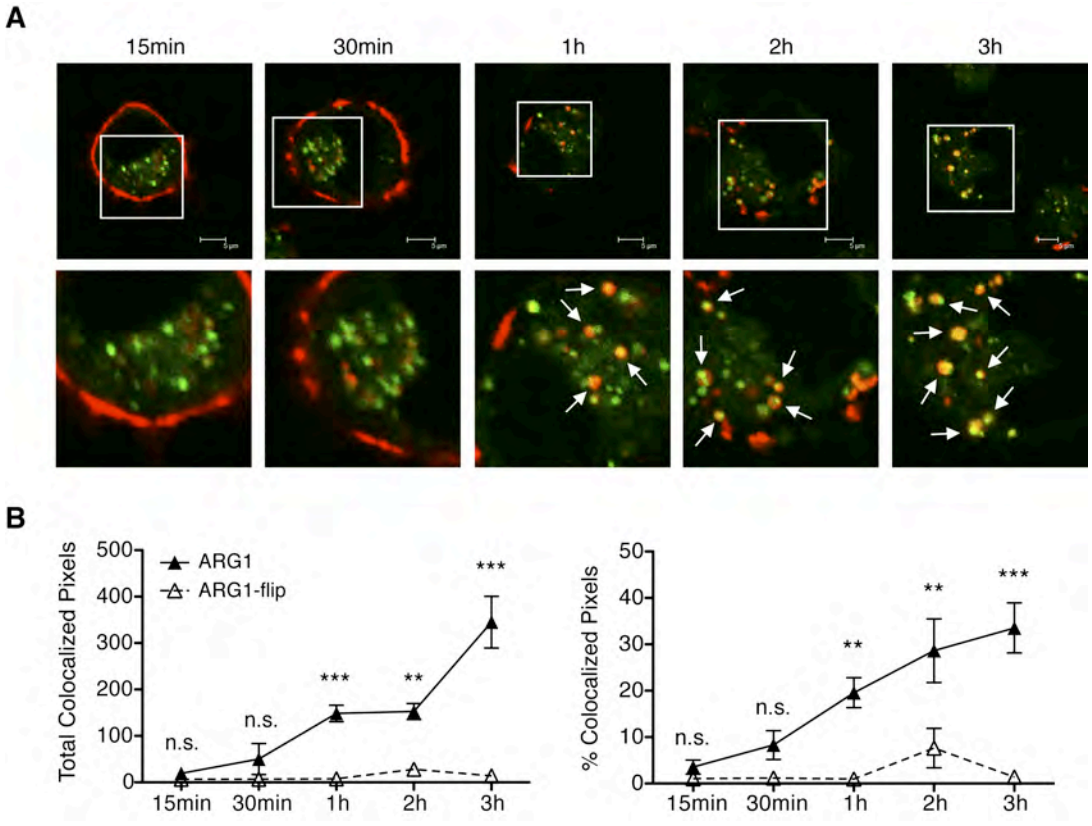


**Figure 2.13. Internalized ARG1 traffics to a lower pH, lysosomal compartment within 3 hours.** (A, B) MNAG cells were incubated with ARG1 (red) and LysoTracker Green DND-26 (50 nM) for 30 min in complete medium. Top panels display the original image. Bottom panels display a magnified region of interest (boxed areas in top panels). Arrows indicate regions of co-localization. (B) Analysis of total and percent ARG1/Lysotracker co-localized pixels (n ≥ 3 per time point). Background co-localization, flipped images, was generated by rotating red and green pictures 180 degrees relative to each other. Data are representative of three separate experiments. Graphs show the mean ± s.e.m. Significance values are shown relative to background levels. P-values are shown as *** ≤ 0.0001; ** < 0.01; n.s. = not significant. Scale bar: 5 μm.

Rab9-positive late endosomes and finally to a lower pH, lysosomal-like compartment within 3 hours, similar to that seen with the αCD71-bound TfR, but in contrast to the results observed with Tf-bound TfR, which localizes with early and recycling endosomes, excluding Rab9, as characterized above.

Taken together, our data suggests that binding of an antibody to a cell surface protein induces a shift from the natural intracellular trafficking of that protein. In addition, our data proposes that antibodies to any cell surface protein, endogenous or viral, mediate predictable trafficking to late endosomal compartments.

## D. DISCUSSION

Studies have shown that monoclonal antibodies can be used as a therapeutic delivery system to specifically target cells expressing the appropriate receptor protein. Several publications have indicated the benefit to using monoclonal antibodies to specifically deliver drugs, including the targeted delivery of cytokines and siRNAs to tumor cells (81, 85, 87, 88, 151, 152).

Critical to the use of antibodies as a drug delivery system is understanding how these antibodies traffic and where the complex is localized and/or degraded. Studies have indicated that the use of antibodies as stand-alone or conjugated therapeutics is useful to either a) target specific cells for destruction through Fc-mediated killing or b) specifically bind to and internalize the cell surface protein to which it is specific. This internalization pathway occurs through receptor-mediated endocytosis, with movement from clathrin-coated vesicles to early endosomes to late endosomes and eventually to

lysosomes where the antibody and cell surface protein are likely degraded (78, 80, 89). Based on these observations, we hypothesized that the internalization pathway seen when an antibody is bound to a cell surface protein may remain the same, regardless of the natural internalization pathway of the membrane protein to which the antibody is specific. In other words, we theorized that there might be a common antibody-mediated internalization pathway that exists when an antibody is bound to a cell surface protein. In order to examine this, we analyzed the internalization of an endogenous cell surface protein, the TfR. We observed a significant increase in localization to Rab9-positive late endosomes when the receptor was bound to an antibody, indicating that the internalization pathway had been shifted to include degradation-associated endosomes, in agreement with our hypothesis (Figure 2.14). As expected, when bound to its natural ligand, Tf, the receptor internalized exclusively through a recycling endosomal pathway, including localization with endosomal proteins Rab4, Rab5a, and Rab11, but not with Rab9. These results suggest that there is a specific antibody-mediated internalization pathway that occurs when an antibody is bound to a cell surface protein.

Virus-specific antibodies are known to modulate or neutralize viral infection and decrease virus-induced cell death (89). One potential mechanism for inhibition of viral release from infected cells is to mediate the internalization of the viral glycoproteins on infected cells. It is possible that this internalization renders virus within a cell unable to appropriately bud from an infected cell, leading to a decrease in viral titers and an ineffective viral infection (90, 91). Additionally, it has been shown that antibody-mediated internalization of viral proteins can be used to target antiviral therapeutics

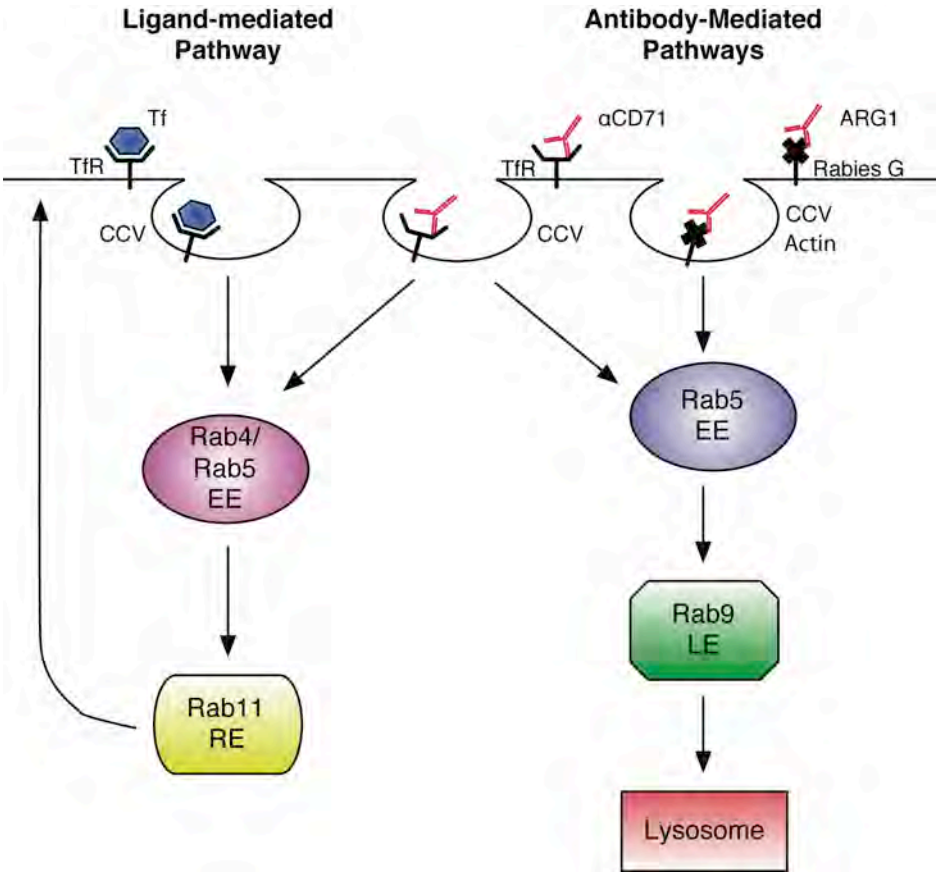


**Figure 2.14: Diagram of generalized antibody-mediated internalization pathway.** Antibodies specific for both viral (Rabies G = ARG1) and endogenous proteins (Transferrin receptor, TfR = αCD71) mediate localization to Rab9-positive late endosomes.

specifically to infected cells. Song et al. reported that an antibody against the HIV glycoprotein can specifically deliver functional siRNA to infected cells only, leading to a decrease in viral protein expression (79). Others have shown that antibodies directed against the hepatitis B surface antigen can effectively deliver antiviral siRNAs to infected cells both in vitro and in vivo leading to decreased viral gene expression (92).

Rabies virus infections are worldwide and once the symptoms of rabies develop, there is no treatment and the disease is almost always fatal (153). Disease can be prevented by post-exposure prophylaxis, which consists of wound care and administration of both the rabies vaccine and rabies immune globulin, which helps to neutralize the virus. Taking advantage of the ability of antibodies and antibody-conjugates to specifically bind to and subsequently internalize target proteins expressed on the surface of cells has broad applicability for the treatment of a variety of viral infections. As such, we examined the antibody-mediated internalization pattern of rabies G expressed on the surface of mouse neuroblastoma cells, to mimic an infected cell state (154). Using a rabies G specific antibody, ARG1, we show that the ARG1/rabies G complex internalizes via a clathrin- and actin- dependent mechanism, followed by movement into endosomes associated with the degradation pathway, including localization with Rab5a, Rab9 and low pH lysosomes.

Although we have defined a role for actin polymerization in the internalization of antibody-bound rabies G, we did not see a requirement for actin in the internalization of antibody-bound TfR (data not shown). It is known that the natural ligand-mediated internalization pathway of TfR does not require actin (35, 36). However, since the

αCD71 antibody was able to alter this pathway to include localization with late endosomes, we suspected that actin may play a general role in antibody-mediated endocytosis. Surprisingly, the actin inhibitor, LA had no effect on the localization of internalized, antibody-bound TfR to Rab9-positive late endosomes (data not shown). It has previously been determined that the TfR localizes to and is internalized via large patches of clathrin on the cell membrane (144, 145), allowing for its rapid internalization in cells. This would suggest that, perhaps, actin is required to re-locate surface-expressed rabies G to areas on the membrane that would allow for clathrin-mediated endocytosis. Since the TfR is already localized to these patches, actin is not required, even if internalization occurs via antibody binding, rather than ligand. Further analysis of the role of actin in endocytosis events may shed more light on this interesting result.

Overall, these findings have broad implications for the use of antibodies as therapeutics to either mediate the degradation of cell surface proteins or to be used as drug-delivery vehicles, via endogenous and viral cell surface proteins. As previously described, it is thought that in order for an antibody or antibody conjugate to be functional, it must internalize and localize with early and late endosomes, and potentially lysosomes, so that the antibody/protein complex will be degraded or, in the case of a drug-conjugate, the drug, e.g. siRNA or inhibitors, will be released into the cytoplasm. Studies thus far examining the potential of an antibody to be used as a therapeutic have either focused on determining whether or not an antibody will localize with late endosomes (78) or have involved the use of antibodies specific to proteins

known to internalize through a degradation pathway, e.g. EGFR. Our findings suggest that one may not have to choose an antibody therapeutic based on the intrinsic property of a cell surface protein, since the binding of an antibody to that protein would guide internalization to include the degradative compartments. This may allow for the development of new therapeutics to targets originally overlooked due to their internalization pathway, including, but not limited to, recycling receptors.

# CHAPTER III

## Characterizing the innate immune response to titanium wear-particles

### A. INTRODUCTION

With over one million total joint replacements performed every year (136), joint replacement surgery is a major advance in treatment of people with arthritis (155). It is estimated that six million total hip and knee replacements will be performed per year in the US by 2015 making this a significant health issue. Long-term studies of hip and knee replacements have indicated that loosening of joint replacements, as well as bone-loss surrounding the replacement, increases over time. Approximately 10-20% of patients who undergo joint replacement surgery will develop joint loosening, eventually requiring replacement of the joint (134, 135). Patients who develop significant inflammation surrounding a fixed implant, if left untreated, will eventually develop joint loosening and, in some cases, bone loss surrounding the joint. This type of aseptic inflammation is associated with activation of macrophages in the tissue surrounding the prosthesis and the destruction of bone. Studies have shown that over time, small wear-particles generated from implants become dislodged and are released into the surrounding area (135) where they can be phagocytosed by monocytes and macrophages (136). This uptake of particles stimulates cells to release pro-inflammatory cytokines such as tumor necrosis factor (TNF), interleukin-6 (IL-6),

prostaglandin E2 ($PGE_2$), and IL-1β (156-160). These cytokines, especially IL-1β, have been implicated in mediating osteoclast activation and/or bone resorption (123-125).

The role of the NLRP3 inflammasome in the response to titanium (Ti) wear-particles has not previously been characterized. We hypothesized that Ti particles activate a pro-inflammatory response in patients through activation of the inflammasome complex, leading to loosening and failure of the joint replacement. To assess this, we first determined whether injection of Ti particles into mice led to neutrophil recruitment, a hallmark of acute inflammation, and whether this neutrophil influx was dependent on the expression of IL-1R and IL-1α/β. To examine the potential for an antagonist-based therapy, we also tested whether treatment of mice with IL-1Ra could decrease neutrophil recruitment. We next characterized the *in vitro* response to Ti particles, starting with determining whether Ti particles could be internalized in mouse macrophages. We also examined the inflammatory cytokine response, including IL-1β production, induced by Ti particles in mouse and human macrophages. Finally, in order to define a role for the NLRP3 inflammasome in Ti-induced inflammation, we examined whether Ti particles could activate IL-1β secretion in mouse and human macrophages deficient in key components of the inflammasome signaling complex: NLRP3, ASC, and Caspase-1.

## B. MATERIALS AND METHODS

### Reagents:

Lipopolysaccharide (LPS), Nigericin, and poly(dA:dT) sodium salt were from Sigma-Aldrich. CA-074-Me, Phorbol 12-myristate 13-acetate (PMA), and GeneJuice transfection reagent were from EMD Chemicals. Commercially pure titanium (Ti) particles (Alfa Aesar, a Johnson Matthey Company) were autoclaved in $H_2O$, washed with 100% ethanol, dried under UV light in a laminar flow hood, and resuspended in sterile PBS for subsequent studies. Particles were determined to have <1EU/ml of endotoxin using the Pyrochrome LAL endotoxin assay (Associates of Cape Cod). Particles (n=6708) had a median diameter of 1.86 μm with a mean diameter of 3.805 μm (SD = 6.065 μm) as determined by confocal microscopy and (NIH) ImageJ software.

**Mice:**

C57BL/6 (WT) and IL-1R-deficient (IL-1R KO) mice were from Jackson Laboratories. CD14 KO and MD2 KO mice were a gift from D. Golenbock (UMass Medical School). IL-1α/β KO mice were a gift from Y. Iwakura (University of Tokyo). All mouse strains, age and sex-matched with appropriate controls, were bred and maintained in the animal facilities at the University of Massachusetts Medical School. All experiments involving live animals were in accordance with guidelines set forth by the University of Massachusetts Medical School Department of Animal Medicine and the Institutional Animal Care and Use Committee.

**Intraperitoneal (i.p.) injections:**

Mice were injected i.p. with sterile PBS (500 μl), 4% thioglycolate (1 ml), or 30 mg Ti particles (600 μl at 50 mg/ml). For IL-1Ra studies, mice were injected subcutaneously with 200 μl (1 mg/kg final dose) of IL-1Ra (Anakinra™; Amgen) in 2% Hyaluronic Acid carrier (Calbiochem) 2 h prior to and 1h following Ti injections. Mice were sacrificed by isoflurane inhalation followed by cervical dislocation. Peritoneal exudate cells (PECs) were isolated 16-18 h after injections as previously described (127).

**Flow cytometric analysis:**

To enumerate neutrophils, PECs ($1x10^6$) were incubated with anti CD16/CD32 monoclonal antibody (clone 2.4G2; BD Biosciences) for 30 minutes to block FcγRIIB/III receptors and stained with Ly6G-FITC (BD Biosciences) and 7/4-Alexa647 (AbD Serotec) for 30 minutes at 4°C. Following staining, cells were washed with PBS and analyzed on a LSRII (BD Biosciences). Neutrophil numbers in PECs were calculated by multiplying total cell numbers by the percentage of Ly6G+, 7/4+ cells. Data were acquired by DIVA (BD Biosciences) and were analyzed with FlowJo 8.8.6 software (Tree Star Inc.).

**Scanning Electron Microscopy (SEM):**

Macrophages were plated at 50-60% confluency in plastic tissue culture dishes. The following day, Ti particles (100 μg/ml) were added to cells for 30 minutes at 37°C. Cells were prepared for imaging as described in (161). Briefly, cells were fixed in 2.5%

glutaraldehyde in phosphate buffer (pH 7.2). Cells were then dehydrated though a graded series of ethanol followed by Critical Point Drying in $CO_2$. The bottoms of the culture dishes were mounted onto scanning stubs and coated with a 3 nm film of carbon. Images were acquired on a FEI Quanta 200 FEG MKII scanning electron at an accelerating voltage of 10kV. Images were collected in both secondary electron imaging (SEI) and back-scattered electron-imaging (BSI) modes for topographic and atomic contrast using FEI Scandium software. Final images, combining both the SEI (brown) and the BSI (blue) signals were generated using Cameo software.

**Spectrum Analysis:**

The elemental composition of titanium particles was analyzed using the Oxford-Link X-ray spectrometer on the microscope. Energy Dispersive Spectroscopy (EDS) scans were collected for 200 s and the elements identified using the Oxford-Link INCA software package.

**Tissue section preparations:**

Tissue sections were obtained from soft tissue (synovial membranes) around failed hip prostheses. Sections were embedded in paraffin and stained with hematoxylin and eosin (H&E) for analysis. Alternatively sections were incubated in the presence of xylenes, to remove paraffin, then prepared for scanning electron microscopy imaging using protocol described in (161). Breifly, xylenes were removed by passing the tissue sections through 100% ethanol followed by Critical Point Drying

in $CO_2$. Areas in the sections that had particles of interest were removed from the tissue section using a small piece of double sided conductive carbon tape and placed onto a scanning stud. The mounted tissue pieces were then coated with a thin film of carbon to make them conductive to ground. Sections were imaged as described above. All experiments involving human samples were in accordance with guidelines set forth by the University of Massachusetts Medical School Committee for the Protection of Human Subjects in Research.

**Cell culture:**

Immortalized mouse macrophages from WT, NLRP3-deficient, ASC-deficient, and Caspase 1-deficient mice were made as previously described (104). Briefly, bone marrow cells were cultured in L929-conditioned media to induce macrophage differentiation. Macrophages were then infected with a J2 retrovirus expressing v-*myc* and v-*raf* and cultured for 3-6 months until they could grow in the absence of L929-conditioned media. Cells were grown in DMEM supplemented with 10% fetal calf serum (FCS), 1% L-glutamine, and 1% penicillin/streptomycin at 37˚C with 5% $CO_2$. Cells were plated in granulocyte macrophage colony-stimulating factor (GM-CSF) (1 ng/ml; eBioscience)-containing media for 18 h prior to stimulations. THP-1 cells (ATCC) were differentiated into macrophages with 10 nM PMA for 48 h and grown in RPMI-1640 supplemented with 10% FCS, 1% L-glutamine, 1% penicillin/streptomycin, 50 μM β-Mercaptoethanol, and 10 mM HEPES at 37˚C with 10% $CO_2$.

**Cell stimulations:**

For particle stimulations, mouse and human macrophages (4-5 x $10^5$) were primed for 3 h with LPS (100 ng/ml) to up-regulate pro-IL-1β expression or left unprimed (Media), then stimulated with Ti particles at given concentrations (mg/ml), transfected with 400 ng of poly(dA:dT) using GeneJuice, or treated with Nigericin (5 mM) for an additional 6 h (mouse) or 18 h (human).

**RNA interference:**

Differentiated THP-1 macrophages were transfected with siGENOME SMARTpools (40 nM) against human NLRP3 or ASC or non-targeting (NT) siRNA #2 using DharmaFECT 4 transfection reagent for 72 h. Cells were then stimulated as described above. All siRNA reagents were obtained from Dharmacon (Thermo Fisher Scientific).

**ELISA:**

Cell culture supernatants were assayed for murine or human IL-1β or IL-6 with ELISA kits from BD Biosciences according to the manufacturer's instructions.

**Statistical Analysis:**

An unpaired, two-tailed Student's t-test was used to determine statistical significance of independent experiments where two groups were compared. When more than two groups were compared, a one-way ANOVA or two-way ANOVA

followed by Bonferroni's correction for post test comparisons was used. Values of $p < 0.05$ were considered significant. Statistics were performed using GraphPad (Prism v5.0a) software.

## C. RESULTS

### Ti particles induce an IL-1-dependent neutrophil influx *in vivo.*

IL-1 plays an important role in the acute inflammatory response through activation and recruitment of neutrophils, a hallmark of acute inflammation (162). Previous studies have shown that intra-peritoneal (i.p.) injections of MSU crystals lead to an increase in neutrophil recruitment and that this recruitment was dependent on the expression of the IL-1R (127). To examine the role of IL-1 and inflammation in the response to Ti particles *in vivo,* WT mice were injected i.p. with Ti (30 mg) and analyzed for neutrophil influx 16 hours later. Mice injected with Ti exhibited a significant increase in neutrophils (Ly6G+7/4+) compared to injections of PBS (Figure 3.1a). As expected, increased neutrophil numbers were seen in mice injected with the positive control, thioglycolate. To control for the possibility that LPS or endotoxin present on the surface of the titanium particles was responsible for the apparent immune response to injections, we used MD2-deficient (MD2 KO) and CD14-deficient (CD14 KO) mice. Both MD2 and CD14 facilitate LPS signaling through TLR4, and deficient mice are unresponsive to LPS (163, 164). Ti injections were able to induce neutrophil influx in MD2 KO and CD14 KO mice at levels similar to WT control mice (Figure 3.1b, c), indicating that LPS did not contribute to neutrophil recruitment by Ti.

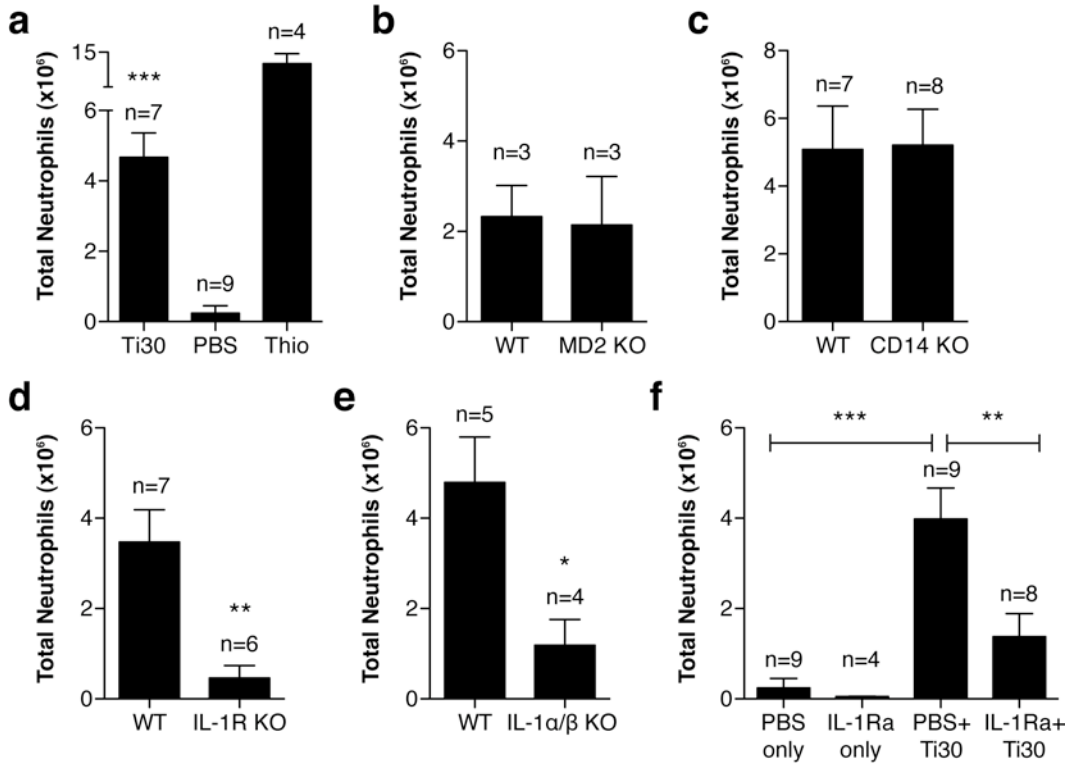


**Figure 3.1: Neutrophil recruitment following Ti injections in various mouse strains.** (a) WT (b) MD2 KO (c) CD14 KO (d) IL-1R KO and (e) IL-1α/β KO. (f) Effect of IL-1Ra treatment on neutrophil recruitment. Graphs show the mean ± s.e.m. from the total number of mice indicated. Each graph represents an average at least two separate experiments. To control for injection errors, separate WT controls were included for each deficient mouse tested. Significance values are shown relative to (a) PBS, (b-e) WT, or as indicated on the graph. P-values are shown as *** ≤ 0.0001; ** < 0.01; * < 0.05

IL-1R has been shown to be required for neutrophil recruitment following exposure to stimulants in mice (104, 126, 127). To determine whether expression of IL-1R was required for Ti-induced neutrophil influx, IL-1R-deficient (IL-1R KO) mice were injected with Ti and compared to WT mice. Ti injections were unable to induce a neutrophil influx in IL-1R KO mice (Figure 3.1d). Both IL-1α and IL-1β signal through the IL-1R. In order to examine the role of IL-1 cytokine production on neutrophil recruitment, IL-1α/β KO mice were injected with Ti. Deficient mice exhibited significantly lower numbers of neutrophils (Figure 3.1e), confirming a role for IL-1 associated signaling in the immune response to Ti wear-particles *in vivo*.

IL-1Ra, the soluble receptor antagonist of IL-1, has been used as a therapeutic drug to treat patients with rheumatoid arthritis to help slow or reverse progression of the disease. Patients receiving the drug have exhibited a significant decrease in joint inflammation (130-132). In order to examine the effects of IL-1Ra treatment on Ti-induced inflammation, mice were injected with IL-1Ra 2 h prior and 1 h post injection of Ti particles. Mice treated with IL-1Ra showed a significant decrease in neutrophil recruitment after injection with Ti, compared to control treated WT mice (Figure 3.1f). Taken together, these results indicate a critical role for IL-1 in Ti-induced neutrophil recruitment and introduce the possibility for a potential therapeutic treatment.

**Ti induces IL-1β cytokine production in mouse and human macrophages.**

In order to determine the molecular pathways involved in IL-1 production we analyzed the immune response of murine and human macrophages to titanium. Studies

have shown that the immune response to Ti wear-particles involves the release of inflammatory cytokines, including IL-1β (157). In order to determine whether the response to Ti was similar in mice, WT immortalized mouse macrophages were incubated with varying concentrations of purified Ti particles for 6 hours. In order to specifically examine IL-1β production, macrophages were primed for 3 hours with LPS, to induce up-regulation of pro-IL-1β transcription, prior to Ti stimulation. WT immortalized mouse macrophages responded to Ti particles in a dose-dependent manner with high levels of secreted IL-1β (Figure 3.2a, c). Supernatants from macrophages that received an LPS prime only did not exhibit an increase in IL-1β production (Figures 3.2 and 3.3). As a positive control, macrophages were transfected with double-stranded DNA, poly-dA:dT (dA:dT). WT macrophages produced a significant amount of IL-1β in response to dA:dT stimulation. As additional controls, macrophages incubated with titanium particles alone produced low to un-detectable levels of IL-6, when compared to LPS stimulation, and IL-1β, when compared to primed cells (Figure 3.3), verifying that endotoxin levels associated with Ti particles did not play a role in observed cytokine responses.

A similar IL-1β response to Ti particles was seen in PMA-differentiated THP-1 human macrophages. Ti particles induced significantly higher levels of IL-1β secretion when compared to un-stimulated controls (Figure 3.2b). As a control, human macrophages exhibited mature IL-1β secretion in response to Nigericin, a potassium ionophore known to stimulate IL-1β through induction of potassium efflux, lysosomal

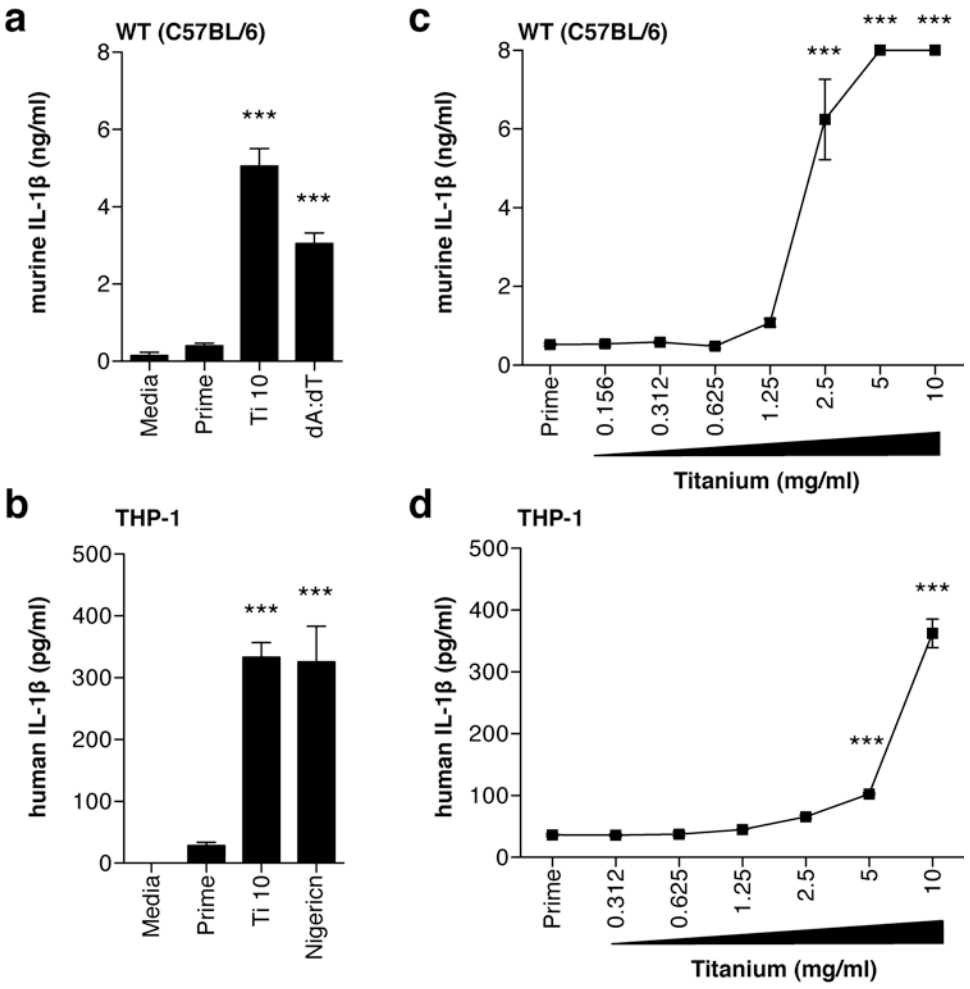


**Figure 3.2: IL-1β secretion following Ti stimulation.** (a, b) WT immortalized mouse macrophages (a) and THP-1 human macrophages (b) were primed for 3 h with LPS (Prime) followed by stimulation with 10 mg/ml of Ti particles (Ti 10) or left unprimed and unstimulated (Media). (c, d) Dose-response curves to Ti in WT immortalized mouse macrophages (c) and THP-1 human macrophages (d). Data are representative of at least two separate experiments performed in duplicate. Secreted IL-1β levels are mean ± s.e.m. Significance values are shown relative to Prime levels. P-values are shown as *** ≤ 0.0001

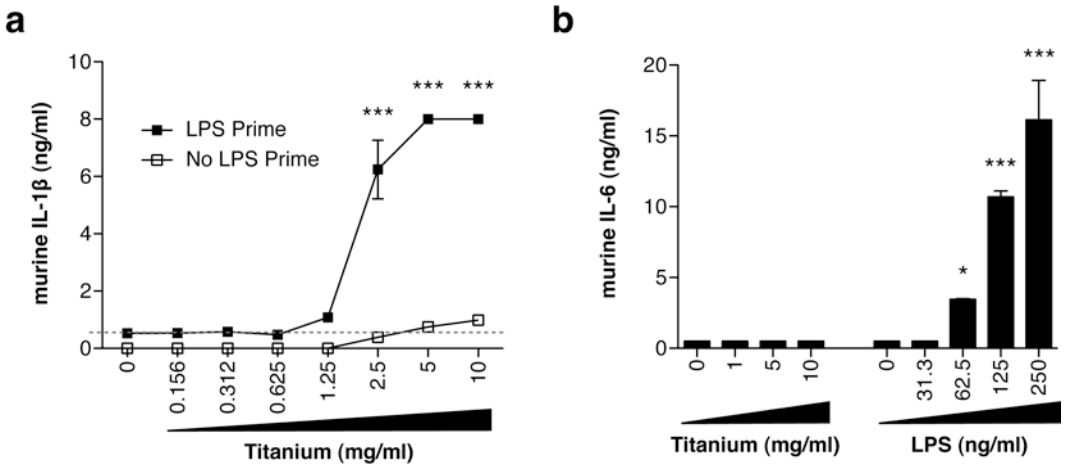


**Figure 3.3: Titanium particles do not induce cytokine production in the absence of an LPS prime.** (a) IL-1β secretion in WT immortalized mouse macrophages incubated for 6 h with Ti particles only or Ti particles following an LPS prime for 3 h. Dashed line represents LPS prime only values. (b) IL-6 secretion following incubation with Ti particles only or LPS only for 6 h. Data are representative of at least two separate experiments performed in duplicate. Secreted cytokine levels are mean ± s.e.m. Significance values are shown relative to (a) LPS prime only or (b) no stimulant (0) values. P-values are shown as *** ≤ 0.0001; * < 0.05

destabilization, and cathepsin B release (165). Ti-induced IL-1β production was also dependent on particle concentration (Figure 3.2d). Together, these results demonstrate that Ti particles induce a variety of inflammatory cytokines in mouse macrophages, and that both human and mouse macrophages respond to Ti particle stimulation with mature IL-1β secretion.

**Ti particles are internalized in macrophages.**

It has been well established that part of the inflammatory response to Ti in patients involves the uptake of wear particles by macrophages surrounding the joint replacement (135, 136). To visualize phagocytosis of Ti particles, immortalized mouse macrophages were incubated with Ti particles then analyzed through SEM. Ti particles were highly internalized in macrophages (Figure 3.4a), with the majority of all Ti particles located within cells by 30 minutes. Using confocal microscopy and Image J software (NIH), the overall diameter of macrophage-associated particles was determined. Macrophage-associated particles had a median diameter of 1.02 μm with a mean diameter of 1.21 μm (S.D. = 0.79 μm) (Figure 3.4b), similar to that seen in failed joints (137, 138).

We also examined several human tissue samples from the membranes surrounding failed joint replacements. Small black particles could be seen throughout the sections when examining H&E stained membranes (Figure 3.5a). In order to further characterize the identity of these small particles, we examined the sections through

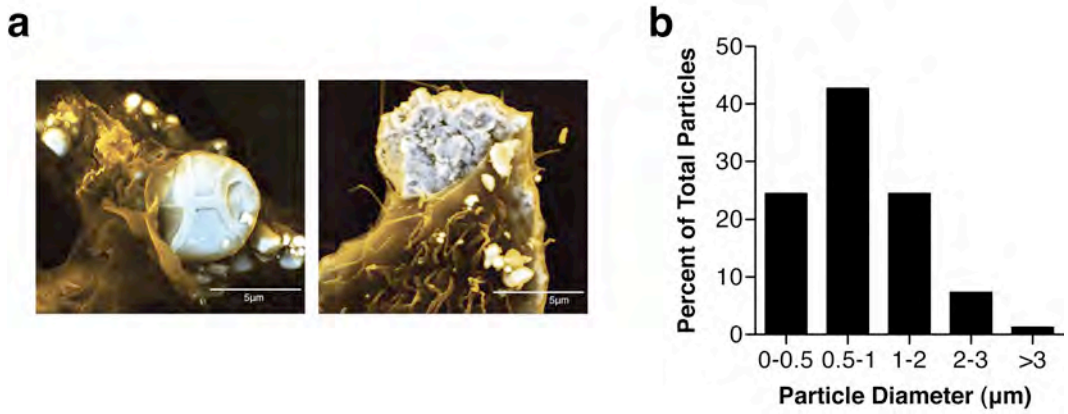


**Figure 3.4: Ti particles are internalized in mouse macrophages.** (a) SEM image of immortalized mouse macrophages incubated with Ti particles (blue) for 30 min. Pseudo-coloring based on electron (brown) and back scattered electron (blue) images. (b) Diameter of macrophage-associated particles (n = 82) as determined by confocal microscopy and NIH ImageJ software.

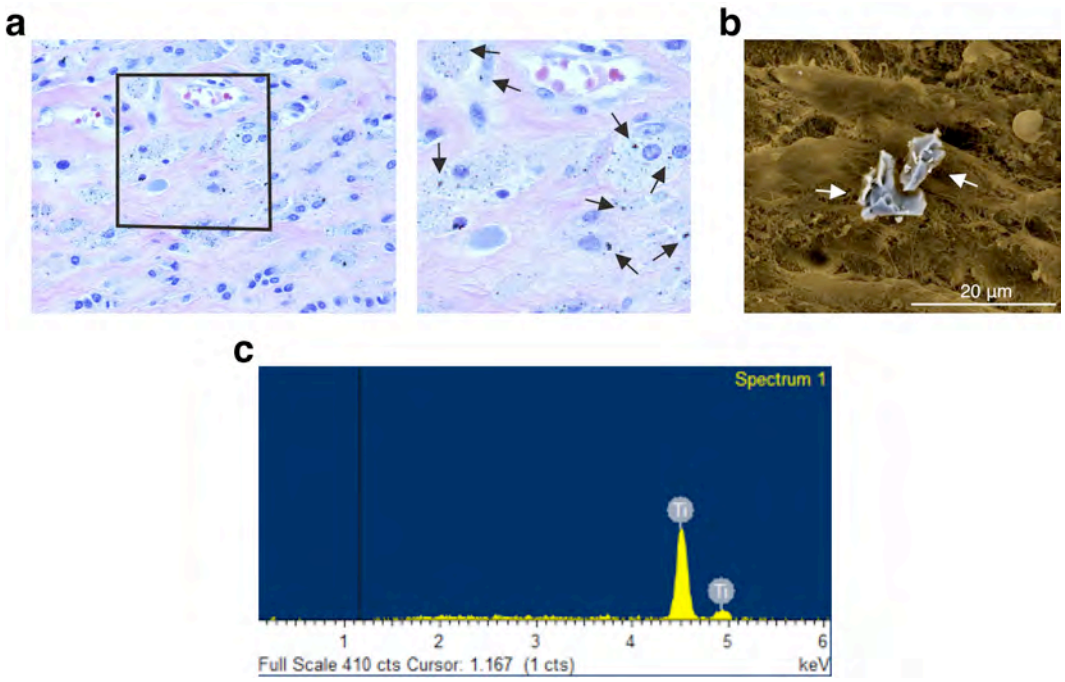


**Figure 3.5: Ti particles are found within patient synovial membranes**. Human tissue sections of membranes surrounding failed joint replacements (a) stained with H&E or (b) analyzed through SEM. Arrows indicate Ti particles. (c) Spectrum analysis of Ti particles within membranes. Images are representative of four separate sections.

scanning electron microscopy. We were able to detect small fragments of Ti particles (Figure 3.5b), verified through spectrum analysis (Figure 3.5c), within these membranes, providing direct evidence that Ti particles are present in the membranes surrounding failed joint replacements.

Following phagocytosis, particles or crystals can cause lysosomal destabilization, with the associated activation and release of cathepsin B into the cytosol. Cathepsin B is required for optimal inflammasome activation in response to silica crystals, alum, and amyloid-β (104, 110). In order to determine whether cathepsin is required for inflammasome activation and subsequent IL-1β production in response to Ti, WT immortalized mouse macrophages were treated with the cathepsin B inhibitor CA-074-Me. Supernatants from cells pre-treated with CA-074-Me had significantly lower levels of IL-1β following Ti stimulation compared to untreated cells (Figure 3.6a). Treated and untreated cells produced comparable levels of the inflammasome-independent cytokine, IL-6, in response to LPS, confirming that inhibition was inflammasome-specific (Figure 3.6b). Together, these results indicate that optimal Ti-induced IL-1β production requires cathepsin B release.

**Immune response to Ti requires the NLRP3 inflammasome.**

Supernatants from immortalized macrophages generated from NLRP3- (NLRP3 KO), ASC- (ASC KO), and Caspase-1- (CASP1 KO) deficient mice exhibited undetectable levels of secreted IL-β in response to Ti while IL-1β secretion from WT

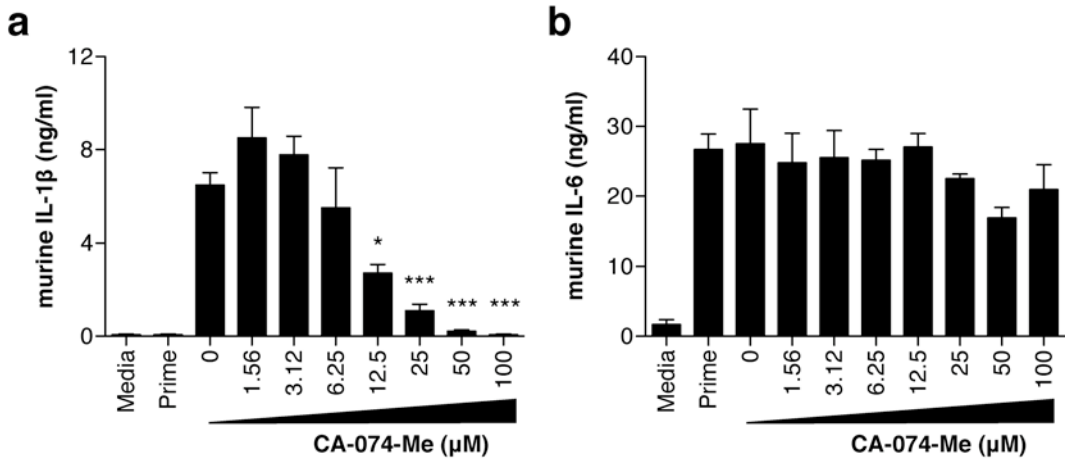


**Figure 3.6: Response to Ti particle uptake is cathepsin B dependent.** (a) IL-1β and (b) IL-6 secretion following Ti stimulation (10 mg/ml) in LPS-primed (Prime) WT immortalized mouse macrophages treated with the cathepsin-B inhibitor, CA-074-Me. Data are representative of two separate experiments performed in duplicate. Secreted cytokine levels are mean ± s.e.m. Significance values are shown relative to untreated (0 μM) samples. P-values are shown as *** ≤ 0.0001; * < 0.05.

macrophages was readily detected (Figure 3.7a). Stimulation with dA:dT induces mature IL-1β production in a NLRP3-independent manner (166). As expected, NLRP3 KO macrophages were able to respond to dA:dT similar to WT cells, while ASC KO and CASP1 KO macrophages were unable to respond to dA:dT. As a control, WT and deficient cells were able to produce similar levels of IL-6 in response to LPS stimulation for 6 hours (Figure 3.7b).

A similar result was observed in THP-1 human macrophages. Cells transfected with siRNAs against NLRP3 and ASC exhibited a significant reduction in the secretion of IL-1β in response to Ti particles (Figure 3.7c) compared to no siRNA or luciferase-specific, non-targeting (NT) siRNA controls.

Together, these results implicate a critical role for components of the NLRP3 inflammasome complex in the IL-1 response to Ti particles in both *in vitro* and *in vivo*.

## D. DISCUSSION

Our results show that Ti wear-particles induce IL-1β cytokine production in both human and mouse macrophages leading to IL-1-associated signaling and subsequent neutrophil recruitment (Figure 3.8). Although Ti is rarely used in bearing surfaces currently, Ti remains an important alloy used in many hip and knee replacements and understanding of the immune response to Ti particles is an important contribution to our understanding the mechanisms of implant loosening and periprosthetic osteolysis. Studies have shown that among failed arthroplasties, patients with cemented Titanium-Aluminum-Vanadium prostheses had the highest amounts of

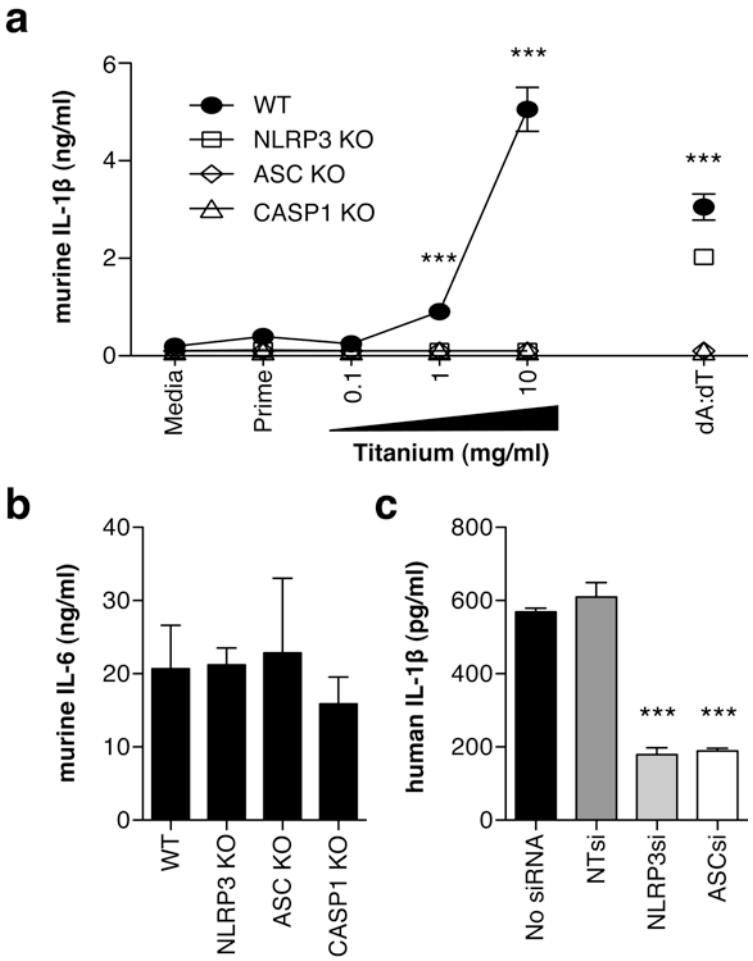


**Figure 3.7: Ti-induced IL-1β secretion is inflammasome-dependent.** (a) IL-1β and (b) IL-6 secretion in WT, NLRP3 KO, ASC KO, and CASP1 KO immortalized mouse macrophages primed for 3 h with LPS (Prime) then stimulated with Ti (10 mg/ml) for 6 h. (c) IL-1β secretion following a 3 h LPS prime and 18 h Ti stimulation (10 mg/ml) in THP-1 human macrophages transfected with siRNA pools specific for NLRP3, ASC, or luciferase (NTsi). Data are representative of at least two separate experiments performed in duplicate. Secreted cytokine levels are means ± s.e.m. Significance values are shown relative to (a) Prime levels or (c) NT-siRNA control levels. P-values are shown as *** ≤ 0.001

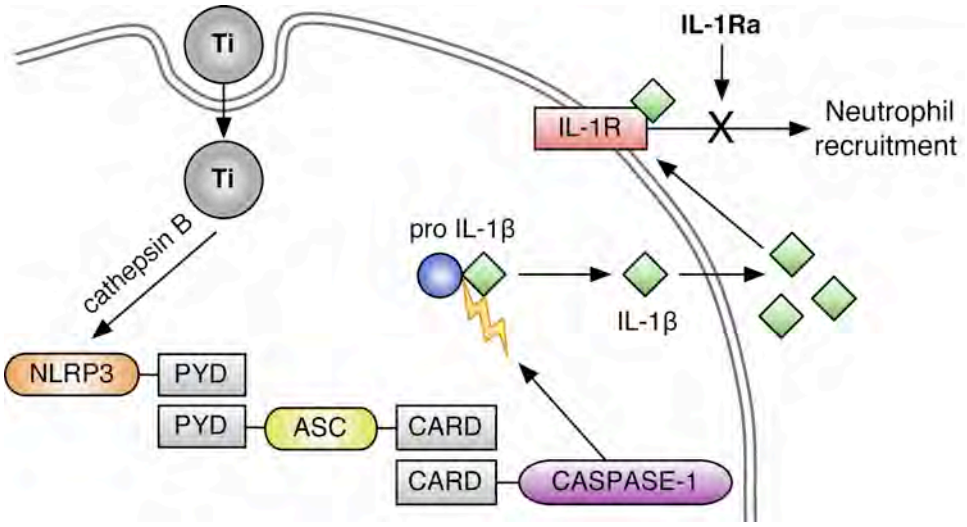


**Figure 3.8: Diagram of Ti induced immune activation.** Ti particle internalization triggers the release of Cathepsin B from lysosomes, which together activate NLRP3. Activated NLRP3 recruits ASC through PYD domain interactions. This complex triggers cleavage and recruitment of activated Caspase-1 through CARD domain interactions. This inflammasome complex then cleaves pro-IL-1β into its active, secreted form IL-1β, which can trigger downstream IL-1 associated signaling, including neutrophil recruitment, through activation of the IL-1R. This acute inflammatory response can be inhibited with IL-1Ra treatment.

IL-1β in serum, compared to patients with cemented implants comprised of other metals, such as Co and Cr (157), which had lower IL-1β serum levels. Additionally, it has been demonstrated that patients with failed cementless total hip arthroplasties have significantly higher levels of TNF, IL-6 and IL-1β and increased macrophage numbers when osteolysis is evident (167). Our data support these findings and suggest a potential mechanism for increases in IL-1β surrounding failed prostheses.

A role for IL-1-associated pro-inflammatory cytokine production following Ti rod implantation has been demonstrated in a murine intramedullary model (160), where a Kirshner wire was implanted into the femur of either WT or IL-1RKO mice along with titanium particles. Mice deficient for the IL-1R exhibited significantly lower levels of pro-inflammatory cytokine production and inflammation. Our studies support these observations and suggest that neutrophil recruitment may also play a role in inflammation. Previous reports have also shown that implantation of $4 \times 10^8$ Ti particles (30 mg) onto the calvarium of mice leads to significant pro-inflammatory cytokine production and bone resorption after only one week (168). Our results show that peritoneal injection of 30 mg of Ti particles induces acute inflammation, as seen by neutrophil recruitment in mice within 16 h through IL-1-associated signaling. These results are consistent with other groups' findings that neutrophils are recruited/activated following stimulation with particles including silica, asbestos, and MSU crystals (104, 105, 126, 127, 169). Our results support the hypothesis that Ti wear-particles activate a pro-inflammatory response in humans through IL-1-associated signaling (Figure 3.8). Additionally, we have shown that neutrophil recruitment following titanium injections

is significantly reduced in mice treated with recombinant IL-1Ra. IL-1Ra, also known as Anakinra ™, has proven to be highly effective at decreasing bone erosion and joint space narrowing in rheumatoid arthritis patients (130-132). Studies have shown that retroviral delivery of IL-1Ra was able to decrease inflammation and inflammatory cytokine production in a murine air pouch model of osteolysis (170). It has also been shown that IL-1Ra treatment diminishes the amount of bone loss in ovariectomized rats and mice (171, 172), a model for post-menopausal osteoporosis. Polymorphisms within the IL-1 gene cluster associated with increased IL-1Ra mRNA expression have also been associated with decreased susceptibility to osteolysis after total hip arthroplasty (173). Along with these results, the ability of IL-1Ra to decrease neutrophilia following Ti injections in mice introduces the potential for antagonist-based therapies for Ti and other wear-particle induced inflammation.

We further demonstrate that Ti particles induce IL-1β secretion through activation of the NLRP3 inflammasome complex (Figure 3.8). The role of the NLRP3 inflammasome in these events is consistent with previous observations in responses to other implant materials, including Co and Cr metal alloys (107). We have also demonstrated a role for cathepsin B in the IL-1β response to Ti particles. This suggests that uptake of Ti particles induces lysosomal destabilization, releasing lysosomal contents and activating NLRP3. Other particulate material, such as silica crystals, have been shown to induce lysosomal destabilization in this manner (104). A role for cathepsin B in implant particle-induced NLRP3 activation has not previously been illustrated. It is also possible that Ti particles induce NLRP3 activation through

production of ROS, as the IL-1β response to Co and Cr metal alloys is significantly diminished in cells treated with the NADPH/ROS inhibitor, DPI (107).

A growing number of systemic inflammatory diseases, characterized by fever, anemia, and elevated levels of acute-phase proteins, have been linked to abnormalities in NLR signaling pathways. It is known that some patients have increased inflammation secondary to particulate debris and are more likely than others to develop osteolysis and subsequent mechanical loosening of the implant ultimately requiring revision joint replacement. The mechanism associated with increased susceptibility remains unclear. Defining the underlying causes of susceptibility to osteolysis will influence the appropriate treatment and management of particulate-induced osteolysis. Taken together, our results increase the understanding of how implant materials, and particulate material in general, interact with the host immune system and provide further insight into the development of treatments for Ti-particle-induced inflammation.

# CHAPTER IV

## Examining the role of surface curvature in innate immune activation by synthetic microparticles

### A. INTRODUCTION

The human immune system is poised to recognize and respond to foreign particulate substances, like crystals, pollen, bacteria and fungal spores. Studies have indicated that following internalization, NLR protein family members are activated, leading to the formation of inflammasomes. The NLRP3 inflammasome has been shown to recognize a variety of particulate material, including silica, asbestos, MSU crystals, and Co/Cr metal alloys (104-107). The physical and chemical characteristics that determine the response to different particles, however, are unclear. Pioneering work from Mitragotri's group (139) and subsequent studies (139, 174-179), have clearly demonstrated that the *shape* of a polymer microparticle has dramatic effects on the processes of phagocytosis and immune activation. The local curvature of the particle surface first encountered by the phagocyte dictates whether the actin cup necessary to engulf the particle can be formed (139). While a striking correlation between geometry and engulfment rate was reported for "simple" particle shapes (i.e., ellipsoids, discs) (139) there has been no systematic study of how phagocytic rates and immune signaling vary with complex particle shapes. Furthermore, the questions of how complex particle shapes influence these processes, as well as how particle morphology dictates the immune response, have not been addressed. Our understanding of these effects remains

fairly limited, primarily because it has been difficult until recently to produce uniform microparticles with controlled surface chemistry and systematically varying shapes.

We have previously developed a method to create polymeric microparticles with complex, but well-controlled, surface morphologies that relies on emulsion processing of amphiphilic block copolymers such as polystyrene-block-poly(ethylene oxide) (PS-PEO) (180). This system provides a simple platform to tune particle morphology independent of other material properties. Using this technique, formation of these particles is highly reproducible, with at least 90% of the particles in any batch forming the same morphology, and consistent from sample to sample. The surface protrusions associated with particles also show a characteristic, and uniform size and density that depends on processing conditions.

Using this novel micro-capillary flow focusing technique, we aimed to define the role of microparticle shape in activating the immune response, which has important implications for engineering of delivery vehicles and implant materials. We compared the ability of particles with different surface structure to be phagocytosed by mouse macrophages. We also examined how particle morphology influences the level of immune cell activation and inflammasome activity through IL-1β cytokine release. Finally, we characterized the ability of particles with varying shapes to induce acute inflammation via neutrophil recruitment in a mouse model.

By systematically varying particle size, shape and surface texturing it should be possible to design particles with optimal immune inducing activity for their desired target usage. Thus, particles for use as vaccine adjuvants could have physical properties

to maximize uptake and the subsequent immune response, while particles used for drug or siRNA delivery could have properties that maximize biodistribution but minimize phagocytic uptake and degradation, allowing slow release of drugs in targeted tissues.

## B. MATERIALS AND METHODS

### Microparticle sample preparation:

Generation of solvent-in-water emulsion droplets of well-controlled sizes, flow-focusing, and particle suspensions were conducted as previously described (181). The resulting suspensions of PS-PEO microparticles were dialyzed against deionized water for 2 – 3 days to remove glycerol and residual chloroform. Budding and spherical particles used in this study were approximately 7-8 μm in diameter.

### Scanning Electron Microscopy (SEM):

Microparticle morphologies were observed by SEM. Particles were placed onto a layer of conductive carbon tape and then coated with a 4 nm layer of iridium metal. The images were acquired on a FEI Quanta 200 FEG MKII scanning electron at an accelerating voltage of 10kV. Images were analyzed using FEI Scandium software.

### Cell culture:

Immortalized mouse macrophages from WT, NLRP3-deficient, ASC-deficient, and Caspase-1-deficient mice were made as previously described (104) and grown in DMEM supplemented with 10% FCS, 1% L-glutamine, and 1% penicillin/streptomycin

at 37˚C with 5% $CO_2$. Cells were plated in media supplemented with GM-CSF (1 ng/ml; eBioscience) for 18 h prior to stimulation.

**Cell Stimulations:**

For particle stimulations, mouse macrophages (4-5 x $10^5$) were primed for 3 h with LPS (100 ng/ml; Sigma) to up-regulate pro-IL-1β expression or left unprimed (Media), then stimulated with microparticles (budding or spherical) at given concentrations (μg/ml), or transfected with 400 ng of poly(dA:dT) (Sigma) using GeneJuice (EMD Chemicals) for an additional 6 h.

**Confocal Microscopy:**

Cells were cultured on glass-bottom 35-mm tissue-culture dishes (MatTek) in complete medium. Images were taken on a Leica SP2 AOBS confocal laser-scanning microscope with a 63x objective, using Leica Confocal Software. Multicolor images were acquired by sequential scanning with only one laser active per scan to avoid cross-excitation. Overall brightness and contrast of images were optimized using Adobe Photoshop CS3.

**Mice injections:**

C57BL/6 (WT) and IL-1R-deficient (IL-1R KO - 96% C57BL/6 background based on microsatellite analysis) were obtained from Jackson Laboratories (Bar Harbor,

ME). All mouse strains, along with age and sex-matched controls, were bred and maintained in the animal facilities at the University of Massachusetts Medical School.

Mice were injected i.p. with sterile PBS (400 μl), 4% thioglycolate (1 ml), or 450 μg of microparticles (300 μl at 1.5 mg/ml). Mice were sacrificed by isoflurane inhalation followed by cervical dislocation. PECs were isolated 6 or 16 h after injections as previously described (127). All experiments involving live animals were in accordance with guidelines set forth by the University of Massachusetts Medical School Department of Animal Medicine and the Institutional Animal Care and Use Committee.

**Flow cytometric analysis:**

To enumerate neutrophils, PECs ($1x10^6$) were incubated with anti-CD16/CD32 monoclonal antibody (clone 2.4G2; BD Biosciences) for 30 minutes to block FcγRIIB/III receptors and stained with Ly6G-FITC (BD Biosciences) and 7/4-Alexa647 (AbD Serotec) for 30 minutes at 4°C. Following staining, cells were washed with PBS and analyzed on a LSRII (BD Biosciences). Neutrophil numbers in PECs were calculated by multiplying total cell numbers by the percentage of Ly6G+, 7/4+ cells. Data were acquired by DIVA (BD Biosciences) and were analyzed with FlowJo 8.8.6 software (Tree Star Inc.).

**Statistical Analysis:**

An unpaired, two-tailed Student's t-test was used to determine statistical significance of independent experiments where two groups were compared. When more than two groups were compared, a one-way ANOVA or two-way ANOVA followed by Bonferroni's correction for post test comparisons was used. Values of $p < 0.05$ were considered significant. Statistics were performed using GraphPad (Prism v5.0a) software.

## C. RESULTS

### Budding particles are more likely to be associated with and internalized in mouse macrophages than spherical particles.

It has been well established that part of the inflammatory response to particulate material involves the uptake of particles by macrophages. Recent studies have indicated that macrophages are more likely to internalize particles containing regions of high surface curvature, compared to those with low or no surface curvature (139). Additionally, particulates, such as alum and polystyrene, have been shown to induce inflammatory responses in mouse dendritic cells (182). In order to examine this further, we generated PS-PEO polymer microparticles of phagocytosable size (7-8 μm) exhibiting regions of high surface curvature, budding particles, or low surface curvature, spherical particles (Figure 4.1). To visualize phagocytosis of microparticles, immortalized macrophages from WT mice were incubated with budding or spherical microparticles incorporated with a fluorescent dye, Vibrant DiI, for 6 hours. Using confocal microscopy, we found that a significantly higher percentage of budding

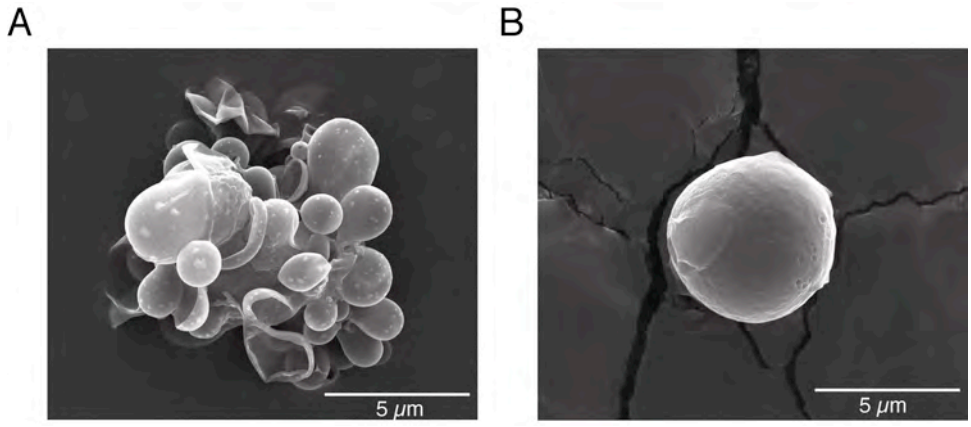


**Figure 4.1: Images of budding and spherical microparticles.** SEM images of (A) budding and (B) spherical particles generated. Scale bars = 5μm.

particles, greater than 85%, were associated with or internalized in macrophages when compared to spherical particles, approximately 20% (Figure 4.2).

**Budding particles associate with more cells on a per particle basis.**

We also examined the number of macrophages associated with each particle. Through confocal microscopy, we found that budding particles were associated with more macrophages on a per particle basis (Figure 4.3b, c), whereas spherical particles were only associated with one macrophage per particle (Figure 4.3a, c). This data is trending towards significance with a p-value of 0.0632. These results suggest that particles with higher surface curvature are not only more efficiently phagocytosed by macrophages, but that they recruit the 'help' of more cells, which may play important roles in cellular activation and subsequent immune responses.

**Budding particles stimulate more IL-1β than spherical particles.**

In order to determine if uptake efficiency played a role in the subsequent immune response to budding and spherical particles, we analyzed the response of murine macrophages to microparticles. Immortalized macrophages from WT mice were primed for 3 hours with LPS to induce up-regulation of pro-IL-1β transcription, then incubated with budding or spherical microparticles for 6 hours to assess pro-IL-1β processing to mature IL-1β. Levels of mature, secreted IL-1β were measured via ELISA using cell supernatants. WT macrophages responded to both types of microparticles in a dose-dependent manner with significantly higher levels of secreted

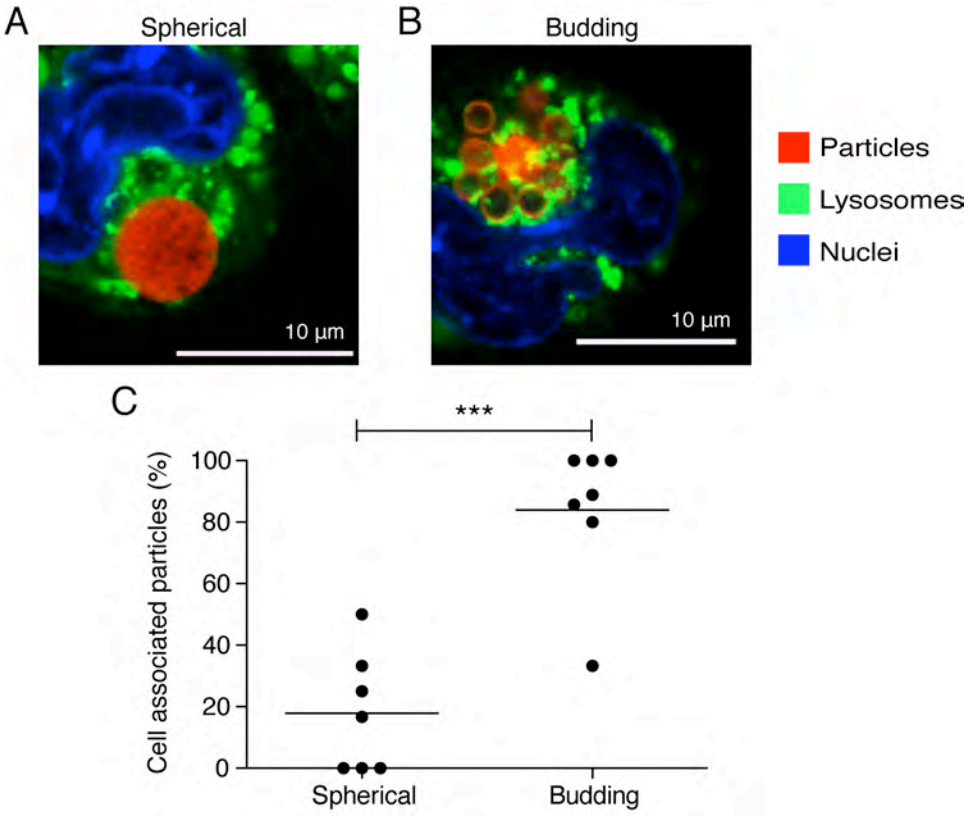


**Figure 4.2: Budding particles are more efficiently phagocytosed by macrophages.** Confocal microscopy images of macrophage-phagocytosed spherical (A) and budding (B) particles. Lysosomes were visualized with LysoTracker Green (Molecular Probes). Nuclei were visualized with Hoechst 34580 (Molecular Probes). (C) Graph shows the percent of and average (line) particles associated with cells per field of view. Analysis was performed on seven independent fields of view per particle type. Scale bars = 10 µm. P-value shown as ***<0.0001.

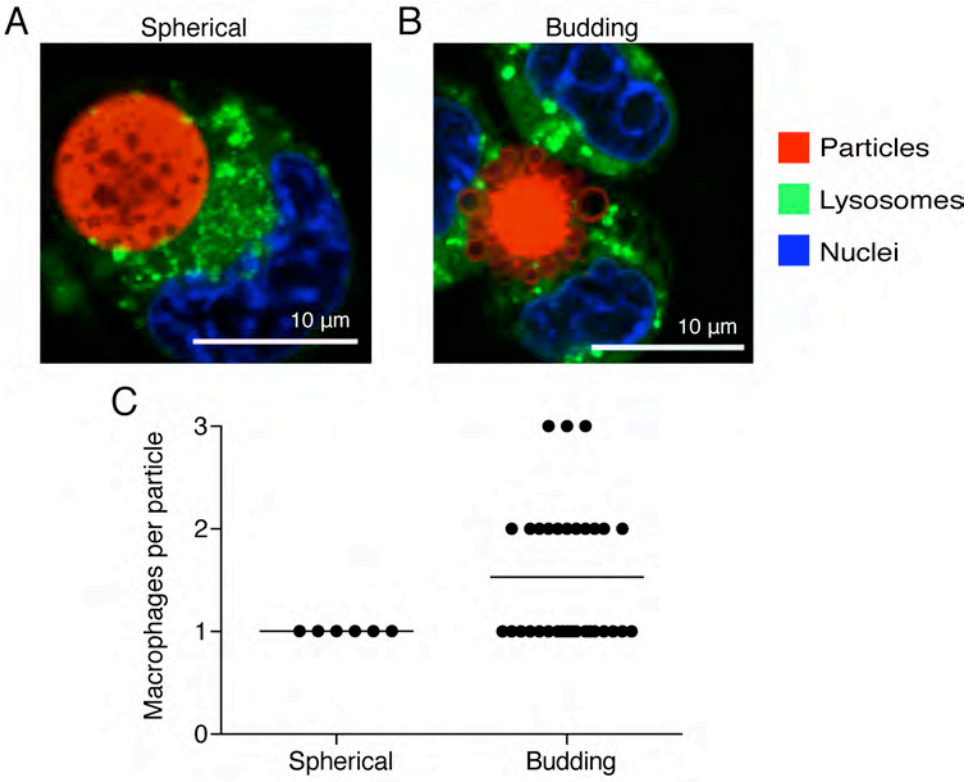


**Figure 4.3: Budding particles associate with more macrophages on a per particle basis.** Confocal microscopy images of macrophages associated with spherical (A) and budding (B) particles. Lysosomes were visualized with LysoTracker Green (Molecular Probes). Nuclei were visualized with Hoechst 34580 (Molecular Probes). (C) Total and average (line) number of macrophages associated with a single particle per field of view. Analysis was performed on seven independent fields of view per particle type. Scale bars = 10 µm.

IL-1β compared to priming alone at the 100 μg/ml dose for both particles as well as the 50 μg/ml dose for budding particles (Figure 4.4a). We also found that budding particles were able to induce significantly higher levels of IL-1β secretion (Figure 4.4a, black bars) compared to spherical particles (Figure 4.4a, white bars). As a positive control, macrophages were transfected with synthetic double-stranded DNA, poly-dA:dT (dA:dT). WT macrophages produced a significant amount of IL-1β in response to dA:dT stimulation (Figure 4.4b). As negative controls, supernatants from macrophages that received media (Media) or an LPS prime only (0) did not exhibit an increase in IL-1β production (Figure 4.4b).

**Microparticle-induced IL-1β production requires the NLRP3 inflammasome.**

Several NLR proteins have been implicated in inflammasome complex formation. More specifically, it has been shown that the NLRP3 inflammasome plays a role in the response to particulate materials (104, 105, 127, 182). In order to determine if the NLRP3 inflammasome signaling complex was also involved in the immune response to polystyrene particles in macrophages, immortalized macrophages generated from NLRP3 KO, ASC KO, and CASP1 KO deficient mice were analyzed for IL-1β production in response to microparticle stimulation. Supernatants from NLRP3 KO, ASC KO, and CASP1 KO macrophages each exhibited undetectable levels of secreted IL-β in response to budding and spherical microparticles while IL-1β secretion from WT macrophages was readily detected (Figure 4.5a). As expected, NLRP3 KO

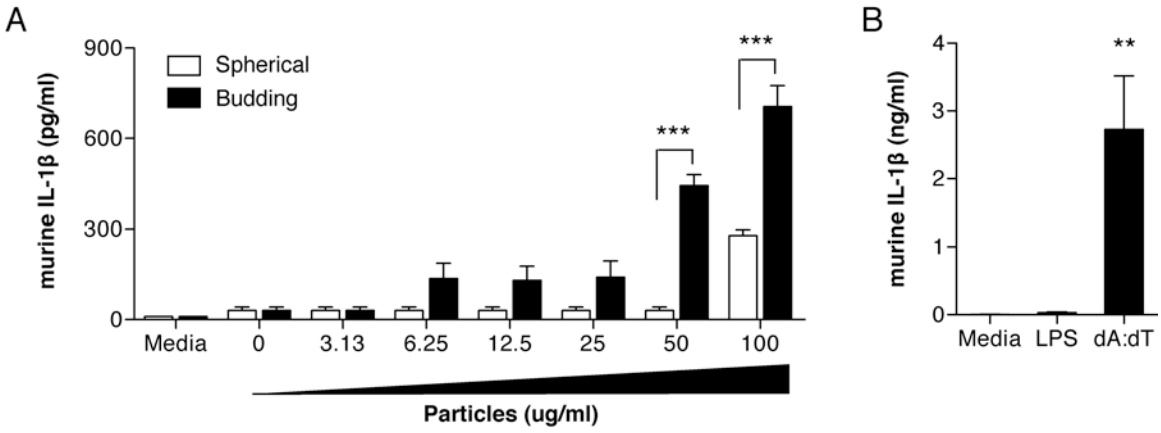


**Figure 4.4: Particle-induced IL-1β cytokine secretion is dependent on surface curvature.** WT immortalized mouse macrophages were primed with LPS for 3 h (0) or left unprimed (Media), then stimulated for 6 h with increasing concentrations of budding (black bars) or spherical (white bars) particles (μg/ml) (A) or transfected with 400 ng poly dA:dT (B). Data are representative at least two separate experiments performed in duplicate. Secreted IL-1β levels are mean ± s.e.m. Significance values are shown as budding versus spherical. P-values are shown as *** ≤ 0.0001, ** ≤ 0.01.

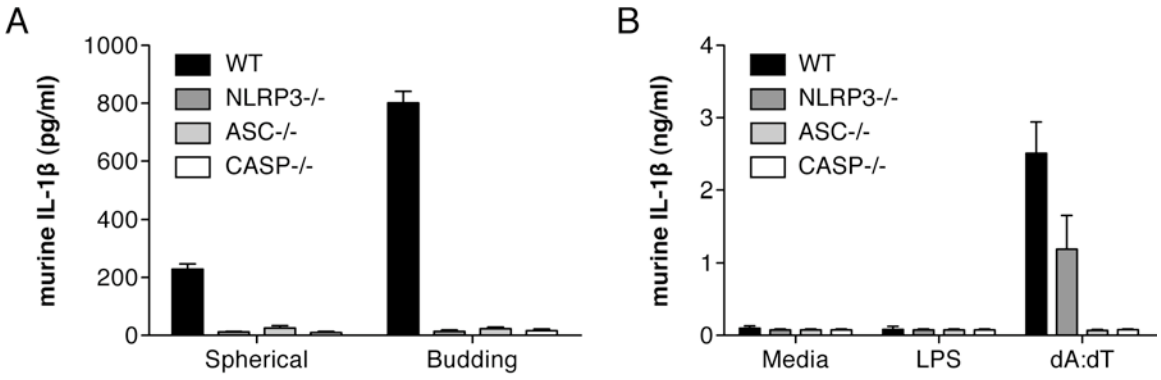


**Figure 4.5: Particle-induced IL-1β cytokine secretion requires the NLRP3 inflammasome.** Immortalized mouse macrophages from WT, NLRP3 KO (NLRP-/-), ASC KO (ASC-/-), and CASP1 KO (CASP1-/-) mice were primed for 3 h with LPS then stimulated with 100 μg/ml spherical or budding microparticles for 6 h (A) or transfected with poly dA:dT (B). Data are representative of at least two separate experiments performed in duplicate. Secreted cytokine levels are mean ± s.e.m.

macrophages were able to respond to dA:dT similar to WT cells, while ASC KO and CASP1 KO macrophages were unable to respond to dA:dT (Figure 4.5b).

**Budding particles stimulate a more robust neutrophil response at early time points.**

Previous studies have shown that i.p. injections of MSU crystals lead to an increase in neutrophil recruitment and that this recruitment was dependent on the expression of the IL-1R(127). In order to determine whether microparticles induced a similar increase in neutrophil recruitment, WT mice were injected i.p. with budding or spherical particles (450 μg) and the peritoneal cavity was analyzed for neutrophil influx 6 or 16 h later. Budding particles induced a more robust neutrophil response (Ly6G+, 7/4+ cells) than spherical particles at 6 h following injection (Figure 4.6) at levels similar to injection with the positive control, thioglycolate (Figure 4.6a). By 16 h post injection, both budding and spherical particles induced a similar increase in neutrophils that was significantly higher than the PBS-carrier only control (Figure 4.6b). These results indicate a direct relationship between high IL-1β production *in vitro* and high neutrophil recuitment *in vivo* in the immune response to particulate material, specifically polystyrene microparticles.

**Microparticle-induced neutrophil recruitment involves IL-1-associated signaling.**

The IL-1R has been shown to be required for neutrophil recruitment following

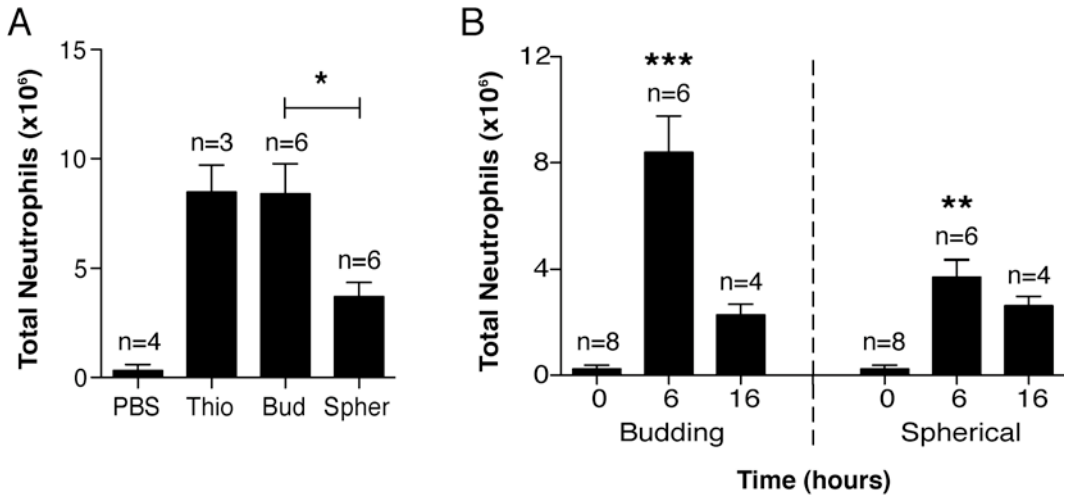


**Figure 4.6: Levels of neutrophil recruitment following particle injections depends on surface curvature.** Flow cytometric analysis on peritoneal neutrophil (Ly6G+, 7/4+ cells) recruitment 6 h (A) or 0, 6, and 16 h (B) after microparticle (450 μg) injections in WT (C57BL/6) mice. Peritoneal neutrophil numbers were compared to PBS only (PBS or 0) or thioglycolate (Thio) controls. Data are representative of at least two separate experiments. Graphs show mean ± s.e.m of number of mice indicated. Significance values are shown as budding versus spherical (A) or timed particle versus time 0 injections (B). P-values are shown as *** ≤ 0.0001; ** < 0.01; * < 0.05

exposure to stimulants in mice (104, 126, 127). To determine whether expression of IL-1R was required for microparticle-induced neutrophil influx, IL-1R KO mice were injected with budding or spherical particles for 16 h and compared to WT mice. As expected, microparticle injections were unable to induce a neutrophil influx in IL-1R KO mice (Figure 4.7). These results suggest that surface curvature plays a critical role in both the *in vitro* and *in vivo* response to polymeric microparticles, where high surface curvature leads to increased internalization, increased IL-1β cytokine production, and a more robust neutrophil response.

## D. DISCUSSION

This study illustrates a significant role for surface curvature in polymer microparticle-induced stimulation, both *in vitro* and *in vivo*. We have shown that large (7-8 μm) polymer particles are efficiently phagocytosed by macrophages. Interestingly, greater than 80% of budding particles were found associated with macrophages compared to 20% of spherical particles under the same conditions. We also noted higher concentrations of lysosomes surrounding the engulfed budding particles (Figure 4.2b) suggesting that the budding particles trigger a stronger cellular response. A recent study indicated that macrophages are more likely to internalize particles if they contain regions of high surface curvature compared to regions of low or no surface curvature (139). Therefore, it is possible that the budding particles are more likely to be phagocytosed because they contain higher local surface curvature compared to spherical particles.

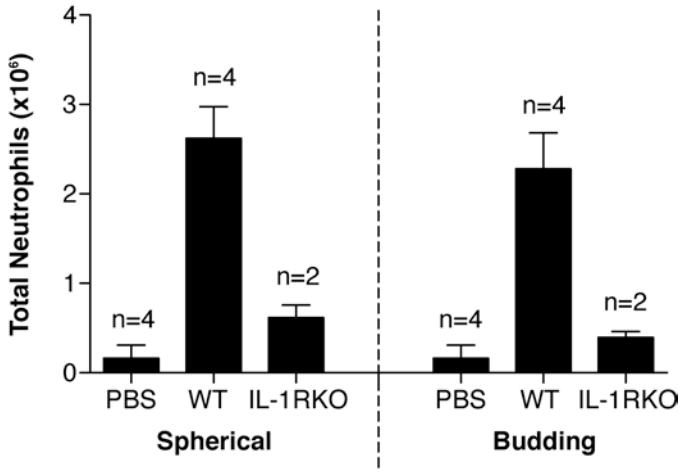


**Figure 4.7: Particle-induced neutrophil recruitment requires IL-1-associated signaling.** Flow cytometric analysis on peritoneal neutrophil (Ly6G+, 7/4+ cells) recruitment 16 h after microparticle (450 μg) injections in WT or IL-1RKO mice. Data are representative of two separate experiments. Graphs show mean ± s.e.m of the number of mice indicated.

We have also shown that budding particles induce a significantly more robust innate immune response in immortalized mouse macrophages. Furthermore, this response is dependent on components of the NLRP3 inflammasome signaling pathway, similar to that seen with other particulate stimuli (104, 105, 127). Recent work has shown that polymer particles measuring 1 μm in diameter stimulate higher amounts of IL-1β than larger particles of the same composition (182). Based on this, our results suggest that budding particles induce higher levels of IL-1β secretion than spherical particles because the macrophage senses the "buds" as smaller particles.

Budding particles induce a higher neutrophil response at early time points (6 h) after peritoneal injections than spherical particles. Conversely, both types of particles are able to induce similar levels of neutrophil recruitment by 16 h after injection. These results suggest that budding particles are able to induce immune responses faster *in vivo*, but that this increased induction is not sustained and spherical particles will ultimately stimulate similar induction levels. This may be a result of the fact that budding particles are more likely to be phagocytosed by macrophages and induce higher levels of cytokines, when compared to spherical particles.

We, and others, have demonstrated a critical role for IL-1-associated signaling in neutrophil responses following injections of particulate stimuli (104, 105, 127). Here we show that IL-1R KO mice exhibit a diminished neutrophil response following microparticle injections, further implicating IL-1 signaling in the innate immune response to budding and spherical polymer microparticles.

Overall, this data has broad implications for the future development of vaccine adjuvants and therapeutic delivery agents, as variation in surface curvature will modulate the resultant immune response. We suggest that particles with low surface curvature would be ideal for use as delivery vehicles, as they exhibit a low level of uptake and induce a slow immune response, and thus, may exhibit a broader biodistribution, ideal for delivery of therapeutic agents. On the other hand, we suggest that particles with high surface curvature would be ideal for the use as vaccine adjuvants, as they are more efficiently phagocytosed in cells and induce a more robust immune response.

# CHAPTER V

## A. SUMMARY

Endocytotic and phagocytotic pathways are important for many cellular functions including cell maintenance, cell survival, receptor recycling, receptor signaling, antigen presentation, and protection from extracellular pathogens. Both pathways involve receptor binding at the surface of the cell followed by internalization and movement through portions of the endosomal pathway.

In this dissertation, the differences between antibody-mediated and ligand-mediated internalization of cell surface proteins were examined. Results indicate that antibodies directed to cell surface proteins will divert internalization and localization to compartments associated with the degradative endosomal pathway. This has broad applicability for antibody therapeutics and antibody-based delivery vehicles. Work described here also examined the immune response to titanium wear-particles. Results show that phagocytosed titanium particles generated from joint replacements activate the NLRP3 inflammasome, leading to pro-inflammatory cytokine production and neutrophil recruitment. Further understanding the basis for joint replacement failure may aid in the development of specific treatments for affected patients. Finally, the role of surface curvature in the immune response to polymeric microparticles was examined. Results indicate that surface curvature plays a pronounced role, independent of chemical composition and surface ligand recognition, in the immune response to phagocytosed microparticles. This data may help guide the development of future particulate-based delivery vehicles and adjuvants. Overall, work on the above projects

demonstrates how basic cell functions, such as endocytosis and phagocytosis (and their downstream effects) can be utilized to develop therapeutics against a variety of diseases, including cancers, viral infections, periprosthetic osteolysis, and more.

In the first chapter, the ability of antibodies to mediate internalization of cell surface-expressed target proteins through receptor-mediated endocytosis was examined. Although antibodies have most commonly been utilized to target specific cells for Fc-mediated killing, in recent years, antibodies have also been utilized to mediate internalization and degradation of target proteins and to deliver a variety of therapeutic agents to a preferred subset of cells. Some of these approaches involve targeting cell surface receptor proteins expressed by tumors or viral proteins selectively expressed on infected cells. This defined targeting of antibodies has been shown to mediate internalization of β-amyloid from the surface of neuronal cells (80, 82-84), to deliver anti-tumor drugs using tumor-specific cell markers (81, 87, 88), and to deliver antiviral siRNAs exclusively to infected cells (79, 92).

It has been suggested that in order for an antibody therapeutic to be efficacious at either mediating down-regulation of the surface proteins, or to deliver drugs or siRNAs into the cytoplasm of cells, it must internalize through a degradation pathway, including localization with low pH compartments, such as late endosomes and lysosomes, where the drugs would be released from the antibody or the target protein will be degraded (78-80). Through examination of a variety of antibody-mediated delivery studies, it was clear that most antibody-protein conjugates were delivered to a degradative compartment. Due to the broad-range of cell surface proteins that have

been successfully utilized for antibody-based internalization or delivery, we hypothesized that one may not have to choose therapeutic targets based on their natural localization to degradative endosomes following internalization, but that perhaps, antibody binding would divert internalization of cell surface proteins, to some extent, through this pathway.

The transferrin receptor is expressed on most cell types, including cells in the brain and is highly expressed in tumor cells (183). As such, groups have studied the ability to use the TfR as a therapeutic target. Some groups have looked at conjugating drugs or DNA to Tf to mediate delivery into cells, while other groups have examined conjugating drugs or DNA to antibodies specific for the TfR (183). We examined whether an antibody specific for the TfR could divert internalization of the protein into a degradation pathway. When bound to its natural ligand, transferrin, the receptor progressively co-localizes with clathrin, followed by the early endosomal proteins Rab5a, Rab4, and the recycling endosomal marker Rab11. If binding of an antibody to the TfR could divert localization to include late endosomes, this would suggest that antibody binding alone could guide internalization through a degradation internalization pathway.

Using an antibody specific for the exofacial, or extracellular, domain of the TfR, αCD71, the internalization of the TfR/αCD71 complex based on its localization to endosomal proteins was examined. Although localization to recycling-associated endosomes remained intact following antibody binding, the TfR/αCD71 complex was also diverted to include localization with the late endosomal marker, Rab9, in

agreement with our hypothesis. This indicates that antibody binding can induce a shift in endosomal localization to degradation endosomes, even if the 'natural-ligand' mediated pathway does not include these compartments.

Taking advantage of the ability of antibodies and antibody-conjugates to bind to and subsequently internalize target proteins expressed on the surface of a particular subset of cells could also be utilized for the treatment of a variety of viral infections, by specifically targeting infected cells. As such, the antibody-mediated internalization pattern of rabies G expressed on the surface of mouse neuroblastoma cells, to mimic an infected cell state (154), was characterized. Rabies virus infections occur in over 100 countries and territories and are fatal once symptoms develop (153). To prevent development of the disease, treatment of exposed individuals includes administration of the rabies vaccine and human rabies immune globulin, which helps to neutralize the virus.

There are several ways that rabies G-specific antibodies have been shown to mediate inhibition of the virus. Neutralizing antibodies can bind to the virion-expressed glycoprotein to either block infection of target cells or to inhibit escape of the virus from endosomal compartments following entry (184), an important step in viral uncoating. Antibodies can also bind to rabies G expressed on the surface of infected cells to inhibit cell-to-cell spread (185). Given that other virus-specific antibody therapeutics have been used for either down regulation of viral glycoproteins or to introduce virus specific siRNAs to cells (79, 92), the ability of an antibody binding to rabies G to induce internalization and localization of the protein to degradative

endosomal compartments was examined. Using a humanized monoclonal antibody specific for rabies G, ARG1, we found that the ARG1/rabies G complex exhibited an internalization pathway similar to that of the antibody-bound TfR, including localization with endosomal compartments associated with the degradation pathway, including Rab5a, Rab9, and lysosomes.

Although these studies suggest that antibodies bound to cell surface proteins can mediate localization to degradative compartments within a cell, it would be of great interest to examine how these antibodies are guiding this internalization pathway. Studies have shown that internalization of plasma membrane receptors through a degradation pathway involves ubiquitination. The EGF receptor, for example, is ubiquitinated by the ubiquitin ligase c-Cbl following ligand binding, which induces internalization and sorting of the receptor to multivesicular bodies (186-188). It is possible that when an antibody binds to a cell surface protein/receptor like the TfR or rabies G, a signal for ubiquitination is induced.

This potential mechanism does not address why fluorescent antibody bound to the TfR is localized to compartments associated with both the recycling pathway and degradative pathway. One simple explanation might be that the observed localization to degradative endosomes is simply a visualization of antibody no longer complexed to the TfR. However, preliminary data using fluorescent TfR-expressing cells has shown that fluorescent antibody remains complexed with the receptor throughout the time course examined in the above studies (data not shown). Therefore, it is unlikely that localization to late endosomes is a visualization of antibody alone. Further

characterization of the signaling mechanisms involved following binding of the TfR to antibody, including the cytosolic proteins involved, would help increase the general understanding of how different ligands bound to TfR, in this case antibody versus Tf, can mediate differential localization to certain endosomal compartments.

In the next two chapters, the downstream signaling events involved following phagocytosis of particulate material in macrophages were examined. As previously mentioned, phagocytosis can occur through binding of opsonized particles to complement-receptors and Fc-receptors, or through binding of particles to PRRs, including TLRs, mannose receptors, and scavenger receptors, expressed on the surface of immune cells, including macrophages. Binding to these receptors stimulates intracellular signaling events associated with the immune response as well as eventual internalization of the particles. Following phagocytosis, particulate material such as silica, asbestos, MSU crystals, and cobalt/chromium metal alloys activate NLRP3 (104-107), a NOD-like receptor protein located in the cytosol of macrophages. Activation of the NLRP3 inflammasome pathway results in the cleavage of pro-IL-1β into its mature secreted form, IL-1β. In this dissertation, uptake, inflammasome activation, and subsequent immune responses to two clinically relevant particulate materials, titanium and polymeric microparticles, were examined.

Osteolysis, or degradation, of bone following total joint replacements is a major clinical problem. Examination of the areas surrounding failed implants has indicated an increase in wear particles, including titanium particles, as well as an increase in the bone-resorption-inducing cytokine, IL-1β. Here, we've shown that titanium particles

injected into the peritoneum of mice induced neutrophil recruitment that was dependent on the expression of the IL-1 receptor (IL-1R) and IL-1α/β. Moreover, treatment with the IL-1R antagonist (IL-1Ra) diminished this response. *In vitro*, titanium-induced IL-1β secretion from macrophages was dependent on the expression of components of the NLRP3 inflammasome. Together, these results suggest that titanium wear-particle induced inflammation and subsequent joint replacement failure may be due to activation of the NLRP3 inflammasome, leading to increased IL-1β secretion and IL-1 associated signaling.

Our data, and the work of others, indicate that the NLRP3 inflammasome signaling pathway is critical in the host response to implant materials, including titanium, cobalt, and chromium (107). It is known that certain patients have increased inflammation secondary to particulate debris and are more likely than others to develop osteolysis and subsequent mechanical loosening of the implant ultimately requiring revision surgery. Until recently, the mechanism associated with increased (or decreased) susceptibility has been unclear. A growing number of systemic inflammatory diseases, characterized by fever, anemia, and elevated levels of acute-phase proteins, have been linked to abnormalities in NLR signaling pathways, as exemplified by the 'cryopyrinopathies', also termed 'the CIAS1-associated periodic syndromes' (reviewed in (115)). These cryopyrinopathies constitute a subfamily of the hereditary periodic fever syndromes, and the clinical presentation includes unexplained episodes of fever and severe localized inflammation, including arthritis and joint destruction. One study has shown that patients containing a polymorphism in the IL-

1Ra gene exhibit decreased susceptibility to osteolysis following a cemented, polyethylene-on-metal total hip arthroplasty (173). This data suggests that patients who are more susceptible to joint inflammation may express polymorphisms in inflammasome-related genes that predispose to this condition, analogous to cryopyrinopathies like Muckle-Wells syndrome which is characterized by spontaneous secretion of active IL-1β (114).

Defining the underlying causes of osteolysis following joint replacements will influence the appropriate treatment and management of particulate-induced osteolysis and possibly identify those patients at high risk for this condition pre-operatively before the primary total joint replacement. For example, these patients at increased risk may benefit from IL-1R antagonists as prophylaxis or treatment at the time of joint replacement. In an ideal situation, different polymorphisms will be associated with the response to different implant materials. This would allow surgeons to specifically select the implant material that would cause the least amount of damage long-term. A more realistic outcome, however, is that all susceptible patients exhibit a variety of polymorphisms associated with NLR- or IL-1-associated genes. At the very least, patients identified as 'high-risk' can be watched more closely for potential inflammation and, if it occurs, can be treated appropriately.

Polymeric microparticles have been investigated as platforms for drug delivery, adjuvants, and as imaging contrast agents. Due to the increased use of these types of particles in a variety of clinical settings, it is important to understand how physical characteristics, including size and shape, of these particles play a role in uptake

efficiency and subsequent immune cell activation. Certain types of particles are phagocytosed by macrophages more efficiently than others. Different particles can also induce significant inflammation or may be relatively well tolerated. The physical and chemical characteristics that determine these responses are unclear.

Our results indicate that particles with high surface curvature (budding particles) are phagocytosed by macrophages at a higher frequency than particles with low surface curvature (spherical particles). The efficiency with which a particle is phagocytosed can play a major role in efficacy of either a delivery vehicle or a vaccine adjuvant. For example, if a particle is to be used as a vaccine adjuvant, it is important that efficient phagocytosis takes place, allowing antigens to be presented in MHC complexes on antigen presenting cells. However, if a particle is designed for delivery to a particular subset of non-immune cells, rapid phagocytosis by macrophages can be problematic, since it would lead to accumulation in the undesired cell type, decreasing delivery to target cells. This data suggests that particles that exhibit characteristics similar to budding particles would be optimal as vaccine adjuvants, as they are more likely to be phagocytosed by macrophages. Conversely, particles destined for delivery vehicles should exhibit characteristics similar to spherical particles, which exhibit lower levels of macrophage uptake.

Remarkably, budding particles also induced stronger IL-1β secretion than spherical particles, through activation of the NLRP3 inflammasome-signaling complex. Additionally, compared to spherical particles, budding particles induced more rapid IL-1-dependent neutrophil recruitment *in vivo* to the injection site. Recent findings by

Sharp et al. has suggested that particles within the range of 0.5-1 μm in diameter induce the highest amount of IL-1β in dendritic cells following phagocytosis (182). Although the overall diameter of the budding and spherical particles ranged between 7-8 μm, the 'buds' on the budding particles averaged a relative diameter of about 1-2 μm. It is possible that the budding particles induce a more robust inflammatory response than spherical particles because the macrophage sensed the 'buds' as smaller particles. It would be of interest to directly compare budding particles to small, spherical particles in the range of 0.5-2 μm in diameter to see if uptake efficiency is equivalent and if IL-1β secretion and neutrophil recruitment are at comparable levels.

Adjuvants enhance the ability of vaccines to activate and direct adaptive immune responses. Until recently, the mechanism of how adjuvants drive innate and adaptive immune responses was unclear. The commonly used particulate adjuvant, Alum, has now been shown to induce IL-1β cytokine production in a NLRP3 inflammasome-dependent manner (189, 190). Studies have also shown that the production of pro-inflammatory cytokines, including IL-1, is essential to induce fully active T cell responses and promote protective immunity in mice challenged with a specific antigen (191, 192). When combined with IL-2, IL-1β induces optimal proliferation of naïve CD4+ T cells in response to antigen (191). This data suggests that particulate adjuvants, like Alum, may exhibit their effect in part through activation of the NLRP3 inflammasome to produce active IL-1β, which can, in turn, induce a more robust CD4+ T cell response. Since budding and spherical particles induce different levels of IL-1β secretion and early neutrophil recruitment, it would be of interest to

examine if these characteristics play a role in the level of CD4+ T cell activation. More specifically, it would be of interest to determine whether budding particles would induce a more robust CD4+ T cell response than spherical particles.

Overall, findings in this dissertation have potential applications to not only guide the development of future targeting vehicles for delivery of vaccines, drugs, proteins, and siRNA therapeutics but also to develop more specific treatments for patients suffering from particulate-induced inflammation and bone loss.

# CHAPTER VI

## References


1. Mellman, I. 1996. Endocytosis and molecular sorting. *Annu Rev Cell Dev Biol* 12:575-625.
2. Mayor, S., and R.E. Pagano. 2007. Pathways of clathrin-independent endocytosis. *Nat Rev Mol Cell Biol* 8:603-612.
3. Kirkham, M., A. Fujita, R. Chadda, S.J. Nixon, T.V. Kurzchalia, D.K. Sharma, R.E. Pagano, J.F. Hancock, S. Mayor, and R.G. Parton. 2005. Ultrastructural identification of uncoated caveolin-independent early endocytic vehicles. *J Cell Biol* 168:465-476.
4. Kirkham, M., and R.G. Parton. 2005. Clathrin-independent endocytosis: new insights into caveolae and non-caveolar lipid raft carriers. *Biochim Biophys Acta* 1746:349-363.
5. Sabharanjak, S., P. Sharma, R.G. Parton, and S. Mayor. 2002. GPI-anchored proteins are delivered to recycling endosomes via a distinct cdc42-regulated, clathrin-independent pinocytic pathway. *Dev Cell* 2:411-423.
6. Mukherjee, S., R.N. Ghosh, and F.R. Maxfield. 1997. Endocytosis. *Physiol Rev* 77:759-803.
7. Aderem, A., and D.M. Underhill. 1999. Mechanisms of phagocytosis in macrophages. *Annu Rev Immunol* 17:593-623.
8. Rabinovitch, M. 1995. Professional and non-professional phagocytes: an introduction. *Trends Cell Biol* 5:85-87.

9. Tjelle, T.E., T. Lovdal, and T. Berg. 2000. Phagosome dynamics and function. *Bioessays* 22:255-263.

10. Fratti, R.A., J.M. Backer, J. Gruenberg, S. Corvera, and V. Deretic. 2001. Role of phosphatidylinositol 3-kinase and Rab5 effectors in phagosomal biogenesis and mycobacterial phagosome maturation arrest. *J Cell Biol* 154:631-644.

11. Underhill, D.M., and A. Ozinsky. 2002. Phagocytosis of microbes: complexity in action. *Annu Rev Immunol* 20:825-852.

12. Janeway, C. 2005. Immunobiology : the immune system in health and disease (pp. 55-75). Garland Science, New York.

13. Ravetch, J.V., and S. Bolland. 2001. IgG Fc receptors. *Annu Rev Immunol* 19:275-290.

14. Ghazizadeh, S., J.B. Bolen, and H.B. Fleit. 1994. Physical and functional association of Src-related protein tyrosine kinases with Fc gamma RII in monocytic THP-1 cells. *J Biol Chem* 269:8878-8884.

15. Cox, D., P. Chang, T. Kurosaki, and S. Greenberg. 1996. Syk tyrosine kinase is required for immunoreceptor tyrosine activation motif-dependent actin assembly. *J Biol Chem* 271:16597-16602.

16. Majeed, M., E. Caveggion, C.A. Lowell, and G. Berton. 2001. Role of Src kinases and Syk in Fcgamma receptor-mediated phagocytosis and phagosome-lysosome fusion. *J Leukoc Biol* 70:801-811.

17. Mukhopadhyay, S., and S. Gordon. 2004. The role of scavenger receptors in pathogen recognition and innate immunity. *Immunobiology* 209:39-49.

18. Palecanda, A., J. Paulauskis, E. Al-Mutairi, A. Imrich, G. Qin, H. Suzuki, T. Kodama, K. Tryggvason, H. Koziel, and L. Kobzik. 1999. Role of the scavenger receptor MARCO in alveolar macrophage binding of unopsonized environmental particles. *J Exp Med* 189:1497-1506.

19. Krieger, M., and J. Herz. 1994. Structures and functions of multiligand lipoprotein receptors: macrophage scavenger receptors and LDL receptor-related protein (LRP). *Annu Rev Biochem* 63:601-637.

20. Pearson, A.M. 1996. Scavenger receptors in innate immunity. *Curr Opin Immunol* 8:20-28.

21. Elomaa, O., M. Kangas, C. Sahlberg, J. Tuukkanen, R. Sormunen, A. Liakka, I. Thesleff, G. Kraal, and K. Tryggvason. 1995. Cloning of a novel bacteria-binding receptor structurally related to scavenger receptors and expressed in a subset of macrophages. *Cell* 80:603-609.

22. Hamilton, R.F., Jr., S.A. Thakur, J.K. Mayfair, and A. Holian. 2006. MARCO mediates silica uptake and toxicity in alveolar macrophages from C57BL/6 mice. *J Biol Chem* 281:34218-34226.

23. Kanno, S., A. Furuyama, and S. Hirano. 2007. A murine scavenger receptor MARCO recognizes polystyrene nanoparticles. *Toxicol Sci* 97:398-406.

24. Ungewickell, E., and D. Branton. 1981. Assembly units of clathrin coats. *Nature* 289:420-422.

25. Smith, C.J., and B.M. Pearse. 1999. Clathrin: anatomy of a coat protein. *Trends Cell Biol* 9:335-338.

26. Rappoport, J.Z., S. Kemal, A. Benmerah, and S.M. Simon. 2006. Dynamics of clathrin and adaptor proteins during endocytosis. *Am J Physiol Cell Physiol* 291:C1072-1081.

27. Rappoport, J.Z., A. Benmerah, and S.M. Simon. 2005. Analysis of the AP-2 adaptor complex and cargo during clathrin-mediated endocytosis. *Traffic* 6:539-547.

28. Hinshaw, J.E. 2000. Dynamin and its role in membrane fission. *Annu Rev Cell Dev Biol* 16:483-519.

29. Ungewickell, E., H. Ungewickell, S.E. Holstein, R. Lindner, K. Prasad, W. Barouch, B. Martin, L.E. Greene, and E. Eisenberg. 1995. Role of auxilin in uncoating clathrin-coated vesicles. *Nature* 378:632-635.

30. Umeda, A., A. Meyerholz, and E. Ungewickell. 2000. Identification of the universal cofactor (auxilin 2) in clathrin coat dissociation. *Eur J Cell Biol* 79:336-342.

31. Lamaze, C., L.M. Fujimoto, H.L. Yin, and S.L. Schmid. 1997. The actin cytoskeleton is required for receptor-mediated endocytosis in mammalian cells. *J Biol Chem* 272:20332-20335.

32. Yarar, D., C.M. Waterman-Storer, and S.L. Schmid. 2005. A dynamic actin cytoskeleton functions at multiple stages of clathrin-mediated endocytosis. *Mol Biol Cell* 16:964-975.

33. Jeng, R.L., and M.D. Welch. 2001. Cytoskeleton: actin and endocytosis--no longer the weakest link. *Curr Biol* 11:R691-694.

34. Roth, M.G. 2007. Integrating actin assembly and endocytosis. *Dev Cell* 13:3-4.

35. Sandvig, K., and B. van Deurs. 1990. Selective modulation of the endocytic uptake of ricin and fluid phase markers without alteration in transferrin endocytosis. *J Biol Chem* 265:6382-6388.

36. Gottlieb, T.A., I.E. Ivanov, M. Adesnik, and D.D. Sabatini. 1993. Actin microfilaments play a critical role in endocytosis at the apical but not the basolateral surface of polarized epithelial cells. *J Cell Biol* 120:695-710.

37. Dunn, K.W., T.E. McGraw, and F.R. Maxfield. 1989. Iterative fractionation of recycling receptors from lysosomally destined ligands in an early sorting endosome. *J Cell Biol* 109:3303-3314.

38. Kornfeld, S., and I. Mellman. 1989. The biogenesis of lysosomes. *Annu Rev Cell Biol* 5:483-525.

39. Zerial, M., and H. McBride. 2001. Rab proteins as membrane organizers. *Nat Rev Mol Cell Biol* 2:107-117.

40. Somsel Rodman, J., and A. Wandinger-Ness. 2000. Rab GTPases coordinate endocytosis. *J Cell Sci* 113 Pt 2:183-192.

41. Gruenberg, J. 2001. The endocytic pathway: a mosaic of domains. *Nat Rev Mol Cell Biol* 2:721-730.

42. Geuze, H.J., J.W. Slot, G.J. Strous, H.F. Lodish, and A.L. Schwartz. 1983. Intracellular site of asialoglycoprotein receptor-ligand uncoupling: double-label immunoelectron microscopy during receptor-mediated endocytosis. *Cell* 32:277-287.

43. Marsh, M., G. Griffiths, G.E. Dean, I. Mellman, and A. Helenius. 1986. Three-dimensional structure of endosomes in BHK-21 cells. *Proc Natl Acad Sci U S A* 83:2899-2903.

44. Gruenberg, J., G. Griffiths, and K.E. Howell. 1989. Characterization of the early endosome and putative endocytic carrier vesicles in vivo and with an assay of vesicle fusion in vitro. *J Cell Biol* 108:1301-1316.

45. Maxfield, F.R., and T.E. McGraw. 2004. Endocytic recycling. *Nat Rev Mol Cell Biol* 5:121-132.

46. Schmid, S., R. Fuchs, M. Kielian, A. Helenius, and I. Mellman. 1989. Acidification of endosome subpopulations in wild-type Chinese hamster ovary cells and temperature-sensitive acidification-defective mutants. *J Cell Biol* 108:1291-1300.

47. Sipe, D.M., and R.F. Murphy. 1987. High-resolution kinetics of transferrin acidification in BALB/c 3T3 cells: exposure to pH 6 followed by temperature-sensitive alkalinization during recycling. *Proc Natl Acad Sci U S A* 84:7119-7123.

48. Yamashiro, D.J., and F.R. Maxfield. 1987. Acidification of morphologically distinct endosomes in mutant and wild-type Chinese hamster ovary cells. *J Cell Biol* 105:2723-2733.

49. Schmid, S.L., R. Fuchs, P. Male, and I. Mellman. 1988. Two distinct subpopulations of endosomes involved in membrane recycling and transport to lysosomes. *Cell* 52:73-83.

50. Bucci, C., R.G. Parton, I.H. Mather, H. Stunnenberg, K. Simons, B. Hoflack, and M. Zerial. 1992. The small GTPase rab5 functions as a regulatory factor in the early endocytic pathway. *Cell* 70:715-728.

51. Gorvel, J.P., P. Chavrier, M. Zerial, and J. Gruenberg. 1991. rab5 controls early endosome fusion in vitro. *Cell* 64:915-925.

52. Zerial, M. 1993. Regulation of endocytosis by the small GTP-ase rab5. *Cytotechnology* 11 Suppl 1:S47-49.

53. Nielsen, E., F. Severin, J.M. Backer, A.A. Hyman, and M. Zerial. 1999. Rab5 regulates motility of early endosomes on microtubules. *Nat Cell Biol* 1:376-382.

54. Van Der Sluijs, P., M. Hull, A. Zahraoui, A. Tavitian, B. Goud, and I. Mellman. 1991. The small GTP-binding protein rab4 is associated with early endosomes. *Proc Natl Acad Sci U S A* 88:6313-6317.

55. Mohrmann, K., L. Gerez, V. Oorschot, J. Klumperman, and P. van der Sluijs. 2002. Rab4 function in membrane recycling from early endosomes depends on a membrane to cytoplasm cycle. *J Biol Chem* 277:32029-32035.

56. van der Sluijs, P., M. Hull, P. Webster, P. Male, B. Goud, and I. Mellman. 1992. The small GTP-binding protein rab4 controls an early sorting event on the endocytic pathway. *Cell* 70:729-740.

57. Vitale, G., V. Rybin, S. Christoforidis, P. Thornqvist, M. McCaffrey, H. Stenmark, and M. Zerial. 1998. Distinct Rab-binding domains mediate the interaction of Rabaptin-5 with GTP-bound Rab4 and Rab5. *EMBO J* 17:1941-1951.

58. Sonnichsen, B., S. De Renzis, E. Nielsen, J. Rietdorf, and M. Zerial. 2000. Distinct membrane domains on endosomes in the recycling pathway visualized by multicolor imaging of Rab4, Rab5, and Rab11. *J Cell Biol* 149:901-914.

59. Ren, M., G. Xu, J. Zeng, C. De Lemos-Chiarandini, M. Adesnik, and D.D. Sabatini. 1998. Hydrolysis of GTP on rab11 is required for the direct delivery of transferrin from the pericentriolar recycling compartment to the cell surface but not from sorting endosomes. *Proc Natl Acad Sci U S A* 95:6187-6192.

60. Schmidt, M.R., and V. Haucke. 2007. Recycling endosomes in neuronal membrane traffic. *Biol Cell* 99:333-342.

61. Ullrich, O., S. Reinsch, S. Urbe, M. Zerial, and R.G. Parton. 1996. Rab11 regulates recycling through the pericentriolar recycling endosome. *J Cell Biol* 135:913-924.

62. Wilcke, M., L. Johannes, T. Galli, V. Mayau, B. Goud, and J. Salamero. 2000. Rab11 regulates the compartmentalization of early endosomes required for efficient transport from early endosomes to the trans-golgi network. *J Cell Biol* 151:1207-1220.

63. Clague, M.J., S. Urbe, F. Aniento, and J. Gruenberg. 1994. Vacuolar ATPase activity is required for endosomal carrier vesicle formation. *J Biol Chem* 269:21-24.

64. Hopkins, C.R., A. Gibson, M. Shipman, and K. Miller. 1990. Movement of internalized ligand-receptor complexes along a continuous endosomal reticulum. *Nature* 346:335-339.

65. Geuze, H.J., W. Stoorvogel, G.J. Strous, J.W. Slot, J.E. Bleekemolen, and I. Mellman. 1988. Sorting of mannose 6-phosphate receptors and lysosomal membrane proteins in endocytic vesicles. *J Cell Biol* 107:2491-2501.

66. Piper, R.C., and J.P. Luzio. 2001. Late endosomes: sorting and partitioning in multivesicular bodies. *Traffic* 2:612-621.

67. Ganley, I.G., K. Carroll, L. Bittova, and S. Pfeffer. 2004. Rab9 GTPase regulates late endosome size and requires effector interaction for its stability. *Mol Biol Cell* 15:5420-5430.

68. Barbero, P., L. Bittova, and S.R. Pfeffer. 2002. Visualization of Rab9-mediated vesicle transport from endosomes to the trans-Golgi in living cells. *J Cell Biol* 156:511-518.

69. Riederer, M.A., T. Soldati, A.D. Shapiro, J. Lin, and S.R. Pfeffer. 1994. Lysosome biogenesis requires Rab9 function and receptor recycling from endosomes to the trans-Golgi network. *J Cell Biol* 125:573-582.

70. Lombardi, D., T. Soldati, M.A. Riederer, Y. Goda, M. Zerial, and S.R. Pfeffer. 1993. Rab9 functions in transport between late endosomes and the trans Golgi network. *EMBO J* 12:677-682.

71. Schneider, C., R. Sutherland, R. Newman, and M. Greaves. 1982. Structural features of the cell surface receptor for transferrin that is recognized by the monoclonal antibody OKT9. *J Biol Chem* 257:8516-8522.

72. Dautry-Varsat, A., A. Ciechanover, and H.F. Lodish. 1983. pH and the recycling of transferrin during receptor-mediated endocytosis. *Proc Natl Acad Sci U S A* 80:2258-2262.

73. Huebers, H.A., and C.A. Finch. 1987. The physiology of transferrin and transferrin receptors. *Physiol Rev* 67:520-582.

74. Ward, J.H., J.P. Kushner, and J. Kaplan. 1982. Regulation of HeLa cell transferrin receptors. *J Biol Chem* 257:10317-10323.

75. Aisen, P., and I. Listowsky. 1980. Iron transport and storage proteins. *Annu Rev Biochem* 49:357-393.

76. Sainte-Marie, J., V. Lafont, E.I. Pecheur, J. Favero, J.R. Philippot, and A. Bienvenue. 1997. Transferrin receptor functions as a signal-transduction molecule for its own recycling via increases in the internal Ca2+ concentration. *Eur J Biochem* 250:689-697.

77. Ohno, H., J. Stewart, M.C. Fournier, H. Bosshart, I. Rhee, S. Miyatake, T. Saito, A. Gallusser, T. Kirchhausen, and J.S. Bonifacino. 1995. Interaction of tyrosine-based sorting signals with clathrin-associated proteins. *Science* 269:1872-1875.

78. Perera, R.M., R. Zoncu, T.G. Johns, M. Pypaert, F.T. Lee, I. Mellman, L.J. Old, D.K. Toomre, and A.M. Scott. 2007. Internalization, intracellular trafficking, and biodistribution of monoclonal antibody 806: a novel anti-epidermal growth factor receptor antibody. *Neoplasia* 9:1099-1110.

79. Song, E., P. Zhu, S.K. Lee, D. Chowdhury, S. Kussman, D.M. Dykxhoorn, Y. Feng, D. Palliser, D.B. Weiner, P. Shankar, W.A. Marasco, and J. Lieberman.

2005. Antibody mediated in vivo delivery of small interfering RNAs via cell-surface receptors. *Nat Biotechnol* 23:709-717.

80. Tampellini, D., J. Magrane, R.H. Takahashi, F. Li, M.T. Lin, C.G. Almeida, and G.K. Gouras. 2007. Internalized antibodies to the Abeta domain of APP reduce neuronal Abeta and protect against synaptic alterations. *J Biol Chem* 282:18895-18906.

81. Polson, A.G., S.F. Yu, K. Elkins, B. Zheng, S. Clark, G.S. Ingle, D.S. Slaga, L. Giere, C. Du, C. Tan, J.A. Hongo, A. Gogineni, M.J. Cole, R. Vandlen, J.P. Stephan, J. Young, W. Chang, S.J. Scales, S. Ross, D. Eaton, and A. Ebens. 2007. Antibody-drug conjugates targeted to CD79 for the treatment of non-Hodgkin lymphoma. *Blood* 110:616-623.

82. Solomon, B., and D. Frenkel. 2010. Immunotherapy for Alzheimer's disease. *Neuropharmacology* In press:1-7.

83. Hock, C., U. Konietzko, J.R. Streffer, J. Tracy, A. Signorell, B. Muller-Tillmanns, U. Lemke, K. Henke, E. Moritz, E. Garcia, M.A. Wollmer, D. Umbricht, D.J. de Quervain, M. Hofmann, A. Maddalena, A. Papassotiropoulos, and R.M. Nitsch. 2003. Antibodies against beta-amyloid slow cognitive decline in Alzheimer's disease. *Neuron* 38:547-554.

84. Masliah, E., L. Hansen, A. Adame, L. Crews, F. Bard, C. Lee, P. Seubert, D. Games, L. Kirby, and D. Schenk. 2005. Abeta vaccination effects on plaque pathology in the absence of encephalitis in Alzheimer disease. *Neurology* 64:129-131.

85. Peer, D., P. Zhu, C.V. Carman, J. Lieberman, and M. Shimaoka. 2007. Selective gene silencing in activated leukocytes by targeting siRNAs to the integrin lymphocyte function-associated antigen-1. *Proc Natl Acad Sci U S A* 104:4095-4100.

86. Li, X., P. Stuckert, I. Bosch, J.D. Marks, and W.A. Marasco. 2001. Single-chain antibody-mediated gene delivery into ErbB2-positive human breast cancer cells. *Cancer Gene Ther* 8:555-565.

87. Kamizuru, H., H. Kimura, T. Yasukawa, Y. Tabata, Y. Honda, and Y. Ogura. 2001. Monoclonal antibody-mediated drug targeting to choroidal neovascularization in the rat. *Invest Ophthalmol Vis Sci* 42:2664-2672.

88. Kaspar, M., E. Trachsel, and D. Neri. 2007. The antibody-mediated targeted delivery of interleukin-15 and GM-CSF to the tumor neovasculature inhibits tumor growth and metastasis. *Cancer Res* 67:4940-4948.

89. Sarmiento, R.E., R.G. Tirado, L.E. Valverde, and B. Gomez-Garcia. 2007. Kinetics of antibody-induced modulation of respiratory syncytial virus antigens in a human epithelial cell line. *Virol J* 4:68.

90. Chesebro, B., K. Wehrly, D. Doig, and J. Nishio. 1979. Antibody-induced modulation of Friend virus cell surface antigens decreases virus production by persistent erythroleukemia cells: influence of the Rfv-3 gene. *Proc Natl Acad Sci U S A* 76:5784-5788.

91. Dowdle, W.R., J.C. Downie, and W.G. Laver. 1974. Inhibition of virus release by antibodies to surface antigens of influenza viruses. *J Virol* 13:269-275.

92. Wen, W.H., J.Y. Liu, W.J. Qin, J. Zhao, T. Wang, L.T. Jia, Y.L. Meng, H. Gao, C.F. Xue, B.Q. Jin, L.B. Yao, S.Y. Chen, and A.G. Yang. 2007. Targeted inhibition of HBV gene expression by single-chain antibody mediated small interfering RNA delivery. *Hepatology* 46:84-94.

93. Witko-Sarsat, V., P. Rieu, B. Descamps-Latscha, P. Lesavre, and L. Halbwachs-Mecarelli. 2000. Neutrophils: molecules, functions and pathophysiological aspects. *Lab Invest* 80:617-653.

94. Dale, D.C., L. Boxer, and W.C. Liles. 2008. The phagocytes: neutrophils and monocytes. *Blood* 112:935-945.

95. Akira, S., and K. Takeda. 2004. Toll-like receptor signalling. *Nat Rev Immunol* 4:499-511.

96. Takeda, K., and S. Akira. 2005. Toll-like receptors in innate immunity. *Int Immunol* 17:1-14.

97. Kawai, T., and S. Akira. 2007. TLR signaling. *Semin Immunol* 19:24-32.

98. Martinon, F., and J. Tschopp. 2005. NLRs join TLRs as innate sensors of pathogens. *Trends Immunol* 26:447-454.

99. Mariathasan, S., K. Newton, D.M. Monack, D. Vucic, D.M. French, W.P. Lee, M. Roose-Girma, S. Erickson, and V.M. Dixit. 2004. Differential activation of the inflammasome by caspase-1 adaptors ASC and Ipaf. *Nature* 430:213-218.

100. Martinon, F., A. Mayor, and J. Tschopp. 2009. The inflammasomes: guardians of the body. *Annu Rev Immunol* 27:229-265.

101. Tschopp, J., F. Martinon, and K. Burns. 2003. NALPs: a novel protein family involved in inflammation. *Nat Rev Mol Cell Biol* 4:95-104.

102. Fitzgerald, K.A. 2010. NLR-containing inflammasomes: central mediators of host defense and inflammation. *Eur J Immunol* 40:595-598.

103. Franchi, L., T. Eigenbrod, R. Munoz-Planillo, and G. Nunez. 2009. The inflammasome: a caspase-1-activation platform that regulates immune responses and disease pathogenesis. *Nat Immunol* 10:241-247.

104. Hornung, V., F. Bauernfeind, A. Halle, E.O. Samstad, H. Kono, K.L. Rock, K.A. Fitzgerald, and E. Latz. 2008. Silica crystals and aluminum salts activate the NALP3 inflammasome through phagosomal destabilization. *Nat Immunol* 9:847-856.

105. Martinon, F., V. Petrilli, A. Mayor, A. Tardivel, and J. Tschopp. 2006. Gout-associated uric acid crystals activate the NALP3 inflammasome. *Nature* 440:237-241.

106. Dostert, C., V. Petrilli, R. Van Bruggen, C. Steele, B.T. Mossman, and J. Tschopp. 2008. Innate immune activation through Nalp3 inflammasome sensing of asbestos and silica. *Science* 320:674-677.

107. Caicedo, M.S., R. Desai, K. McAllister, A. Reddy, J.J. Jacobs, and N.J. Hallab. 2008. Soluble and particulate Co-Cr-Mo alloy implant metals activate the inflammasome danger signaling pathway in human macrophages: A novel mechanism for implant debris reactivity. *J Orthop Res* 27:847-854.

108. Martinon, F. 2010. Signaling by ROS drives inflammasome activation. *Eur J Immunol* 40:616-619.

109. Zhou, R., A. Tardivel, B. Thorens, I. Choi, and J. Tschopp. 2010. Thioredoxin-interacting protein links oxidative stress to inflammasome activation. *Nat Immunol* 11:136-140.

110. Halle, A., V. Hornung, G.C. Petzold, C.R. Stewart, B.G. Monks, T. Reinheckel, K.A. Fitzgerald, E. Latz, K.J. Moore, and D.T. Golenbock. 2008. The NALP3 inflammasome is involved in the innate immune response to amyloid-beta. *Nat Immunol* 9:857-865.

111. Hornung, V., and E. Latz. 2010. Critical functions of priming and lysosomal damage for NLRP3 activation. *Eur J Immunol* 40:620-623.

112. Masumoto, J., S. Taniguchi, K. Ayukawa, H. Sarvotham, T. Kishino, N. Niikawa, E. Hidaka, T. Katsuyama, T. Higuchi, and J. Sagara. 1999. ASC, a novel 22-kDa protein, aggregates during apoptosis of human promyelocytic leukemia HL-60 cells. *J Biol Chem* 274:33835-33838.

113. Mariathasan, S., and D.M. Monack. 2007. Inflammasome adaptors and sensors: intracellular regulators of infection and inflammation. *Nat Rev Immunol* 7:31-40.

114. Agostini, L., F. Martinon, K. Burns, M.F. McDermott, P.N. Hawkins, and J. Tschopp. 2004. NALP3 forms an IL-1beta-processing inflammasome with increased activity in Muckle-Wells autoinflammatory disorder. *Immunity* 20:319-325.

115. Neven, B., A.M. Prieur, and P. Quartier dit Maire. 2008. Cryopyrinopathies: update on pathogenesis and treatment. *Nat Clin Pract Rheumatol* 4:481-489.

116. Dinarello, C.A. 1996. Biologic basis for interleukin-1 in disease. *Blood* 87:2095-2147.

117. Dinarello, C.A. 2010. IL-1: discoveries, controversies and future directions. *Eur J Immunol* 40:599-606.

118. Werman, A., R. Werman-Venkert, R. White, J.K. Lee, B. Werman, Y. Krelin, E. Voronov, C.A. Dinarello, and R.N. Apte. 2004. The precursor form of IL-1alpha is an intracrine proinflammatory activator of transcription. *Proc Natl Acad Sci U S A* 101:2434-2439.

119. Bauernfeind, F.G., G. Horvath, A. Stutz, E.S. Alnemri, K. MacDonald, D. Speert, T. Fernandes-Alnemri, J. Wu, B.G. Monks, K.A. Fitzgerald, V. Hornung, and E. Latz. 2009. Cutting edge: NF-kappaB activating pattern recognition and cytokine receptors license NLRP3 inflammasome activation by regulating NLRP3 expression. *J Immunol* 183:787-791.

120. Hise, A.G., J. Tomalka, S. Ganesan, K. Patel, B.A. Hall, G.D. Brown, and K.A. Fitzgerald. 2009. An essential role for the NLRP3 inflammasome in host defense against the human fungal pathogen Candida albicans. *Cell Host Microbe* 5:487-497.

121. Franchi, L., R. Munoz-Planillo, T. Reimer, T. Eigenbrod, and G. Nunez. 2010. Inflammasomes as microbial sensors. *Eur J Immunol* 40:611-615.

122. Daun, J.M., and M.J. Fenton. 2000. Interleukin-1/Toll receptor family members: receptor structure and signal transduction pathways. *J Interferon Cytokine Res* 20:843-855.

123. Stashenko, P., F.E. Dewhirst, W.J. Peros, R.L. Kent, and J.M. Ago. 1987. Synergistic interactions between interleukin 1, tumor necrosis factor, and lymphotoxin in bone resorption. *J Immunol* 138:1464-1468.

124. Assuma, R., T. Oates, D. Cochran, S. Amar, and D.T. Graves. 1998. IL-1 and TNF antagonists inhibit the inflammatory response and bone loss in experimental periodontitis. *J Immunol* 160:403-409.

125. Thomson, B.M., G.R. Mundy, and T.J. Chambers. 1987. Tumor necrosis factors alpha and beta induce osteoblastic cells to stimulate osteoclastic bone resorption. *J Immunol* 138:775-779.

126. Chen, C.J., H. Kono, D. Golenbock, G. Reed, S. Akira, and K.L. Rock. 2007. Identification of a key pathway required for the sterile inflammatory response triggered by dying cells. *Nat Med* 13:851-856.

127. Chen, C.J., Y. Shi, A. Hearn, K. Fitzgerald, D. Golenbock, G. Reed, S. Akira, and K.L. Rock. 2006. MyD88-dependent IL-1 receptor signaling is essential for gouty inflammation stimulated by monosodium urate crystals. *J Clin Invest* 116:2262-2271.

128. Ogilvie, A.C., C.E. Hack, J. Wagstaff, G.J. van Mierlo, A.J. Erenberg, L.L. Thomsen, K. Hoekman, and E.M. Rankin. 1996. IL-1 beta does not cause

neutrophil degranulation but does lead to IL-6, IL-8, and nitrite/nitrate release when used in patients with cancer. *J Immunol* 156:389-394.

129. Evans, R.J., J. Bray, J.D. Childs, G.P. Vigers, B.J. Brandhuber, J.J. Skalicky, R.C. Thompson, and S.P. Eisenberg. 1995. Mapping receptor binding sites in interleukin (IL)-1 receptor antagonist and IL-1 beta by site-directed mutagenesis. Identification of a single site in IL-1ra and two sites in IL-1 beta. *J Biol Chem* 270:11477-11483.

130. Abramson, S.B., and A. Amin. 2002. Blocking the effects of IL-1 in rheumatoid arthritis protects bone and cartilage. *Rheumatology (Oxford)* 41:972-980.

131. Bresnihan, B., J.M. Alvaro-Gracia, M. Cobby, M. Doherty, Z. Domljan, P. Emery, G. Nuki, K. Pavelka, R. Rau, B. Rozman, I. Watt, B. Williams, R. Aitchison, D. McCabe, and P. Musikic. 1998. Treatment of rheumatoid arthritis with recombinant human interleukin-1 receptor antagonist. *Arthritis Rheum* 41:2196-2204.

132. Jiang, Y., H.K. Genant, I. Watt, M. Cobby, B. Bresnihan, R. Aitchison, and D. McCabe. 2000. A multicenter, double-blind, dose-ranging, randomized, placebo-controlled study of recombinant human interleukin-1 receptor antagonist in patients with rheumatoid arthritis: radiologic progression and correlation of Genant and Larsen scores. *Arthritis Rheum* 43:1001-1009.

133. Dinarello, C.A., and R.C. Thompson. 1991. Blocking IL-1: interleukin 1 receptor antagonist in vivo and in vitro. *Immunol Today* 12:404-410.

134. Saeed, S., and P.A. Revell. 2001. Production and distribution of interleukin 15 and its receptors (IL-15Ralpha and IL-R2beta) in the implant interface tissues obtained during revision of failed total joint replacement. *Int J Exp Pathol* 82:201-209.

135. Revell, P.A. 2008. The combined role of wear particles, macrophages and lymphocytes in the loosening of total joint prostheses. *J R Soc Interface* 5:1263-1278.

136. Ingham, E., and J. Fisher. 2005. The role of macrophages in osteolysis of total joint replacement. *Biomaterials* 26:1271-1286.

137. Lee, J.M., E.A. Salvati, F. Betts, E.F. DiCarlo, S.B. Doty, and P.G. Bullough. 1992. Size of metallic and polyethylene debris particles in failed cemented total hip replacements. *J Bone Joint Surg Br* 74:380-384.

138. Margevicius, K.J., T.W. Bauer, J.T. McMahon, S.A. Brown, and K. Merritt. 1994. Isolation and characterization of debris in membranes around total joint prostheses. *J Bone Joint Surg Am* 76:1664-1675.

139. Champion, J.A., and S. Mitragotri. 2006. Role of target geometry in phagocytosis. *Proc Natl Acad Sci U S A* 103:4930-4934.

140. Favoreel, H.W., T.C. Mettenleiter, and H.J. Nauwynck. 2004. Copatching and lipid raft association of different viral glycoproteins expressed on the surfaces of pseudorabies virus-infected cells. *J Virol* 78:5279-5287.

141. Van de Walle, G.R., H.W. Favoreel, H.J. Nauwynck, P. Van Oostveldt, and M.B. Pensaert. 2001. Involvement of cellular cytoskeleton components in

antibody-induced internalization of viral glycoproteins in pseudorabies virus-infected monocytes. *Virology* 288:129-138.

142. Favoreel, H.W., H.J. Nauwynck, H.M. Halewyck, P. Van Oostveldt, T.C. Mettenleiter, and M.B. Pensaert. 1999. Antibody-induced endocytosis of viral glycoproteins and major histocompatibility complex class I on pseudorabies virus-infected monocytes. *J Gen Virol* 80 ( Pt 5):1283-1291.

143. Sloan, S.E., C. Hanlon, W. Weldon, M. Niezgoda, J. Blanton, J. Self, K.J. Rowley, R.B. Mandell, G.J. Babcock, W.D. Thomas, Jr., C.E. Rupprecht, and D.M. Ambrosino. 2007. Identification and characterization of a human monoclonal antibody that potently neutralizes a broad panel of rabies virus isolates. *Vaccine* 25:2800-2810.

144. Bellve, K.D., D. Leonard, C. Standley, L.M. Lifshitz, R.A. Tuft, A. Hayakawa, S. Corvera, and K.E. Fogarty. 2006. Plasma membrane domains specialized for clathrin-mediated endocytosis in primary cells. *J Biol Chem* 281:16139-16146.

145. Leonard, D., A. Hayakawa, D. Lawe, D. Lambright, K.D. Bellve, C. Standley, L.M. Lifshitz, K.E. Fogarty, and S. Corvera. 2008. Sorting of EGF and transferrin at the plasma membrane and by cargo-specific signaling to EEA1-enriched endosomes. *J Cell Sci* 121:3445-3458.

146. Green, E.G., E. Ramm, N.M. Riley, D.J. Spiro, J.R. Goldenring, and M. Wessling-Resnick. 1997. Rab11 is associated with transferrin-containing recycling compartments in K562 cells. *Biochem Biophys Res Commun* 239:612-616.

147. Harding, C., J. Heuser, and P. Stahl. 1983. Receptor-mediated endocytosis of transferrin and recycling of the transferrin receptor in rat reticulocytes. *J Cell Biol* 97:329-339.

148. Axelrod, D. 2003. Total internal reflection fluorescence microscopy in cell biology. *Methods Enzymol* 361:1-33.

149. Axelrod, D. 2001. Total internal reflection fluorescence microscopy in cell biology. *Traffic* 2:764-774.

150. Li, G., and P.D. Stahl. 1993. Structure-function relationship of the small GTPase rab5. *J Biol Chem* 268:24475-24480.

151. Trachsel, E., F. Bootz, M. Silacci, M. Kaspar, H. Kosmehl, and D. Neri. 2007. Antibody-mediated delivery of IL-10 inhibits the progression of established collagen-induced arthritis. *Arthritis Res Ther* 9:R9.

152. Marecos, E., R. Weissleder, and A. Bogdanov, Jr. 1998. Antibody-mediated versus nontargeted delivery in a human small cell lung carcinoma model. *Bioconjug Chem* 9:184-191.

153. WHO. 2007. Rabies vaccines. WHO position paper. *Wkly Epidemiol Rec* 82:425-435.

154. Wiktor, T.J., and H. Koprowski. 1978. Monoclonal antibodies against rabies virus produced by somatic cell hybridization: detection of antigenic variants. *Proc Natl Acad Sci U S A* 75:3938-3942.

155. Jacobs, J.J., K.A. Roebuck, M. Archibeck, N.J. Hallab, and T.T. Glant. 2001. Osteolysis: basic science. *Clin Orthop Relat Res* 393:71-77.

156. Stea, S., M. Visentin, D. Granchi, G. Ciapetti, M.E. Donati, A. Sudanese, C. Zanotti, and A. Toni. 2000. Cytokines and osteolysis around total hip prostheses. *Cytokine* 12:1575-1579.

157. Granchi, D., E. Verri, G. Ciapetti, S. Stea, L. Savarino, A. Sudanese, M. Mieti, R. Rotini, D. Dallari, G. Zinghi, and L. Montanaro. 1998. Bone-resorbing cytokines in serum of patients with aseptic loosening of hip prostheses. *J Bone Joint Surg Br* 80:912-917.

158. Rader, C.P., T. Sterner, F. Jakob, N. Schutze, and J. Eulert. 1999. Cytokine response of human macrophage-like cells after contact with polyethylene and pure titanium particles. *J Arthroplasty* 14:840-848.

159. Boynton, E.L., J. Waddell, E. Meek, R.S. Labow, V. Edwards, and J.P. Santerre. 2000. The effect of polyethylene particle chemistry on human monocyte-macrophage function in vitro. *J Biomed Mater Res* 52:239-245.

160. Epstein, N.J., B.A. Warme, J. Spanogle, T. Ma, B. Bragg, R.L. Smith, and S.B. Goodman. 2005. Interleukin-1 modulates periprosthetic tissue formation in an intramedullary model of particle-induced inflammation. *J Orthop Res* 23:501-510.

161. Hayat, M.A. 1978. Introduction to biological scanning electron microscopy. University Park Press, Baltimore. 323 p. pp.

162. Oliveira, S.H., C. Canetti, R.A. Ribeiro, and F.Q. Cunha. 2008. Neutrophil migration induced by IL-1beta depends upon LTB4 released by macrophages

and upon TNF-alpha and IL-1beta released by mast cells. *Inflammation* 31:36-46.

163. Nagai, Y., S. Akashi, M. Nagafuku, M. Ogata, Y. Iwakura, S. Akira, T. Kitamura, A. Kosugi, M. Kimoto, and K. Miyake. 2002. Essential role of MD-2 in LPS responsiveness and TLR4 distribution. *Nat Immunol* 3:667-672.

164. Wright, S.D., R.A. Ramos, P.S. Tobias, R.J. Ulevitch, and J.C. Mathison. 1990. CD14, a receptor for complexes of lipopolysaccharide (LPS) and LPS binding protein. *Science* 249:1431-1433.

165. Hentze, H., X.Y. Lin, M.S. Choi, and A.G. Porter. 2003. Critical role for cathepsin B in mediating caspase-1-dependent interleukin-18 maturation and caspase-1-independent necrosis triggered by the microbial toxin nigericin. *Cell Death Differ* 10:956-968.

166. Muruve, D.A., V. Petrilli, A.K. Zaiss, L.R. White, S.A. Clark, P.J. Ross, R.J. Parks, and J. Tschopp. 2008. The inflammasome recognizes cytosolic microbial and host DNA and triggers an innate immune response. *Nature* 452:103-107.

167. Chiba, J., H.E. Rubash, K.J. Kim, and Y. Iwaki. 1994. The characterization of cytokines in the interface tissue obtained from failed cementless total hip arthroplasty with and without femoral osteolysis. *Clin Orthop Relat Res* 300:304-312.

168. Schwarz, E.M., A.P. Lu, J.J. Goater, E.B. Benz, G. Kollias, R.N. Rosier, J.E. Puzas, and R.J. O'Keefe. 2000. Tumor necrosis factor-alpha/nuclear

transcription factor-kappaB signaling in periprosthetic osteolysis. *J Orthop Res* 18:472-480.

169. Schumacher, H.R., and C.A. Agudelo. 1972. Intravascular degranulation of neutrophils: an important factor in inflammation? *Science* 175:1139-1140.

170. Sud, S., S.Y. Yang, C.H. Evans, P.D. Robbins, and P.H. Wooley. 2001. Effects of cytokine gene therapy on particulate-induced inflammation in the murine air pouch. *Inflammation* 25:361-372.

171. Kimble, R.B., J.L. Vannice, D.C. Bloedow, R.C. Thompson, W. Hopfer, V.T. Kung, C. Brownfield, and R. Pacifici. 1994. Interleukin-1 receptor antagonist decreases bone loss and bone resorption in ovariectomized rats. *J Clin Invest* 93:1959-1967.

172. Baltzer, A.W., J.D. Whalen, P. Wooley, C. Latterman, L.M. Truchan, P.D. Robbins, and C.H. Evans. 2001. Gene therapy for osteoporosis: evaluation in a murine ovariectomy model. *Gene Ther* 8:1770-1776.

173. Gordon, A., E. Kiss-Toth, I. Stockley, R. Eastell, and J.M. Wilkinson. 2008. Polymorphisms in the interleukin-1 receptor antagonist and interleukin-6 genes affect risk of osteolysis in patients with total hip arthroplasty. *Arthritis Rheum* 58:3157-3165.

174. Champion, J.A., and S. Mitragotri. 2009. Shape induced inhibition of phagocytosis of polymer particles. *Pharm Res* 26:244-249.

175. Hubbell, J.A., S.N. Thomas, and M.A. Swartz. 2009. Materials engineering for immunomodulation. *Nature* 462:449-460.

176. van Zon, J.S., G. Tzircotis, E. Caron, and M. Howard. 2009. A mechanical bottleneck explains the variation in cup growth during Fc gamma R phagocytosis. *Molecular Systems Biology* 5:298.

177. Canelas, D.A., K.P. Herlihy, and J.M. DeSimone. 2009. Top-down particle fabrication: control of size and shape for diagnostic imaging and drug delivery. *Wiley Interdisciplinary Reviews-Nanomedicine and Nanobiotechnology* 1:391-404.

178. Decuzzi, P., B. Godin, T. Tanaka, S.Y. Lee, C. Chiappini, X. Liu, and M. Ferrari. 2010. Size and shape effects in the biodistribution of intravascularly injected particles. *Journal of Controlled Release* 141:320-327.

179. Doshi, N., and S. Mitragotri. 2010. Macrophages Recognize Size and Shape of Their Targets. *PLoS ONE* 5:e10051.

180. Zhu, J., and R.C. Hayward. 2008. Hierarchically structured microparticles formed by interfacial instabilities of emulsion droplets containing amphiphilic block copolymers. *Angewandte Chemie International Edition* 47:2113-2116.

181. Zhu, J., and R.C. Hayward. 2008. Spontaneous generation of amphiphilic block copolymer micelles with multiple morphologies through interfacial Instabilities. *J Am Chem Soc* 130:7496-7502.

182. Sharp, F.A., D. Ruane, B. Claass, E. Creagh, J. Harris, P. Malyala, M. Singh, D.T. O'Hagan, V. Petrilli, J. Tschopp, L.A. O'Neill, and E.C. Lavelle. 2009. Uptake of particulate vaccine adjuvants by dendritic cells activates the NALP3 inflammasome. *Proc Natl Acad Sci U S A* 106:870-875.

183. Qian, Z.M., H. Li, H. Sun, and K. Ho. 2002. Targeted drug delivery via the transferrin receptor-mediated endocytosis pathway. *Pharmacol Rev* 54:561-587.

184. Dietzschold, B., M. Tollis, M. Lafon, W.H. Wunner, and H. Koprowski. 1987. Mechanisms of rabies virus neutralization by glycoprotein-specific monoclonal antibodies. *Virology* 161:29-36.

185. Lodmell, D.L., and L.C. Ewalt. 1987. Immune sera and antiglycoprotein monoclonal antibodies inhibit in vitro cell-to-cell spread of pathogenic rabies viruses. *J Virol* 61:3314-3318.

186. de Melker, A.A., G. van der Horst, and J. Borst. 2004. c-Cbl directs EGF receptors into an endocytic pathway that involves the ubiquitin-interacting motif of Eps15. *J Cell Sci* 117:5001-5012.

187. de Melker, A.A., G. van der Horst, J. Calafat, H. Jansen, and J. Borst. 2001. c-Cbl ubiquitinates the EGF receptor at the plasma membrane and remains receptor associated throughout the endocytic route. *J Cell Sci* 114:2167-2178.

188. Levkowitz, G., H. Waterman, E. Zamir, Z. Kam, S. Oved, W.Y. Langdon, L. Beguinot, B. Geiger, and Y. Yarden. 1998. c-Cbl/Sli-1 regulates endocytic sorting and ubiquitination of the epidermal growth factor receptor. *Genes Dev* 12:3663-3674.

189. Li, H., S.B. Willingham, J.P. Ting, and F. Re. 2008. Cutting edge: inflammasome activation by alum and alum's adjuvant effect are mediated by NLRP3. *J Immunol* 181:17-21.

190. Eisenbarth, S.C., O.R. Colegio, W. O'Connor, F.S. Sutterwala, and R.A. Flavell. 2008. Crucial role for the Nalp3 inflammasome in the immunostimulatory properties of aluminium adjuvants. *Nature* 453:1122-1126.

191. Curtsinger, J.M., C.S. Schmidt, A. Mondino, D.C. Lins, R.M. Kedl, M.K. Jenkins, and M.F. Mescher. 1999. Inflammatory cytokines provide a third signal for activation of naive CD4+ and CD8+ T cells. *J Immunol* 162:3256-3262.

192. Pape, K.A., A. Khoruts, A. Mondino, and M.K. Jenkins. 1997. Inflammatory cytokines enhance the in vivo clonal expansion and differentiation of antigen-activated CD4+ T cells. *J Immunol* 159:591-598.